Urban-Rural Aerosol Characteristics and Solar Insolation over Delhi-NCR Region

Thesis submitted to the Jawaharlal Nehru University
in partial fulfilment of the requirements for the
award of the degree of

DOCTOR OF PHILOSOPHY

PURNIMA BHARDWAJ

SCHOOL OF ENVIRONMENTAL SCIENCES
JAWAHARLAL NEHRU UNIVERSITY
NEW DELHI-110067
INDIA
2017

जवाहरलाल नेहरू विश्वविद्यालय
Jawaharlal Nehru University
SCHOOL OF ENVIRONMENTAL SCIENCES
New Delhi-110067
Tele. 011-26704303, 4304

CERTIFICATE

This is to certify that the thesis entitled **"Urban-Rural Aerosol Characteristics and Solar Insolation over Delhi-NCR region"** embodies the original work, carried out in the School of Environmental Sciences, Jawaharlal Nehru University, New Delhi, India. This work has not been submitted in full or partial for any other degree or diploma to any other University or Institute.

Purnima Bhardwaj
(Candidate)

21/07/2017
Prof. Krishan Kumar
(Co-supervisor)

Prof. V. K. Jain
(Supervisor)

21/7/2017
Prof. S. Mukherjee
(Dean)

प्रो.सौमित्र मुखर्जी / Prof. S. Mukherjee
डीन / Dean
पर्यावरण विज्ञान संस्थान
School of Environmental Sciences
Jawaharlal Nehru University
New Delhi-110067

To My Parents.....

Acknowledgements

"All praise for the Almighty, the ultimate being"

By the abundant grace and blessings of God and His everlasting light of guidance, I was able to accomplish this work. As I reach another milestone in my academic career, I wish to express my eternal feelings to those, whose strong support and motivation made possible to present my research work in the form of dissertation.

First of all, I would like to express my deepest sense of gratitude and special thanks to my supervisor Prof. ***V. K. Jain*** *and Co-supervisor* ***Prof. Krishan Kumar*** *who believed in, encouraged and supported my efforts and provided intellectual stimulation, continuing exhilarating and sagacious guidance throughout the present study. Their scholarly suggestions, prudent admonitions, immense interest, constant help, and affectionate behaviour have been a beacon of light for me.*

I sincerely thank ***Prof. S. Mukherjee****, Dean, School of Environmental Sciences for providing me an opportunity to work and avail the necessary departmental facilities during the course of this work. I would also like to thank my Doctoral Committee Members, Dr. Sudesh Yadav and Dr. Pratima Solanki for giving inspiration and support during the course of research work.*

I would like to acknowledge NASA's MODIS and CERES data dissemination teams for providing open access to the data. I wish to express my gratitude to University Grants Commission (UGC), Govt. of India for BSR scholarship assistance provided to me in the form of Junior Research Fellowship.

I am thankful to the faculty and office staff specially Mr. M. P. Guite, Mr. Umasankar, Mr. M. K. Prabhakar, Mr. Amrik Singh, Mrs. Raj Dulari and Mr. Vinod for providing me the necessary administrative and research facilities. I overwhelmingly acknowledge the services rendered by Gajendra ji, Puran ji and Anil ji for providing ever possible help.

I was bestowed upon with the memorable company of my senior colleague Dr. Amit Prakesh, Dr. Sudeep Shukla, Dr. Bhupendra Pratap Singh and Dr. Amit to whom I owe my heartfelt thanks for taking a keen interest, making useful suggestions and timely help in overcoming numerous problems. I can't forget their constructive suggestions, meticulous attention, wise counsel and scholarly guidance. I would like to thank my seniors Dr. Saiyogita, Dr. Neetu, and Dr. Deepak Singh.

I would specially like to thank my esteemed senior Dr. Alok Kumar Pandey who helped me a great deal in completing my PhD work.

No word would be enough for expressing my gratitude towards my lab members for their immense support all throughout my Ph.D. tenure. I am very much thankful to my lab members Anandam and caring juniors Priyanka, Gayatri , Ritesh, Prabhat and Akash Ajay for bringing in the required fun, enthusiasm and optimism in me at hard times. I would also like to thank Manisha, Saurabh and Dr. Pallavi Saxena for helping me during my analysis for the PhD work.

Words alone cannot express my gratitude I owe to my friends Naba, Shivesh, Disha, Yogender, Hemant, Vinay and Prateek who have stood by me in all circumstances and provided me the constant support.

A special word of thank to Savi Di whose friendship is really an achievement in my life.

Last but not least, I cannot get through without mentioning my family members and the almighty who established a great courage, confidence, patience in me and firm determination for fulfilling my dreams. With gratitude and reverence, I would like to admire my parents who answered to all I needed, tolerated my idiosyncrasies and boosted my morale for the successful completion of the project. Words fall short to express my appreciation for my brothers and sisters whose unconditional love have always cherished in hard times. I would also like to thank my neighbours Sandhya Aunty (Delhi) and Angoori Aunty (Haryana) without whom my work could not have been completed for allowing me to use their home for carrying out the sampling for my work.

Regret and regards to those who have been close enough to be mentioned but not included by name in this acknowledgement. I also expect their grant of forgiveness and acknowledge their help and support.

July 2017 ***Purnima Bhardwaj***

List of Contents

		Page No.
Acknowledgements		I-II
List of Contents		III
List of Figure		IV-V
List of Table		VI
List of Abbreviations		VII-VIII
List of Publications		IX
Chapter - 1	***Introduction***	**1-25**
	1.1 Air Quality	1
	1.2 Aerosols and their Significance	3
	1.3 Physical and Chemical Properties of Aerosols	6
	1.4 Urban and Rural Differences	9
	1.5 Aerosol- Solar radiation Interaction	10
	1.6 Literature Review	12
	1.7 Objectives	25
	1.8 Significance of study	25
Chapter - 2	***Methodology***	**26-40**
	2.1 Study Area	26
	2.2 Measurements of Solar Spectral Irradiance	28
	2.3 $PM_{2.5}$ Sampling	29
	2.4 SEM Analysis	30
	2.5 OC and EC Analysis	30
	2.6 Data Used	34
	2.7 Software Used	37
Chapter - 3	***Results and Discussion***	**41-103**
	3.1 PM2.5 characteristics	41
	3.2 Solar irradiance studies over Delhi NCR	77
	3.3 Urban-Rural aerosol characteristics and Solar Insolation Rel.	86
	3.4 Radiative Forcing	92
Chapter - 4	**Conclusions**	**104-106**
References		**i-xiv**

List of Figures

S. No.		Page No.
Fig- 2.1	Map showing the sampling sites in Delhi-NCR	27
Fig- 2.2	FieldSpec Spectroradiometer (ASD Inc.) used for the solar irradiance (Global and Direct) measurements.	29
Fig- 2.3	Airmetrics Mini-Vol® Air sampler for $PM_{2.5}$ sampling	30
Fig- 2.4	EC/OC Analyser (DRI) used for the analysis of Organic and Elemental carbon in $PM_{2.5}$ samples	33
Fig-2.5	DRI Model 2001 Thermal Optical Carbon Analyzer schematic diagram	33
Fig-2.6	Flowchart of the Methodology	40
Fig- 3.1	Seasonal variation of $PM_{2.5}$ concentration at urban and rural sites.	41
Fig- 3.2	SEM micrographs for the blank quartz fibre filters	45
Fig- 3.3	SEM micrographs for the summer season at two sites Shahdara (a, c, e) and Sampla (b, d, f).	47
Fig- 3.4	SEM micrographs for the Sept-October months at the two sites viz. Shahdara (a, c, e) and Sampla (b, d, f).	49
Fig- 3.5	SEM micrographs for the PoM (N) season at two sites Shahdara (a, c, e) and Sampla (b, d, f).	51
Fig- 3.6	SEM micrographs for the winter (N) season at two sites Shahdara (a, c, e) and Sampla (b, d, f).	53
Fig- 3.7	The size distribution of $PM_{2.5}$ particles at the Shahdara and Sampla site during the Summer season	56
Fig- 3.8	The size distribution of $PM_{2.5}$ particles at the Shahdara and Sampla site during the Post-Monsoon (S-O) season	58
Fig- 3.9	The size distribution of $PM_{2.5}$ particles at the Shahdara and Sampla site during the Post-Monsoon (N) season.	60
Fig- 3.10	The size distribution of $PM_{2.5}$ particles at the Shahdara and Sampla site during the winter season	62
Fig- 3.11	Relationship between OC and EC during summer season at two sites Shahdara (a) and Sampla (b)	64
Fig- 3.12	Relationship between OC and EC during September-October months at two sites Shahdara (a) and Sampla (b).	66
Fig- 3.13	Relationship between OC and EC during November month at two sites Shahdara (a) and Sampla (b).	67
Fig- 3.14	Relationship between OC and EC during winter season at two sites Shahdara (a) and Sampla (b).	69
Fig- 3.15	Variation of Global Irradiance at Shahdara and Sampla during Summer season	77

Fig- 3.16	Variation of Global Irradiance at Shahdara and Sampla during PoM (Sept-October) season.	78
Fig- 3.17	Variation of Global Irradiance at Shahdara and Sampla during PoM (November) season.	79
Fig- 3.18	Variation of Global Irradiance at Shahdara and Sampla during Winter season	80
Fig- 3.19	Variation of Direct Irradiance at Shahdara and Sampla during Summer season	81
Fig- 3.20	Variation of Direct Irradiance at Shahdara and Sampla during PoM (Sept-October) season.	82
Fig- 3.21	Variation of Direct Irradiance at Shahdara and Sampla during PoM (November) season.	83
Fig- 3.22	Variation of Direct Irradiance at Shahdara and Sampla during Winter season	84
Fig- 3.23	Seasonal associations of the $PM_{2.5}$ (difference) concentration and global solar irradiance at the Shahdara and Sampla	86
Fig- 3.24	Seasonal associations of the $PM_{2.5}$ (difference) concentration and direct solar irradiance at the Shahdara and Sampla	87
Fig- 3.25	The seasonal association of the organic carbon (OC) and solar irradiance (global and direct) at Shahdara site.	89
Fig- 3.26	The seasonal association of the organic carbon (OC) and solar irradiance (global and direct) at Sampla site	90
Fig- 3.27	The seasonal association of the elemental carbon (EC) and solar irradiance (global and direct) at Shahdara site	91
Fig- 3.28	The seasonal association of the elemental carbon (EC) and solar irradiance (global and direct) at Sampla site	92
Fig- 3.29	The Radiative Forcing over Delhi using Intercept and Slope Methods in Pre-monsoon (PrM), Post-monsoon (PoM) and Winter (W) season.	93
Fig- 3.30	The radiative forcing over Haryana using Intercept and Slope Methods in Pre-monsoon (PrM), Post-monsoon (PoM) and Winter (W)seasons.	94
Fig- 3.31	Variation of surface (SRF) solar fluxes in PrM, PoM and W seasons at Delhi site	96
Fig- 3.32	Variation of surface (SRF) solar fluxes in PrM, PoM and W seasons at Haryana site.	97
Fig- 3.33	Variation of top of the atmosphere (TOA) fluxes with AOD550 in PrM and W seasons at Delhi site.	98
Fig- 3.34	Variation of top of the atmosphere (TOA) fluxes with AOD550 in PrM and W seasons at Haryana site.	98

List of Tables

S. No.		Page No.
Table 1.1	Different size categories of aerosols	7
Table 3.1	The average, minimum and maximum $PM_{2.5}$ concentration (all in $\mu g/m^3$) at Shahdara and Sampla in different seasons.	44
Table 3.2	The average values of EC, OC (all in $\mu g/m^3$), standard deviation (S.D) and standard error at Shahdara and Sampla in different seasons	71
Table 3.3	The minimum and maximum values of EC, OC (all in $\mu g/m^3$) and OC/EC ratio at Shahdara and Sampla in different seasons	74
Table 3.4	Secondary organic carbon (SOCs) concentrations with standard deviation (SD) and their % contribution to organic carbon at Shahdara and Sampla sites in different seasons.	75
Table 3.5	The global and Direct Irradiance (Wm^{-2}) value for the 325-1075 nm wavelength band	85
Table 3.6	Seasonal variations of the $PM_{2.5}$ concentration difference, Global and Direct Irradiance at Shahdara and Sampla sites	88
Table 3.7	The seasonal radiative forcing efficiency (η) and Clear sky flux (F^o) variation at surface (SRF) and top of the atmosphere (TOA) over Delhi	99
Table 3.8	The seasonal radiative forcing efficiency (η) and Clear sky flux (F^o) variation at surface (SRF) and top of the atmosphere (TOA) over Haryana	99
Table 3.9	Radiative Forcing over Delhi using slope and intercept methods with errors in Pre-Monsoon, Post-Monsoon and Winter seasons	100
Table 3.10	. Radiative Forcing over Haryana using slope and intercept methods with errors in Pre-Monsoon, Post-Monsoon and Winter seasons	101
Table 3.11	The seasonal single scattering albedo (SSA), (AE) and Aerosol Optical Depth (AOD) variations over Delhi and Haryana	102

List of Abbreviations

μm	Micrometer
AE	Angstrom Exponent
AMJ	April-May-June
AOD	Aerosol Optical Depth
ATM	Atmosphere
BC	Black Carbon
CCN	Cloud Condensation Nuclei
CERES	Clouds and the Earth's Radiant Energy System
CO_2	Carbon Dioxide
CPCB	Central Pollution Control Board
DJF	December-January-February
EC	Elemental Carbon
η	Radiative Forcing Efficiency
IN	Ice Nuclei
$\mu g/m^3$	Micrograms per cubic meter
$\mu gC/m^3$	Micrograms Carbon per cubic meter
MODIS	Moderate-Resolution Imaging Spectroradiometer
NAAQS	National Ambient Air Quality Standards
NCR	National Capital Region
NOx	Nitrogen Oxides
O_3	Ozone
OC	Organic Carbon
OM	Organic Matter
PAH	Polycyclic aromatic hydrocarbon
$PM_{2.5}$	Particulate Matter with diameter ≤ 2.5 μm
$PM_{2.5}$(Diff.)	PM2.5 concentration Difference
PoM	Post-Monsoon Season
PoM (N)	Post-Monsoon (November)

PoM (S-O)	Post Monsoon (September – October)
PrM	Pre-Monsoon Season
RF	Radiative Forcing
RH	Relative Humidity
SA	Surface Albedo
SD	Standard Deviation
SEM	Scanning Electron Microscopy
SOA	Secondary Organic Aerosols
SOC	Secondary Organic Carbon
SON	September-October-November
SO_x	Sulphur Oxides
SRF	Surface
SSA	Single Scattering Albedo
SZA	Solar Zenith Angle
TOA	Top of the Atmosphere
US-EPA	United States Environmental Protection Agency
VOC	Volatile organic compounds
WHO	World Health Organization
Wm^{-2}	Watts per square meter
WSOC	Water Soluble organic carbon

List of Publications

- **Bhardwaj, P.**, Singh, B. P., Pandey, A. K., Jain, V. K., & Kumar, K. (2017). *Characterization and Morphological Analysis of Summer and Wintertime PM2. 5 Aerosols over Urban-Rural Locations in Delhi-NCR.* International Journal of Applied Environmental Sciences, 12(5), 1009-1030. (ISSN 0974-0260).

- **Bhardwaj, P.**, Pandey, A. K., Kumar, K., & Jain, V. K. (2017). *Spatial variation of Aerosol Optical depth and Solar Irradiance over Delhi-NCR during Summer season.* Current World Environment, 12(2). (ISSN: 2320-8031). (In-Press)

CHAPTER – I

INTRODUCTION

Chapter 1 *Introduction*

The beginning of 19th century saw the First Industrial Revolution with advancement in urbanization which lead to an increase in the air pollution (Te Brake 1975). During that time, many scientific predictions were made regarding the role of some gases in atmosphere including that of CO_2 in blocking the infrared radiation and their role in the climate change due to change in their concentration (Spencer Weart 2015). The early decades of 20th century saw the World War I & II which further escalated the problem of air pollution. Initially the focus was mainly on the greenhouse effect of various gases in the atmosphere but gradually, with the availability of data, focus shifted towards understanding the role of other species such as tiny particles present in the atmosphere (later called aerosols) and their effects in governing the atmospheric dynamics. Great pollution episodes like Los Angeles Smog (Spencer Weart 2015) also propelled scientists to start considering the problem of air pollution seriously. Air pollution affects not only the human population but the whole ecosystem directly or indirectly. One of the major implications of air pollution is its adverse impact on human health. Lelieveld et al. (2015) estimate that air pollution is responsible for 3.3 million premature deaths per year worldwide. Further, the atmospheric constituents interact with both the incoming (solar) and outgoing (terrestrial) radiation, thereby changing the radiation budget of the earth's atmosphere and hence the climate system. Thus, in addition to health concerns, the air quality also affects the visibility and climate change over a region.

1.1 Air Quality

Air quality can be understood as a measure of the health of the air we breathe. Air quality is affected by the various kinds of air pollutants that are injected into the atmosphere from both natural as well as anthropogenic sources. Air pollutants are the substances present in the atmosphere, which not only has adverse impact on the health of living beings but can cause either a short or in long term damage to the environment. Air pollutants may be classified based on their physical state or origin in the following ways:

1.1.1 Gaseous Pollutants and Aerosols

Based on their physical state in the atmosphere, air pollutants may be classified as gaseous i.e. which are emitted in gas-phase (e.g. CO_2, NO_2, SO_2, CH_4, CO etc.) and aerosols, which are tiny solid or liquid particles which remain suspended in the air (e.g. soot particles, dust particles, smoke, fog etc.)

1.1.2 Natural and Anthropogenic pollutants:

Air pollutants may also be classified on the basis of their origin as either natural or anthropogenic. Natural pollutants may be geogenic or biogenic in nature. Pollutants such as SO_2 and volcanic ash from volcanic eruptions, which are emitted from geological sources are known as geogenic pollutants. Similarly, substances such as isoprene, monoterpenes etc. which are emitted by vegetation or methane which is emitted due to microbial decomposition of organic matter – are examples of air pollutants that are termed as biogenic. Anthropogenic air pollutants are those which are generated as a result of the human activities. Majority of the air pollutants in the atmosphere are anthropogenic in nature. Examples include emissions of particulate matter, sulphates, nitrates and carbon monoxide among others, from sources such as industries, automobiles, thermal power plants (TPPs), agricultural waste burning, incineration units etc.

1.1.3 Primary and Secondary Pollutants

Air pollutants can further be classified as primary pollutants if they are directly introduced in the atmosphere from their respective sources, for e.g., carbon monoxide (CO), sulfur dioxide (SO_2), nitrogen oxide (NO), nitrogen dioxide (NO_2) and particulate matter besides several other substances released directly into the atmosphere. In contrast, air pollutants are termed as secondary pollutants if they are formed in the atmosphere as a result of various chemical reactions among the primary pollutants and other atmospheric constituents. Most important examples of secondary pollutants include pollutants such as tropospheric ozone (O_3), Peroxyacyl nitrates (PAN) and sulphur trioxide (SO_3).

Different air pollutants may have different effects on the human health. Exposure to NO_2 for long duration can cause severe respiratory illnesses especially in children (Hasselblad et al. 1992; Gauderman et al. 2005). SO_2 can cause irritation of lung tissue among other respiratory problems. Carbon monoxide rapidly binds with the haemoglobin and forms a compound Carboxyhaemoglobin (COHb) which reduces the oxygen carrying ability of the blood from lungs to various parts of the body. Major symptoms of these adverse respiratory effects appear as cough, throat dryness, discomfort in the chest and headache (McGranahan and Murray 2003). Short term high levels of VOCs exposure cause irritation in eye and upper respiratory system (Wolkoff et al. 2006).

1.2 Aerosols and their significance

Based on the physical and chemical composition, experts in the various fields call aerosols by different nomenclature. Various regulatory agencies and meteorologists describe aerosols based on their size as particulate matter (PM_{10} or $PM_{2.5}$), toxicologists describes them as ultrafine, fine or coarse matter and various engineering fields refer to them as nano-particles whereas climatologists refer to them based on their chemical composition and colour such as black carbon (BC), sulphates, nitrates etc. (https://earthobservatory.nasa.gov/ Features/Aerosols/).

Aerosols are solid or liquid particles suspended in the gaseous medium. For example, dust, smoke, fog, fine droplets of perfume, pollen grains etc. As discussed above, depending upon their origin, atmospheric aerosols can be both natural and anthropogenic such as wind-blown dust, volcanic emissions, sea salt sprays, grassland/forest fires, pollen, particles originating from various anthropogenic combustion processes such as burning of fossil fuels, incineration plants etc. (Harrison et al 1997; McGranahan and Murray 2003). Aerosols can further be characterized as Primary and Secondary aerosols. The particles which are directly introduced in the gas/atmosphere are termed as primary aerosols e.g. particles from construction sites, vehicular emissions, forest fires, volcanic emissions, sea sprays, re-suspended road dust etc. Particles formed by the various chemical reactions in the atmosphere such as either by gas to particle conversion, reactions among same particles or different particles, interactions of gas-liquid-solid in atmosphere or coagulation are termed as secondary aerosols (Sienfeld and

Pandis 2006). On the basis of aerodynamic diameters the PM is further divided in PM_{10} (particles having size < 10 μm), $PM_{2.5}$ (particles having size < 2.5 μm) and PM_1 (particles having size < 1 μm).

1.2.1 Health effects of aerosols:

Depending upon their sizes and hence deposition, aerosols affect the human health differently. PM_{10} is considered to be inhalable as it generally settles into nasal tract and throat only whereas fine particles of diameter less than 1μg/m^3 are considered to be respirable as they reach the innermost part of the lungs whereas $PM_{2.5}$ aerosols settle somewhere in-between. According to WHO (2016) report, exposure to particulate matter increases the risk of acute respiratory diseases especially in the children under the age of 5 years and chronic respiratory illness such as asthma, heart diseases, stroke and lung cancer in adults. Yadav et al. (2003) conducted a study on the health effects of haze episode of 1998 in Brunei Darussalam and showed increased correlation between PM_{10} and the number of cases reporting respiratory diseases such as bronchitis, asthma and other acute respiratory infections at high PM_{10} levels. However, recent studies show that the finer particulate matter ($PM_{2.5}$) causes a stronger and more consistent adverse health effects than coarser particles (Apte et al. 2015). It is reported that $PM_{2.5}$ long-term exposure is associated with an increase in the cardiopulmonary mortality by 6 – 13% per 10 μg/m^3 of $PM_{2.5}$ (Pope 2002; Beelen 2008; Apte et al. 2015). Chronic obstructive pulmonary disease (COPD) and lung cancer are diseases associated with PM pollution (Lelieveld et al. 2015). The PM along with other pollutants such as Sulphur Dioxide (SO_2), Nitrogen Dioxide (NO_2), Carbon Monoxide (CO) and Ozone (O_3), particulate matter (PM) and Lead (Pb) play an important role in defining the air quality of a region. Together these pollutants are referred to as Criterion Pollutants based on the Clean Air Act of United States of America (https://www.epa.gov/criteria-air-pollutants/naaqs-table).

1.2.2 Aerosols and the earth-atmospheric system

Aerosols are not only important for governing the air quality of a region and hence the health of a general population, but they actively interact with the incoming and outgoing radiations and influence local, regional and global climate systems either indirectly or directly. Since

aerosols' optical properties vary greatly with their composition, there is a great deal of uncertainty about their over-all role in the climate system. One of the important aspects studied worldwide in this regard is the amount of carbon (elemental or black and organic) present in the aerosols which greatly affects the radiative interactions of aerosols with both the shortwave and long wave radiations. Aerosols can scatter/absorb the incoming solar radiation, depending upon their physico-chemical properties, which is known as the direct effect. Aerosols tend to reduce the incoming solar radiation by scattering thereby causing a "cooling effect" whereas a "warming effect" is observed by the absorption of the incoming radiation by them (Bergstrom et al. 2002). Atmospheric aerosols are a mixture of both the scattering and absorbing aerosols and their interaction with the radiation play a major role in the radiation budget of the earth along with the surface and cloud properties. Aerosols are vital for cloud formation, known as the indirect effect, because a subset of them serves as cloud condensation nuclei (CCN) and ice nuclei (IN) (Kaufmann et al. 2002). Absorbing aerosols have the potential to modify cloud properties by heating the air surrounding them which stabilizes the atmosphere and diminishes the convection and thus the potential for cloud formation. They also increase the atmospheric temperature, which reduces the relative humidity, inhibits cloud formation and enhance the evaporation of existing clouds. This is collectively termed as semi-direct aerosol effect. The net effect is uncertain and highly dependent on vertical profile of BC. In addition, BC and other absorbing aerosols deposited on snow or ice surfaces may reduce the surface albedo, leading to reduced reflectance of solar radiation, and hence a heating effect (Myhre et. al., 2013).

One of the most important reasons of studying the aerosol properties other than health hazards is their effect on the visibility over a region. Visibility is the measure of how clear the atmosphere is. The high level of anthropogenic aerosols especially during the winter months greatly affects the visibility of the region which badly hits the transport sector both (air and ground), safety of the public, business and tourism (Malm et al. 1994; Singh and Dey, 2012).

Haziness of the sky, as a result of anthropogenic aerosols, further plays an important role in the solar irradiance attenuation (Ramanathan et al. 2001). Aerosols (e.g. Black carbon and sulphur dioxide) also play a major in the global "dimming" which is the reduction in the

amount of sunlight reaching the earth's surface (Streets et al. 2006). Higher the concentration of the aerosols, higher will be the attenuation of the incoming solar radiation (Streets et al. 2006). Scientists observed dimming through the 1960s-1980s as a result of increasing anthropogenic aerosols but during the period of 1980s-2000s a global increase in the solar radiation (or "brightening") was observed which might be attributed to the reduction in the aerosols because of stringent regulatory laws in various places around the world (Pinker et al. 2005; Wild et al 2005) which may have widespread effect on various processes in the earth's system. As solar radiation is one of the major driving forces of various earth and life processes, understanding the role of the aerosols interactions with the incoming solar radiation is very important for various scientific, academic and industrial applications.

Another important aspect of studying the light attenuation processes by aerosols is their effect on the crop productivity. Aerosols may affect the crop productivity by reducing the amount of solar radiation (Chameides et al. 1999 ; Cohan et al 2002; Greenwald et al. 2006) but some cases report that photosynthesis may increase slightly with the decrease in solar radiation as, in turn, diffuse component of solar radiation will increase. Diffuse radiation can penetrate the canopy of the trees thereby reaching the deeper parts of vegetation (Pinker et al. 2005). Also, the deposition of aerosols in soils due to precipitation may change the soil geochemistry and hence, may affect the vegetation and crops growing in that region (Grantz et al. 2003 ; Soriano et al. 2012).

1.3 Physical and Chemical Properties of Aerosols

Particle shape, size and chemical composition are three important properties of the aerososl which significantly affect their interaction with the incident radiation. Aerosol particles are normally non-spherical or irregular in shape except the water droplets or the hygroscopic particles which by absorption of the moisture become spherical. However, particles are often assumed to be spheres for convenience to use the equivalent diameter. Particles formed as result of attrition are generally non-spherical particles such as dust. Other examples for non-spherical particles include asbestos fibres and chain-like agglomerates, dust particles etc. whereas spherical particles include droplets, fly ash particles, inorganic salt particles (crystals) etc.

The imaging techniques like Scanning Electron Microscopy (SEM) or Transmission Electron Microscopy (TEM) are some of the most useful and powerful techniques to gain an insight into the morphological properties of aerosols (Paoletti et al. 1999; Casuccio et al. 2004). These techniques have been used both nationally and internationally to study the physical and chemical properties of the $PM_{2.5}$ aerosols (Tasic et al. 2006; Rodriguez et al. 2009; Pipal et al. 2011; Tiwari et al. 2015). The shape of the particles play a significant role in the light scattering properties of the aerosols (Buseck et al. 2000) and varies from region to region and sometimes seasonally as well causing a change in the aerosols optical properties like Single Scattering Albedo (SSA), Extinction Efficiency (Q_{ext}) and Asymmetry parameter (g) (Mishra et al. 2015).

Since the shape of the particles is highly variable, therefore, in order to measure their size conventional methods are not used. One of the most widely used methods to estimate aerosol size is based on measuring the Aerodynamic Diameter (AD). It is defined as the diameter of a sphere with unit density having the same aerodynamic property as the particle under study (Reist 1984). Particles of any size and density will have same aerodynamic diameter if their settling velocity is same. There may be other methods like Martin's -, Feret's - and Stokes diameter. The particle size is defined either by the geometrical considerations or the aerodynamic property of the aerosols. Size of the atmospheric aerosols is typically in the range between 0.001-100 μm. Depending upon their size, aerosols are further classified into coarse (AD > 1 μm) and fine (AD<1μm) size modes. Fine mode aerosols are further classified into various size ranges (Janhall et al. 2010) as per the scheme given in the Table 1.1

Table 1.1: Different size categories of aerosols.

Mode	Diameter (d)	Examples
Coarse	>1 μm	Dust, seas spray, pollens
Fine	<1 μm	Soot, NO_x, SO_x
Accumulation	100-1000nm	Particles from combustion processes, Secondary aerosols
Ultrafine	<100nm	Particles from combustion processes, Secondary aerosols
Aitken	10-100nm	Particles from combustion processes, Secondary aerosols
Nucleation	1-10nm	Particles from combustion processes, Secondary aerosols

Size of the aerosols has a great effect on the lifetime and their physico-chemical properties making it imperative to understand their size distribution. Out of all the other distributions, the Power-Law (or Junge) and log-normal size distributions of aerosols are of the utmost importance in the atmospheric sciences (Sienfeld and Pandis 2006). However, here only the log-normal distribution is discussed briefly. Log-normal distribution tends to spread out the smaller size ranges and compress the larger ones (Reist 1984). The log-normal distribution is defined by the *geometric mean diameter* (d_g or μ_g) and *geometric standard deviation* (σ_g).

The concentration and chemical composition of the aerosols in the air of a region/country is a major concern for human health and well-being. Various studies have been conducted to analyze the concentration of the aerosols around the world (Chow et al. 2004, Hueglin et al. 2005; Khan et al. 2010; Yang et al. 2012). The chemical composition of aerosols is strongly influenced by their formation and post-formation processes as well as the geographical location. The fine mode aerosols are often rich in toxic metals like Cu, Zn, Ni, Pb, As etc. and are anthropogenic in nature (Hueglin et al. 2005, Hays et al. 2011; Patil et al. 2013). Large particles (AD > 2.5 μm) come from mineral ores constituting mineral dust and from desert regions such as Thar Desert in India, African Saharan Desert or China (Pandithurai et al. 2008).

The aerosols can be further classified into the carbonaceous and non-carbonaceous aerosols. The non-carbonaceous aerosols include inorganic pollutants such as ammonium ion, sulphates (SO_x), nitrates (NO_x), aluminosilicates from mineral dust (K^+ or Al^+) etc. from both the natural and anthropogenic sources. According to Sienfeld and Pandis (2006), the carbonaceous aerosols include the organic matter (OM) and elemental (EC) or black carbon (BC). However, there is still no universal definition of EC and BC even after an extensive research in the field of aerosols and soot. The differences between EC and BC have been made on the basis of thermal and optical measurement techniques. Even though in some cases these techniques largely agree with each other but mostly a deviation of 100% or more in results has been found (Poschl 2005).

OM is generally given as the factor (a) multiplied by organic carbon (OC). The OM is a complex mixture of many compounds, like volatile organic carbons (VOCs), water soluble

organic carbons (WSOCs), polycyclic aromatic hydrocarbons (PAHs) etc., as it can be either directly emitted from the emission sources or produced from chemical reactions among various constituents of the atmosphere. These complex compounds pose a serious health threat which makes it highly important to study the organic matter. However, elemental carbon is primary in nature as it is produced by the combustion sources only. The EC or BC has a graphite-like structure (Castro et al. 1999). Also, the graphitic carbon particles are the most abundant light-absorbing aerosol species in the atmosphere. Primary BC and OC containing aerosols are generally smaller than 1 micrometer (Myhre et al. 2013).

1.4 Urban and Rural Differences

The concentration of the pollutants in the rural areas is expected to be lower than that observed in the urban areas as the number of pollution sources are less than those present in the urban areas. The particles shape and size, however, may differ on the basis of their formation in the rural areas. The sources in the rural areas generally include the wind-blown dust, seasonal biomass burning, automobiles emissions, woods and coal usage for cooking purposes, the transport of pollutants by air, smoke from brick kilns situated in the agricultural fields at some places etc. Whereas urban areas are dominated by the numerous anthropogenic sources, which generally lies in the fine mode fractions, such as emissions from vehicles, industries, thermal power plants, waste burning plants, wind-blown/re-suspended roadside dust etc. all the year round.

The increasing pollution has a tremendous effect on the air quality and in the long run may affect the climate of a region as well as is discussed above. However, various studies on the air pollutants including particulate matter have been conducted worldwide but they have mostly focused on the indoor air pollution in urban and rural areas (Chengappa et al. 2007; Colbeck et al. 2010; Joon et al. 2011; Mukhopadhyaya et al. 2012). Few studies have reported on the health effects of the PM in the rural areas (Lelieveld et al. 2015; Kumar et al. 2014). Even though various studies have been carried out over the urban and rural regions throughout the world they have mostly focused on the chemical composition of the aerosols such as Castro et al. 1999; Putaud et al. 2004 &2010; Liu et al. 2005; Viana et al. 2008; Aldabe et al. 2011; Pachauri et al. 2013; Shubhankar and Ambade 2016 to name a few.

However, the effects of aerosols on the solar irradiance at the urban and rural surroundings have not been studied as extensively. A few studies such as those by Elminir et al. 2007; Codato et al. 2008 have reported the urban-rural variation of solar irradiance due to PM. As the distinction between the urban and rural areas especially in the developing world is fast diminishing, the change in the micro-climatology of the region will also be evident.

1.5 Aerosols –Solar radiation Interaction

The interaction of the aerosols with the incident solar radiation is studied with the help of various parameters such as the aerosol optical depth (AOD), Single Scattering Albedo (SSA), Angstrom Exponent (AE). These are called the optical properties of aerosols. AOD is the measurement of radiation extinction by aerosols. It gives a value of how much solar radiation gets attenuated before reaching the ground surface and is a dimensionless quantity measured by the vertical column of aerosol load in atmosphere.

Wavelength dependence of aerosol optical depth is given by (Liou 2002),

$$\frac{\tau\lambda}{\tau\lambda 0} = \left(\frac{\lambda}{\lambda 0}\right)^{-\alpha}$$

Where τ_λ is the optical thickness at wavelength λ, $\tau_{\lambda 0}$ is the optical thickness at the wavelength λ_0 and α is Angstrom exponent.

Angstrom Exponent (AE or α) is related with the size distribution of the aerosols and is related with the wavelenth and AOD by the above formula (equation 5). Smaller the particle size, larger will be the exponent. In general, if according to Gadhavi and Jayaraman, 2010:

$AE < 1$ or $AE \approx 0$ (Coarse mode particles)

$AE > 1$ (Fine mode particles)

For coarse mode particles, α could be around 0 as well. For small spherical particles coming from single sources like soot, α could be 1.

Single Scattering Albedo (SSA): It is the ratio of the scattering efficiency by the particles to the total extinction upon impingement of radiation (Iqbal 1980). If the ratio is unity then it

implies that total extinction is solely due to scattering by the aerosols but if the ratio is zero then extinction is due to the absorption processes.

Surface Albedo is defined as the ratio of the amount of the incident to radiant energy reflected back or scattered by the aerosols. It is a dimensionless quantity, usually representing the amount of light reflected from the earth into the space.

The amount of the sunlight reaching the surface of the earth depends upon various factors such as latitude, solar zenith angle and seasons. The incoming solar radiation/insolation is further divided in Global, Direct and Diffuse components. According to Iqbal (1980), Global radiation refers to the total of diffuse, direct and reflected radiation. Direct radiation or "beam" radiation is the measured radiation which is directly coming from the solar disk by blocking all the other radiations. Direct beam travels in straight line path. Diffuse radiation, is the radiation that reaches the surface of the earth after being scattered by the atmospheric constituents such as gases, molecules and aerosols. Diffuse radiation has no specific direction. It travels in all the directions after scattering.

The major purpose of studying the aerosols properties both physical and chemical is the kind of "forcing" they introduce at the surface, top of the atmosphere (TOA) and in the atmosphere. Among other processes, the interaction of the aerosols with the radiation, both incoming and outgoing, is of utmost importance as it governs the amount of heat added/removed by the aerosols from the atmosphere. This removal/addition of the heat from the atmosphere plays a profound role in governing the weather patterns and hence the climatology of a region (Xu 2001; Meehl et al. 2007). Radiative forcing, in general, is the radiative effects as a consequence of the increasing concentrations of the atmospheric pollutants - greenhouse gases or aerosols (Kaufmann et al. 2002). RF basically gives the net change in the incoming solar and outgoing thermal energy absorbed as well as emitted by the earth's system and hence is vital for the climate change.

1.6 Literature Review

The quality of air gets affected by aerosols, from various sources, either directly or indirectly via chemical reactions that form secondary pollutants. Aerosols produced as a result of the anthropogenic activities are estimated to contribute significantly to the climate change in the future (Chung et. al. 2002). Extensive studies have been carried out on monitoring, source apportionment and characterization (Chow et al. 2004; Putaud et al. 2004 & 2010; Hueglin et al. 2005; Liu et al. 2005; Larson et al. 2012; Li et al. 2014) of the aerosols with a view to study their likely impact on the air quality of a region and human health (Balakrishanan et al. 2002; Slezakova et al. 2011; Lelieveld et al. 2015; Apte et al. 2015). However, in recent times, the radiative properties of the aerosols and their role in visibility and climate change (both regional and global) have attracted a great deal of attention of the scientific community (DeLuisi et al. 1976; Malm et al.1994; Jacobson 2001; Meloni et al. 2005; Sarangi et al. 2016). Brief details of the research carried out at both international and national levels are given below:

1.6.1 International

Bergstrom (1967) discussed the effects of size distribution and chemical composition on the spectral absorption and extinction coefficients of aerosols mixture containing variable mixture of non-absorbing (quartz), absorbing (carbon) and metallic particles (Nickel). Their study report that for a given aerosol load and size distribution, the influence of chemical composition on the extinction coefficient varies with the part of solar spectrum under study. It was observed that carbon particles produce wavelength independent spectral absorption coefficient whereas metallic particles have negligible influence owing to their low concentrations in urban atmospheres. They also report that absorption coefficient decreases with wavelength on account of constant refractive index.

Quenzel (1970) determined the extinction coefficient in a vertical atmospheric column using solar irradiance measurements as well as size distributions using Mie calculations over Atlantic Ocean. The study reported the finding of a log-normal distribution (which

superimposed the power-law distribution) with maximum concentration of particles around 0.4μm radius.

Unsworth and Monteith (1972) measured the solar radiation (total and diffuse fluxes) in Sutton Bonington (English Midlands) and Scotland using a pyrheliometer. They calculated the aerosols attenuation coefficient (τ_a) for maritime ($\tau_a = 0.05 – 0.15$) and continental ($\tau_a = 0.1 – 0.5$) air. They reported a decrease in the τ_a for tropical maritime air from sea level to a height of 1340m.

DeLuisi et al. (1976) studied various optical properties of the aerosols in 11 field experiments involving surface based and aircraft measurements in Blythe California (desert) and Big Spring, Texas (agricultural land). They measured vertical distributions of aerosol concentrations, size distributions, optical depths and radiation fluxes to determine the radiation absorption and refractive indices. Aerosol concentration was found to be variable indicating the transport of aerosols in both the vertical and horizontal directions. A satisfactory agreement was observed between the spectral extinction and transmission measurements of direct solar beam measurements. From the measured aerosol properties, they concluded that mean aerosol size distribution in their study can be represented by Junge distribution with slope = 2.

Tanre et al. (1988) attempted to validate the satellite data using the derived optical properties of the desert aerosols from ground based solar radiation measurements for the period of April to May 1986 at Senegal. The study observed the dependence of aerosol characteristics on the background and dust storms conditions of the dust. The aerosol optical depth was observed to be highly variable and strong enough to be measured by satellites for the monitoring of desert aerosols. They also observed that a persistent desert background component may have an effect on solar radiation budget.

Nakajima et al. (1986) carried out measurements for the direct and diffuse solar radiations as well as aerosols over Sendai, Japan using various instruments. They concluded that the bimodal volume spectra of aerosols to be the best to describe the observed data. They found that the three estimated refractive indices were consistent with each other and suggested that

inversion-library method may give better results for determining the aerosol refractive index. They also calculated absorption index using the diffuse to global ratio. Their study found higher absorption index at the study area which was attributed to the presence of high elemental carbon in the atmosphere.

Lam et al. (1996) studied the global, direct and diffuse components of the solar radiance at City University, Hongkong for the period of 1991-1994. They reviewed the correlation of clearness index (K_t) with the diffuse coefficient (K_d), the diffuse fraction (K), and the direct normal (I_{dn}). They also proposed a hybrid model for calculating the diffuse and direct solar radiances from measured global solar radiances. Their model was reported to perform better than other existing models. Their study signifies that missing data of diffuse and direct solar radiations can be generated using their technique.

Meywerk and Ramanathan (1999) measured the spectral global and direct solar irradiance over the Indian Ocean in the months of February and March, 1998. They reported a decrease in optical depth (500 nm) from northern Arabian Sea to south of the Intertropical Convergence Zone. They also observed a remarkable shift in the wavelength of maximum intensity (~460 nm to 580 nm) in the direct component of the irradiance.

Roderick (1999) used the daily and monthly global and diffuse radiation measured over Australia and Antarctica for the period 1975-1991 to calculate correlations between diffuse fraction (R_d/R_s) and clearness index (R_s/R_o) where R_o is the extra-terrestrial solar irradiance. Daily irradiance data and a derived set of parameters were found to be in good correlation (typical R^2 =0.90). They also developed an empirical model to estimate the monthly average daily diffuse radiation.

Jacobson (2001) studied the forcing due to black carbon (BC) by simulating various chemical compositions of aerosols. The study reported that the mixing state and direct forcing due to the black carbon approaches that of the internally mixed BC on account of coagulation and coatings of other aerosols implying a higher positive forcing (warming) by BC which may balance the cooling by other constituents of anthropogenic aerosols. He also reported that the

radiative forcing due to the BC exceeds that due to methane (CH_4) in magnitude and that BC may be the second most global warming component after CO_2.

Chow et al. (2004) carried out observations for $PM_{2.5}$ and PM_{10} to identify and chemically characterize various sources in Texas and northern Mexico during the period of July 1999 to October 1999. They reported a high elemental concentration of Ca, Se and Antimony in geological dust, coal-based power stations and oil refinery catalytic cracker emissions respectively during this period. The study also reported that the thermally evolved fractions of organic and elemental carbon varied with the combustion sources.

Hueglin et. al. (2005) chemically characterised $PM_{2.5}$, PM_{10} and the coarse PM particles from urban, rural and kerbside in Switzerland during a time period from April 1998 to March 1999. Their study focused on variation of elemental concentration among different types of sites. Their study reported that the road traffic was the major contributor of trace elements like Ba, Ca, Cu, Fe, Mo, Mn, Pb etc. whereas long range transport accounted for Al, As, Cd, K etc. at these sites.

Meloni et al. (2005) calculated radiative forcing (RF) using radiative transfer model of Saharan dust at a Mediterranean site. Their study examined the dependence of RF on solar zenith angle, single scattering albedo and aerosol absorption. They concluded that the aerosol radiative forcing was weakly dependent on vertical profile of aerosol, whereas a strong dependence for absorbing particles is observed at the top of atmosphere (TOA).

Tasic et al. (2006) tried to identify the sources of PM_{10} and $PM_{2.5}$ based on their physico-chemical properties (shape, size, morphology and chemical composition) in Belgrade for the period of 2002-2004 using Scanning Electron Microscopy (SEM) and Energy Dispersive X-Rays (EDX). Morhological and chemical anlysis identified the soil and road dust, emissions from traffic, and fossil fuel combustion as the major sources of particulate matter at the study site.

Kaskaoutis et al. (2007) investigated the effect of atmospheric turbidity and solar zenith angle (SZA) on the diffuse-to-direct-beam ratio ($E_{d\lambda}/E_{b\lambda}$) under different atmospheric turbidity conditions (same SZA) and different SZAs (same atmospheric turbidity) at Athens in

September 2002 using a spectroradiometer. A rapid exponential decrease of the diffuse-to-direct-beam ratio with wavelength ($E_{d\lambda}/E_{b\lambda}=a\lambda^{-b}$) was reported. The spectral dependence of the $E_{d\lambda}/E_{b\lambda}$ revealed a significant departure from the linearity and single scattering albedo, size distribution and SZA were found to be responsible for this departure. The $E_{d\lambda}/E_{b\lambda}$ ratio was found to exhibit a strong wavelength and aerosol-loading dependence.

Duan et al. (2007) studied the carbonaceous content (EC and OC) of $PM_{2.5}$ at Guangzhou and Hong Kong in PRDR, China. They reported the highest OC and EC concentrations in urban Guangzhou followed by urban Hong Kong and Hong Kong background site. Contribution of TCA to $PM_{2.5}$ was reported highest in urban Hong Kong (43–57%) than urban Guangzhou (32–35%) suggesting the dominance of transportation sources in Hong Kong and industrial sources in Guangzhou.

Husain et al. (2007) measured concentrations of BC and EC from 22 November 2005 –31 January 2006 at Lahore, Pakistan, by an Aethalometer and thermal optical method. The city was reportedly heavily polluted with fine PM. About 69% of the $PM_{2.5}$ mass came from carbonaceous aerosols. A high correlation ($r^2 = 0.71$) between BC and EC concentration was found.

Meng et al. (2007) examined the $PM_{2.5}$ and carbonaceous species in Taiyuan, China. This study showed high level of $PM_{2.5}$ and its carbonaceous species in winter indicating the coal combustion as a major OC and EC source. They reported strong positive correlations between $PM_{2.5}$ and OC, OC/EC ratio and relative humidity and negative correlations in winter between $PM_{2.5}$ and OC, OC/ EC ratio, wind speed and precipitation.

Alpert and Kishcha (2008) studied solar dimming effect using the Gridded Population of the World version 3 (GPWv3) database of population density as a proxy for anthropogenic activities. They found that solar radiation received by the urban areas was less as compared to the rural areas.

Campa et al. (2009) carried out the carbonaceous and chemical characterization studies for particulate matter (PM_{10}, $PM_{2.5}$) at an urban and rural area in SW Spain during June 2005 and June 2006. The mean OC concentration was reported to be higher in the urban region

compared to the rural due to local emissions (e.g. traffic). The rural site reported a total of 82% of TC as OC whereas the urban background station revealed 70% and 73% of TC in the PM_{10} and $PM_{2.5}$ mass, respectively.

Feng et al. (2009) investigated seasonal characteristics of $PM_{2.5}$ and carbonaceous species at two sites at Shanghai, China. Annually, average $PM_{2.5}$ concentration at these sites indicated a severe pollution threat whereas seasonally, the highest average levels of $PM_{2.5}$ and carbonaceous content were observed during fall were higher by a factor of 2 than in summer. They reported a strong OC and EC correlation ($r = 0.79 – 0.93$) suggesting the contributions from common sources and similar atmospheric process taking place during each season.

Kaskaoutis et al. (2009) investigated the clear sky daily variation of the solar radiation components (diffuse, global and direct-beam) in addition to their ratios (diffuse-to-global, DGR, and diffuse-to-direct-beam, DDR) under different atmospheric conditions. They also discussed the significant effect of solar zenith angle (SZA) on both the ratios at the shorter wavelengths. They reported that only DDR can be used as a measurement technique to calculate atmospheric turbidity at longer wavelengths.

Safaripour et al. (2011) compared the measured data for the average monthly global and diffuse irradiation with the results from the existing linear models using seven relevant parameters in Kerman, Iran. The measured results were in agreement with the model results and could be used to predict irradiation data in various parts of Iran.

Blackburn and Vignola (2012) measured the global horizontal and diffuse irradiance solar spectral irradiance for solar zenith angles of 53.5º to 86.3º during the months of January, February, and March in Eugene, Oregon between 31 January 2012 and 8 March 2012. They compared the measurements of a spectroradiometer and a pyranometer for clear and cloudy days. They observed similarity in spectral distribution for global horizontal irradiance for both clear and cloudy days and concluded that diffuse horizontal component was majorly affected during the said periods.

Yin et al. (2012) studied the seasonal variation in $PM_{2.5}$ concentration and its chemical composition (Organic carbon (OC), Elemental carbon (EC), water soluble inorganic ions

(WSIIs), and various elements) during the haze period in Yong'an, China from 2007 to 2008. No significant seasonal variation in the PM2.5 mass concentration was observed. Presence of crustal elements during spring and secondary inorganic ions during the autumn and winter seasons in PM2.5 indicated the dominance of dust in spring and anthropogenic emission sources (coal combustion and vehicles) during autumn and winter seasons.

Huang et al. (2013) observed the local aerosol properties affected by regionally transported pollutants in urban Shanghai for three days in October 2011. The sampling period was divided into three periods. Period 1 reported fresh aerosols and negative variation of SSA with elemental carbon indicating the dominance of local sources. Period 2 was characterized by the aged aerosols, high amount of secondary ions (nitrate, sulphate and ammonium), the highest loading of PM mass and lowest acidity of particles. Period 3 reported an event of new particle formation and low PM1/PM10 ratio. They also studied the effect of pollutants on the aerosol optical properties and found that particle mixing state greatly influences the extinction efficiency of particulate matter.

Bilbao et al. (2014) studied interactions of the global, diffuse, direct and erythemal ultraviolet (UVER) solar irradiance as function of solar zenith angle (SZA) with atmospheric constituents such as ozone, scattering by gases, and aerosols in Malta, Mediterranean sea from May to October 2012. Ozone and Rayleigh scattering were found to be the main factors affecting the behavior of UVER variations with SZA. However, aerosols were reported to be the dominant factors affecting the global and diffuse irradiance.

Li et al. (2014) determined the effect of residual biomass burning to $PM_{2.5}$ in the harvesting period of June 2013 in eastern China using a positive matrix factorization model. They reported the average concentrations of $PM_{2.5}$ and its constituents (organics, EC, K and Cl^-). The sampling period was studied in the pre-local burning phase (Phase 1), the local-burning phase (Phase 2) and the post-local-burning phase (Phase 3). Phase 2 reported a very high concentration of $PM_{2.5}$ and its constituents than those in Phases 1 and 3 resulting in severe health concerns.

Gharibzadeh et al. (2017) studied the raditive effects and various aerosol optical properties during two dust storm events in the year 2013 using ground based Aerosol RObotic NETwork (AERONET) over Zanjan, Iran. They observed the dominance of coarse mode particles during the study period. They also simulated the solar irradiance during the study period using Santa Barbara DISORT Atmospheric radiative Transfer (SBDART) model over the surface, TOA, and in the atmosphere and observed the cooling effect due to dust particles at the earth's surface. A good correlation between the AERONET and SBDART results was observed.

1.6.2 National

The deteriorating air quality in megacities and surrounding rural areas has become a matter of concern in India. Because of their impact on human health and regional climate, monitoring of aerosols and their properties have drawn the attention of a large number of workers in the Indian context.

Srivastava and Jain (2007) used the chemical mass balance receptor model to study the coarse and fine particle sources in Delhi in different seasons in the year 2001. It was found that in fine mode particulates, vehicular emissions were the dominant source whereas, in coarse mode, other than site specific sources, contribution came largely from vehicular emissions, soil and crustal dust.

Badarinath et al. (2009) compared the urban and rural black carbon (BC) aerosol mass concentration in Hyderabad and Anantapur India for August 2006. The study period corresponds to the monsoon season over the Indian region. Higher BC mass concentrations were found over Hyderabad compared to those over Anantapur.

Behera et al. (2010) found that crustal matter, chloride, ammonium, sulfate, nitrate, organic matter and EC accounted for 64–85% of the $PM_{2.5}$ mass in Kanpur city of India. Organic matter and sulfate were found to be major $PM_{2.5}$ components in the city. The sequence for percentage of contribution of these components to $PM_{2.5}$ mass was: organic matter > sulfate > crustal matter > nitrate > ammonium > EC > chloride.

Ram et al. (2010) studied elemental carbon (EC), organic carbon (OC) and water-soluble organic carbon (WSOC) over urban, rural and high altitude areas in northern India during winter time (2004-2008). The OC/EC ratios over urban areas were found to be much higher than the rural areas and significantly lower abundances of EC and OC in the higher latitudes. However, WSOC/OC ratios were found to be constant over urban areas and higher at high altitude areas signifying the presence of secondary organic aerosols.

Sahu et al. (2011) developed an Emission Inventory (EI) for PM_{10} and $PM_{2.5}$ as part of the System of Air quality Forecasting and Research (SAFAR) project developed for air quality forecasting during the Delhi Commonwealth Games (CWG) - 2010. For this study, transport, thermal power plants, industrial, residential and commercial cooking in addition to windblown road dust was considered as major sources of pollution. The PM_{10} emission reported a major contribution from windblown dust from both paved and unpaved roads.

Srimuruganandam and Nagendra (2012) examined $PM_{2.5}$ and PM_{10} emission sources at urban roadside in the city of Chennai, India during winter, summer and monsoon seasons over a period from November 2008 to April 2009. They reported higher concentrations of ambient $PM_{2.5}$ and PM_{10} in winter and monsoon seasons as compared to those in summer. They applied Positive matrix factorization (PMF) to estimate the sources and their contribution in the concentrations of particulate matter. Study reported that major contribution to the PM10 and PM2.5 concentrations came from sources like marine aerosol, secondary particulate matter, biomass burning and other sources.

Tiwari et al. (2012) conducted simultaneous measurement for the organic carbon (OC) and elemental carbon (EC) and continuous measurements of black carbon (BC) and $PM_{2.5}$ aerosols in the winter season in the year 2010-2011 at Delhi. They reported that total carbonaceous aerosol mass contributed ~46 % to $PM_{2.5}$ mass. Also, the average OC/EC ratio (5 ± 2) suggested the presence of SOAs in Delhi's atmosphere.

Kaushar et al. (2013) studied the measurements of coarse and fine particles across the nine monitoring sites under SAFAR program during the CWG-2010 in Delhi. It was found that during the Commonwealth Games, due to pollution control policies implemented in and

around the city of Delhi, the level of coarse ($PM_{10-2.5}$) and fine ($PM_{2.5}$) particles plunged to those close by or even below their NAAQ standards. The pollution reduction measures for the Delhi's CWG-2010 (well before the Games) and washout of air pollutants by monsoonal rain till end of the September, 2010 were effective in reducing atmospheric concentrations of both coarser and fine particles.

Pachauri et al. (2013) characterized $PM_{2.5}$ and carbonaceous aerosols in Agra during Nov 2010 to Feb 2011. The average mass concentrations of TCA were observed to be greater at traffic sites followed by rural and campus site. SEM/EDX results indicated branched chain-like aggregates of carbon bearing spheres at the traffic and rural sites, while at the campus site carbon-rich and minerogenic (mineral dust) particles were the dominant ones.

Tiwari et al. (2013) for a year studied the BC and $PM_{2.5}$ at Delhi for daily, monthly and seasonal temporal scales and the meteorological influence on the concentrations of $PM_{2.5}$. The lower and higher $PM_{2.5}$ concentration was reported respectively during monsoon and post-monsoon. Correlation analysis between BC and meteorological parameters (wind speed (WS), rainfall, and visibility) showed a negative correlation of BC with WS and visibility during the entire duration of study.

Pipal et al. (2014) studied the 24 hourly diurnal variation of EC and OC of $PM_{2.5}$ using the semi-continuous carbon analyser at Agra, UP during winter (2011-2012). They reported the high concentrations of EC and OC during daytime. The vehicular activities, biomass and fossil fuel combustion were attributed to the high concentration of $PM_{2.5}$ and the carbonaceous aerosols at the site. A very strong correlation between OC, EC and $PM_{2.5}$ ($r = 0.83$-0.97) was observed for 24-h samples.

Srivastava et al. (2014) investigated the major aerosol types to understand their different characteristics over an urban station at Delhi during 2009 using a ground-based automatic sun/sky radiometer. They reported four categories of aerosol such as polluted dust (PD), polluted continent (PC), mostly black carbon (MBC) and mostly organic carbon (MOC), contributing nearly ~48%, 32%, 11% and 9%, respectively to the total aerosols. The highest and lowest atmospheric forcing was observed for PC and MBC aerosol types respectively.

Yadav et al. (2014) revealed a significant increasing trend (upto 37%) in the concentration of particulate matter in the city of Udaipur during a period of 2010 to 2012. Their study showed highly significant impact of rainfall for PM_{10} while, it is found to be less significant for $PM_{2.5}$. The impact was found to be significant during winter when the inversion layer is found to be low.

Pant et al. (2015) characterized ambient $PM_{2.5}$ samples collected at a high traffic location in the city of New Delhi, India during summer and winter 2013. Higher concentrations were found in winter when it surpassed the Indian $PM_{2.5}$ air quality standards on various occasions as compared to those in summer. Crustal material was found as the major component contributing during the summer, while wood burning, nitrates and chlorides were found as important contributors in the winter.

Singh et al. (2015) studied the effect of anthropogenic emissions and open biomass burning on carbonaceous aerosols in an urban (NPL, Delhi) and rural (Nurpur, Haryana) environment during June 2012-May 2013. OC and EC values were observed to increase from monsoon to winter season respectively. The month of November reported very high values of OC and EC as a consequence of post-harvesting agricultural residue burning. Vehicular emission accounted for OC/EC ratios in range (1–4) at the urban site whereas at the rural site (OC/EC > 4), residential wood smoke and biomass residue burning were found to be major emission sources.

Singh et al. (2015) studied the variability of aerosols characteristics over Patiala, India from December 2011 to November 2013. They observed the highest concentration of PM_{10} during summer of 2012, and those of $PM_{2.5}$ and PM_1 during autumn of 2013. The particle size distribution was found to be skewed towards particles with size < 1.00 μm. AOD_{500} was observed to be highest during summer of 2012 and autumn of 2013 whereas minimum in spring of 2013, further reflecting the different effects of aerosols on climate during different seasons. They observed that the concentration of PM_1 affected the AOD_{500} more compared to $PM_{2.5}$ and PM_{10}.

Rastogi et al. (2016) examined temporal variability of primary and secondary aerosols over northern India during a period from October 2011 to September 2012. Their results showed that PM2.5 mass concentration varied in a range from ~20 to 400 μg/m^3. Further, their study showed dominance of biomass burning emissions over this region where the average OC/EC varied in a range from 3.2 to 12 and K+/EC ratio ranged from 0.26 to 0.80. Their study also revealed that contribution of secondary inorganic matter was maximum (~40%) in winter.

Tiwari et al. (2016) analyzed significant cooling effect on the surface due to soot particles in Guwahati, India during a period from 1st July 2013 to 30th June 2014. They reported daily concentrations of BC to be lying in the range from 2.86 to 11.56 μg/m^3 while, CO varied from 0.19 to 1.20ppm during this period. The concentration of BC and OC were found to be higher in dry period (October to March) as compared to those in wet months i.e. April to September.

The uncerainty in the role played by the aerosols has led to a number of studies that have focused their attention on the optical properties of aerosols and the estimation of radiative forcing caused by them at the regional scale in India, but majority of them are focussed on the urban areas only (Choudhary 1967; Bhattacharya et al. 1996; Singh et al. 2005; Tripathi et al. 2005; Badrinath et al. 2009). Though studies regarding the air pollution and their effect on solar radiation has been going on for quite some time in India but it has only recently gained momentum and importance especially in regard of air quality and climate change studies. A few studies in this respect have been discussed briefly below:

Latha and Badarinath (2005) investigated seasonal variation of aerosol optical properties over the urban area of Hyderabad by using sun-photometer at different wavelength. They proved that aerosol optical depth value gradually increases during dry season and falls down in monsoon season.

Singh et al. (2005) studied aerosols characteristics and their effects on surface radiation forcing over city of Delhi, India during pre-monsoon period i.e. April to June 2003. Their results found small value (~ 0.328) of average Angstrom parameter due to high concentration of total suspended particulate matter which further become negative (~ 0.06) because of high dust content during this period.

Tripathi et al. (2005) measured aerosol black carbon over Kanpur during December 2004. Their study reported the highest BC concentration especially during morning hours and daily average BC concentration to be between 6– 20 μg/m^3. They reported a decrease in short wave radiation reaching the earth's surface over North India and TOA due to black carbon. They also estimated the forcing due to BC over northern India as 62 W/m^2 and at the TOA reflected radiation to be 9 W/m^2.

Simultaneous measurements were conducted using the semi-continuous thermo-optical EC-OC analyzer (for EC & OC), and Aethalometer (for BC) by Srivastava et al. (2014) at Delhi for the duration of January 2011 to May 2012. They reported that OC, EC and BC concentrations were ~ 2 times higher in winter compared to summer. A high correlation between OC and EC indicated the common emission sources. The fossil fuel emissions were suggested as a major source of lower OC/EC ratio (range 1.0–3.6, mean 2.2±0.5) over the concerned site. On average, mass concentration of EC was found to be higher than BC by ~ 38 % in the duration of study. The significant correlation between measured absorption co-efficient (b_{abs}) with EC, suggested EC is a major absorbing species in ambient aerosols at Delhi.

Singh et al. (2015) studied the variability of aerosols characteristics over Patiala, India from December 2011 to November 2013. They observed the highest concentration of PM_{10} during summer of 2012, and those of $PM_{2.5}$ and PM_1 during autumn of 2013. The particle size distribution was found to be skewed towards particles with size < 1.00 μm. AOD_{500} was observed to be highest during summer of 2012 and autumn of 2013 whereas minimum in spring of 2013. They observed that the concentration of PM_1 affected the AOD_{500} more compared to $PM_{2.5}$ and PM_{10}.

Tyagi et al. (2017) studied the impact of BC and $PM_{2.5}$ on the planetary boundary layer (PBL) and solar fluxes over the National capital region (NCR) of Delhi during the winter months of 2014. They observed high concentration of BC and $PM_{2.5}$ during the months of December and January of the study duration. High BC concentrations during morning and evening hours were attributed to peak traffic time. Daily solar fluxes were also observed and were found to be negatively correlated with the BC in the fog events. Reduced ventilation Coefficient (VC)

from “fog” to “no-fog” indicated the high level of pollution in the NCR. The observed mean aerosol optical depth (AOD_{500} nm) was found to be highest in the foggy episodes in agreement with BC and $PM_{2.5}$ concentrations. The study reported the dominance of fine mode aerosols during the study period.

In the context of aerosol – radiation interaction, most studies in India (as mentioned above) have focused on the estimation of radiative forcing of aerosols on local or regional scale using radiative transfer models. However, very few studies in India till date, have examined the role of aerosols in the attenuation/dimming of solar radiation reaching the surface of earth utilizing the field based observational data on surface solar spectral irradiance. Padma Kumari et al. (2007) evaluated monthly mean solar radiation over 12 stations distributed over the Indian region and reported decline in solar radiation at all the stations. Badrinath et al (2010) studied the solar dimming over Hyderabad and reported that anthropogenic aerosols and cloud effect contributed considerably to the reduction in the solar radiation over the study site. in a comprehensive study over Hyderabad.

1.7 Objectives

1. To measure the concentration, shape and size of aerosols ($PM_{2.5}$) and their EC & OC content in urban and rural aerosols in Delhi-NCR.
2. To monitor the solar insolation over Delhi and rural area outside Delhi.
3. To study the relationship between urban-rural aerosol characteristics and solar insolation in Delhi-NCR region.

1.8 Significance of the study

The present study attempts to investigate the urban-rural relationship of aerosol characteristics with the solar insolation over Delhi and rural area outside Delhi. This is important as this information will provide insight into the role of aerosols in the local and regional climate over Delhi-NCR region.

CHAPTER – II

METHODOLOGY

In the present study, measurement of solar spectral irradiance along with $PM_{2.5}$ sampling were conducted at a typical urban site (Shahdara) and a rural site (Sampla) situated in north west of Delhi in the National Capital Region, at a distance of approximately 66 km from the urban site in Delhi. The two sites i.e. urban and rural were chosen for a comparative study to evaluate the impact of particulate matter in the ambient atmosphere on the solar spectral irradiance reaching the surface of earth.

2.1 Study Area

Shahdara, Delhi (28.68°N, 77.29°E) is one of the oldest and highly urbanized areas in the eastern part of Delhi, consisting of both the residential as well as industrial establishments around it. The sampling site is located near the main Loni Road which is a major arterial road connecting Delhi and Saharanpur, (Uttar Pradesh). It is one of the busiest roads experiencing heavy traffic 24 hours of the day. Loni Road comprises of many shops such as of utilities, local eateries (*dhabhas*), printing presses, mechanics shops or motor repairing workshops and businesses mainly of plywood and timber. The Shahdara Railway Station and Metro Station are located around two kilometers from the sampling site.

Sampla (28.77°N, 76.76°E) is situated in the Rohtak district of Haryana and is surrounded mainly by the vast agricultural fields and village settlements in its neighbourhood on all sides. A few factory establishments and one or two brick kilns are situated approximately 10 kms away from the sampling site. The national highway (NH-9) and Sampla railway station are located approx. 1-1.5 kms away from the sampling site. Bahadurgarh, Rohtak, Sonepat and Jhajjar are some of the prominent towns/cities of Haryana that are located within a distance of 20 - 40kms away Sampla.

The two sites fall in a semi arid climate zone experiencing different seasons during the course of a year namely, Summer (April-June), Monsoon (July-August), Post-Monsoon (September-November), winter (December- January). Summers are usually long with temperature going up to as high as 45°C during daytime (Guttikunda and Gurjar, 2012).

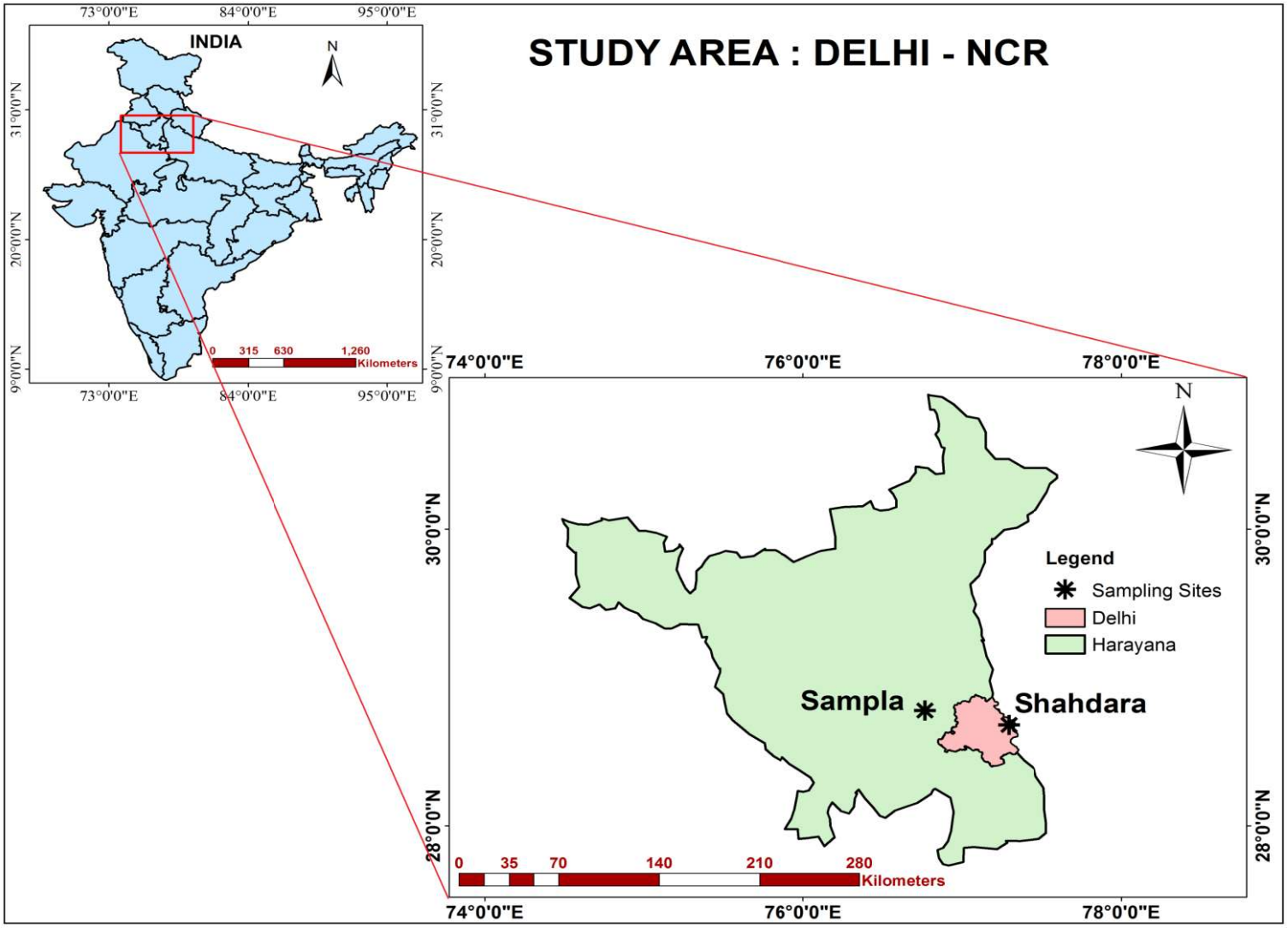

Figure 2.1. Map showing the sampling sites in Delhi-NCR.

The winters are generally cold with calm winds and temperatures going as low as 4-5°C or even less. A strong inversion layer forms over the region during the winters. The average annual rainfall in this region is approximately 670 mm. The wind direction is generally north-westerly throughout the year except during monsoon period when it is south-westerly. Sampling was carried out for summer (May-June), September to November months as Post-Monsoon (PoM) and winter (December-January) seasons for the year 2015 at the two sites. PoM has been studied as two separate cases of September-October (SO) and November (N) months. Sampling sites are shown in Figure 2.1.

2.2 Measurements of Solar Spectral Irradiance

The measurements of solar spectral irradiance (both global and direct) were made with the help of a Fieldspec spectroradiometer (Figure 2.2). The equipment measures radiation in the visible/near infrared spectrum in the wavelength range 325 – 1075 nm with a spectral resolution of 3 nm using a 512 channel silicon photodiode array detector. The equipment measures radiation in both the photon count mode and the irradiance mode and has the automatic facility of collecting dark current. The equipment comes with the attachments for making measurements of global as well as direct solar spectral irradiance. The data collected by the equipment is transferred directly to a field controller unit (computer) via a standard RS-232 serial port interface where it is visualized and recorded using the RS^3 software.

For the purpose of making measurements, the equipment was installed on the rooftops of buildings located at both the urban and rural site. The sampling sites were so chosen that they gave a nearly 180 degree (solid angle) field of view. The solar irradiance, both global and direct irradiance components, sampling was carried out under clear sky conditions between 11.00 am to 4.00 pm at a sampling interval of 15 minutes during different seasons in the year 2015. For the measurement of global irradiance, a remote cosine receptor (RCR) was attached to the spectroradiometer using an optical fiber cable. For the direct irradiance measurement, 2π field of view for measuring global irradiance was restricted using a narrow pipe whose inner surface was coated with black carbon and fitted with a 2 degree FOV disc (Figure 2.4). This narrow pipe was then pointed manually towards the solar disc and observations were carried out using the shadow technique. Prior to every measurement, the dark current was

collected and automatically subtracted from the final measurements by the software. A set of three files in ".asd" format at an interval of 1 second was recorded for both global and direct irradiance measurements respectively.

Further analysis of the collected data for both global and direct components of solar irradiance was carried out using View Spec pro software as follows:

1. The .asd files were first converted to the ".irr" format.

2. Using the statistics tool of the software, a mean file for all the files was calculated.

3. From the calculated mean file, the value of irradiances at every wavelength band was extracted.

4. Global and Direct insolation values of solar irradiance were calculated by performing the Lambda Integration in the 325-1075 nm wavelength range.

Figure 2.2. FieldSpec Spectroradiometer (ASD Inc.) used for the solar irradiance Global and Direct) measurements.

2.3 $PM_{2.5}$ Sampling

$PM_{2.5}$ sampling was carried out with the help of Airmetrics Mini-Vol® Air sampler (Figure 2.3) at a constant flow rate of 5 L/min for 24 hours a day. The sampler operates with a rechargeable lead-acid battery with a 24 hour backup. $PM_{2.5}$ sampling was carried out using Whatman quartz fibre filters (47mm) for 5-9 days each in three seasons viz. summer, post-monsoon and winter at both Shahdara and Sampla sampling sites. The sampler was mounted on a tripod stand (1.5 m high) above the rooftops of residential buildings at each sampling site throughout the study.

Filter papers were kept in desiccators with silica gel for 24 hours both pre and post-sampling. Blank filters were also treated in the same way. The air drawn by the sampler pump is made to pass through an impactor leading to collection of $PM_{2.5}$ on the quartz filter paper. After sampling, the samples were put in the aluminium foil covered petri dishes which were sealed with the plastic cover and cello tape and stored in the refrigerator till further analysis. Samples were weighed pre and post-sampling using microbalance (SARTORIUS GD603) with 0.0001mg accuracy. Samples were handled with the forceps all the time to avoid any impurities. Weight of the samples was calculated gravimetrically. A total of 56 samples were collected at both the sampling sites in the summer, post-monsoon and winter seasons.

Figure 2.3. Airmetrics Mini-Vol® Air sampler for $PM_{2.5}$ sampling.

2.4 SEM Analysis

SEM technique was used to analyze $PM_{2.5}$ samples collected from the two sites at Advanced Instrumentation Research Facility (AIRF) in Jawaharlal Nehru University (JNU), New Delhi. The SEM analysis was carried out with the help of a computer controlled scanning electron microscope SEM (Carl Zeiss EVO 40, Cambridge). Prior to the SEM analysis, the samples were mounted on aluminium stubs using double sided carbon tape for gold coating to make the samples electrically conductive. A very thin film of gold (Au) was deposited on the surface of each sample in vacuum coating unit called Gold Sputter Coater (POLARON-SC7640, UK). The samples were placed in the vacuum chamber of SEM instrument (Silicon Drift detector) at the designated positions for analysis. The SEM working conditions were set at an accelerating voltage of 20 kV, a beam current of 40–50μA. The images were recorded at different magnifications 5000x, 10000x, 15000x, 20000x with a resolution of 20 nm. Furthermore, the particles diameter or size was measured manually by randomly selecting particles which were easily and independently visible from the different SEM images using the ImageJ software and hence, particle size distribution was plotted using the MATLAB software.

2.5 OC and EC Analysis

The carbonaceous content i.e. organic carbon (OC) and elemental carbon (EC) in the $PM_{2.5}$ samples was analysed by using the Desert Research Institute (DRI) Model 2001A Thermal/Optical Analyzer. To determine the OC and EC, Thermal/ Optical Reflectance (TOR) method was selected followed by Interagency Monitoring of PROtected Visual Environments (IMPROVE-A) protocol (Chow et al. 2007). The complete analysis was carried out as follows:

The functioning of the DRI model 2001 Thermal/Optical Carbon Analyzer is based on the principle of the oxidation of organic carbon (OC) compounds and elemental carbon (EC) at different temperatures. It is based on the fact that the organic carbon oxidizes in the He-only environment at low temperatures whereas the elemental carbon oxidizes at high temperatures in the 98%He+2%O_2 atmosphere. A filter punch of 0.5cm^2 area was cut with the help of an

iron punch from the sample which was placed in the sample port of the analyzer. During the differential heating of the samples, four organic carbon fractions (OC1, OC2, OC3 and OC4 at temperatures 140°, 280°, 480° and 580°C respectively) and three fractions of elemental carbon (EC1, EC2 and EC3 at 580°, 740° and 840°C respectively) are generated. The carbon compounds, thus, evolved at different temperatures under different oxidizing atmosphere are converted to CO_2 by passing through a heated manganese dioxide (MNO_2), oxidizer for their eventual removal. This CO_2 is then passed through a methanator – hydrogen enriched nickel catalyst and is converted to methane (CH_4). These methane equivalents are then quantified with a flame ionization detector (FID). Pyrolyzed Organic Carbon (OP) fraction was quantified at 580°C right after the introduction of 98% He + 2% O_2 gas mixture by optical method when reflected laser light reaches its initial value into the analysis environment. In this regard, Quality Assurance / Quality Control procedure has been described by Cao et al. (2003).

OC, EC and TC were determined by using the following equations (Mishra and Kulshreshtha 2016):

$$OC = OC1 + OC2 + OC3 + OC4 + OP \quad (1)$$

$$EC = EC1+EC2+EC3-OP \quad (2)$$

$$TC = OC + EC \quad (3)$$

Where OC1, OC2, OC3, OC4, EC1, EC2, and EC3 are the different fractions of organic carbon and elemental carbon generated at different temperatures.

Samples were analysed in the Central Instrumentational Facility (CIF) of School of Environmental Sciences, Jawaharlal Nehru University, New Delhi. Figures 2.4 and 2.5 respectively show the image of the Thermal/Optical Analyzer installed in CIF and its schematic diagram. Blanks filters were also analyzed for the subtraction from the $PM_{2.5}$ samples OC and EC concentrations to remove the overestimation. For the blanks, OC and EC were observed to be 2.06 $\mu gC/cm^2$ and 0.63 $\mu gC/cm^2$ respectively and were subsequently subtracted from the measured $PM_{2.5}$ sample.

Figure 2.4. EC/OC Analyser (DRI) used for the analysis of Organic and Elemental carbon in $PM_{2.5}$ samples (Source: Central Instrumentation Facility (CIF), School of Environmental Sciences (SES), JNU, New Delhi).

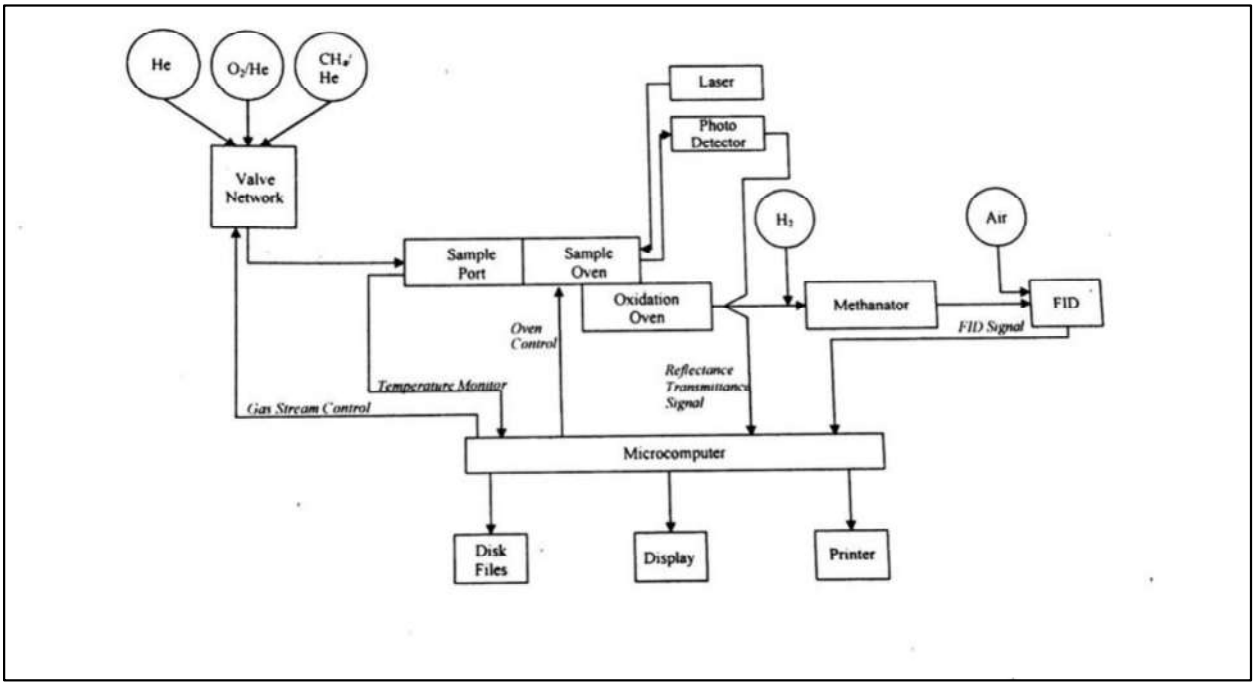

Figure 2.5 DRI Model 2001 Thermal Optical Carbon Analyzer schematic diagram. (Source: DRI Model 2001 Manual)

The equation used for the calculation of OC, EC and Secondary organic Aerosols (SOA) are as follows:

Deposition of OC or EC = Total area of deposition of $PM_{2.5}$ aerosols * (measured) OC or EC (μg C)

$$[OC] \text{ or } [EC]\ (\mu g/m^3) = \text{Deposition } (\mu g)/ \text{ Volume } (m^3)$$

$$SOC = OC_{measured} - EC*(OC/EC)_{min}$$

2.6. Data Used

CERES Data

Clouds and the Earth's Radiant Energy System (CERES) is satellite instruments developed for NASA's Earth Observing System (EOS) to understand the solar - reflected and earth emitted radiation from the top of the Earth's surface. First CERES instrument was launched with the NASA's Tropical Rainfall Measurement Mission. Now CERES instruments are onboard on the NASA's EOS satellites Terra and Aqua. It is also part of the Suomi National Polar-orbiting Partnership observatory.

The CERES 1-hourly (1º × 1º) gridded Single Scanner Footprint (SSF) datasets of fluxes at the surface (SRF) and top of the atmosphere (TOA) were used to estimate the impact of aerosol loading on the incoming and outgoing radiation fluxes. CERES's 1-hourly (1º × 1º) gridded Single Scanner Footprint (SSF) data product considers MODIS-observed cloud and aerosol properties in estimating the outgoing shortwave (SW) radiation fluxes. The fluxes are obtained from measured radiances using angular distribution models (Loeb and Kato, 2002). The CERES_SSFlevel2_Ed4A flux (SWTOA (0.3–5μm) clear-sky) and collocated MODIS-AOD products from AQUA were used for the duration of 1st April 2015 to 28th February 2016. We used linear regression between SZA normalized SW_{TOA}, $SW_{SURFACE}$ and collocated MODIS-AOD over the two regions viz. 28.5–29.0ºN and 77.0–77.5ºE centered at Shahdara, Delhi (28.6ºN, 77.29ºE) and 28.5-29.0ºN and 76.5-77.0ºE centered at Sampla, Haryana (28.77ºN, 76.76ºE) to get a statistically significant estimate of the radiative forcing efficiency due to aerosol load at the Surface and TOA. The radiative forcing efficiency studies using the

CERES datasets at the surface and TOA have previously been carried out over Indo-Gangetic Plain (Gautam et al., 2010, 2011, Sarangi et al., 2016).

The following parameters were downloaded at 50×50 km grid distance on each side from the sampling sites for the period of 1st April 2015 to 28th February 2016:

1. Time and Location (coordinates of the sites)
2. Surface parameters : Single Scattering Albedo, Atmospheric Extinction (AE), Cloud Factor
3. Surface Flux
4. Top of the Atmosphere (TOA) Flux
5. Surface Albedo
6. Aerosol Optical Depth (AOD) at 550nm from MODIS Aqua Sensor

These datasets were further resolved into 20×20 km grid and values were extracted at the interval of 0.5° in the coordinates of each sampling site (Delhi and Haryana). In order to calculate the seasonal variation of the radiative forcing, analysis duration is further divided into seasons: Pre-Monsoon (April, May, June - AMJ), Post-Monsoon (September, October, November - SON), Winter (December, January, February - DJF). The data is further segregated seasonally for both the sites in Delhi and Haryana. The expected uncertainty of MODIS-AOD is $\pm 0.05 \pm 0.15 \times$ AOD over land [*Remer et al.*, 2005].

For the forcing at the surface and TOA respectively, following datasets were chosen for each sampling sites:

(i) AOD and Surface Flux

(ii) AOD, TOA Flux and Cloud factor

For TOA flux, only days with cloud factor $\leq 10\%$ were considered.

The radiative forcing at the surface and TOA over Delhi and Haryana is calculated using the following steps:

I. The TOA and Surface fluxes variation with the AOD was observed. Only those seasons with the p-values < 0.05 were considered for the further analysis of radiative forcing.

II. Radiative forcing was calculated by two methods: slope and intercepts methods using the following equations:

For RF at the surface:

$$\mathbf{F_{\downarrow}{}^{a}_{S} = \eta_s\,(AOD_{550}) + F^{0}_{\downarrow}S} \quad \textbf{(1)}$$

$$\mathbf{\Delta F^{SW}_{S} = (F^{a}_{\downarrow S} - F^{0}_{\downarrow S}) \times (1 - SA)} \quad \textbf{(Intercept method)} \quad \textbf{(2)}$$

$$\mathbf{\Delta F^{SW}_{S} = \eta_s\,(AOD_{550})} \quad \textbf{(Slope Method)} \quad \textbf{(3)}$$

Where,

F^{a}_{S} = Mean surface flux under aerosol laden conditions/atmosphere

F^{0}_{S} = Surface flux under the clear sky conditions (intercept)

η_s = RF Efficiency (in $Wm^{-2}AOD^{-1}$) (at surface) (slope)

AOD_{550} = Aerosol Optical Depth at 550nm wavelength

ΔF^{SW}_{S} = Short wave forcing at the surface (in Wm^{-2})

SA = Mean seasonal Surface Albedo

Similarly, Short Wave radiative forcing at the TOA:

$$\mathbf{F^{a}_{\uparrow T} = \eta_T\,(AOD_{550}) + F^{0}_{\uparrow T}} \quad \textbf{(4)}$$

$$\mathbf{\Delta F^{SW}_{T} = (F^{a}_{\uparrow T} - F^{0}_{\uparrow T})} \quad \textbf{(Intercept method)} \quad \textbf{(5)}$$

$$\mathbf{\Delta F^{SW}_{T} = \eta_T\,(AOD_{550})} \quad \textbf{(Slope Method)} \quad \textbf{(6)}$$

Where,

F^{a}_{T} = Mean TOA flux under aerosol laden conditions/atmosphere

F^{0}_{T} = TOA flux under the clear sky conditions (intercept)

η_T = RF Efficiency (in $Wm^{-2}AOD^{-1}$) (at TOA) (slope)

AOD_{550} = Aerosol Optical Depth at 550nm wavelength

ΔF^{SW}_{T} = Short wave forcing at the TOA (in Wm^{-2})

SA = Mean seasonal Surface Albedo

RF in the atmosphere ($\mathbf{F^{SW}_{ATM}}$) is calculated as follows:

$$\mathbf{F^{SW}_{ATM} = F^{SW}_{T} - F^{SW}_{S}} \quad \textbf{(7)}$$

III. Error Estimation:

Following error in the fluxes, slopes and intercepts were calculated as follows:

Standard errors in mean values of surface and TOA fluxes = ε_{mean}

Standard errors in mean values of AOD = ε_{mAOD}

Error in the slope = ε_1

Error in the intercepts = ε_2

Final errors in the forcing:

Slope Method: $$\boldsymbol{\varepsilon = \sqrt{\varepsilon mAOD^2 + \varepsilon 1^2}} \quad \textbf{(8)}$$

Intercept Method: $$\boldsymbol{\varepsilon = \sqrt{\varepsilon mean^2 + \varepsilon 2^2}} \quad \textbf{(9)}$$

Meteorological data

Meteorological data for the parameters wind speed, wind direction, relative humidity (RH), precipitation for the study sites have been used from wunderground (www. wunderground.com)

2.7 Software Used

Image J

ImageJ is an open access Java image processing and analysis program inspired by NIH Image program which was developed at the Research Services Branch (RSB) of the National Institute of Mental Health (NIMH) (https://imagej.nih.gov/nih-image/about.html). *Image* can read and write, display, edit, analyze, process, save and print 8-bit, 16-bit and 32-bits images of wide variety of image formats such as TIFF, GIF, JPEG etc. Various parameters such as diameter, area, perimeter, among others can be measured using this software. It also performs automated particle analysis and provides tools for measuring path lengths and angles. Further information about the software can be obtained from - https://imagej.nih.gov

/ij/docs/intro.html. Being an open program, Java plugins can be modified by the users to solve almost any image processing or analysis problem.

ImageJ software has been used in the present study to measure the size (diameter) of the $PM_{2.5}$ particles.

ViewSpec Pro

ViewSpec™ Pro is trademark software developed by the ASD Inc. This software is used for post-processing of the spectral data which has been saved in the .asd format.

Radiometric Correction

The .asd format is converted to ".irr" format using the Radiometric Correction. Radiometric correction converts the RawDN values to radiance or irradiance using the formula:

$$L = \frac{(\text{lampfile}) \times (\text{calpanelfile}) \times (\text{inputfile}) \times (\text{calITG})}{(\text{calibrationfile}) \times (\text{inputITG}) \times \pi}$$

Where,

L	= radiance to be calculated
lampfile	= calibrated irradiance file for the lamp
calpanefile	= calibrated Spectralon® reflectance file
inputfile	= unknown, dark current corrected input file
*cal*ITG	= Integration time and/or gain of the calibration file
calibrationfile	= Dark current corrected raw data collected at ASD
*input*ITG	= Integration time and/or gain of the input file

The π in the denominator is automatically left out by the software in calculating the Irradiance measurements. The Irradiance is defined as the radiant flux per unit of area in W/m^2, whereas, Radiance (L) is defined as the radiant flux emitted from the source per unit area per unit solid angle.

Statistics

This process performs the standard statistical methods: Mean, Median and Standard Deviation on the selected spectral files. These methods distinguish the noise of each spectrometer.

Lambda Integration

The average values of the spectral data can be calculated using the Lambda Integration option from the view spec application. Lambda Integration averages or integrates wavelengths under the area as per the end limits set by the user. (Source: ViewSpec Pro Manual, www.asdi.com)

MATLAB

Matlab (Matrix Laboratory) from MathsWorks, is a high-performance, fourth generation and technical computing proprietary programming language which integrates the computation, visualization and programming all in a common environment. The in-built libraries of Matlab facilitate the signal processing, data analysis, image processing, modelling, simulations etc. Matlab has been used for the CERES satellite data processing and the particle size distribution trends.

Methodology Flowchart

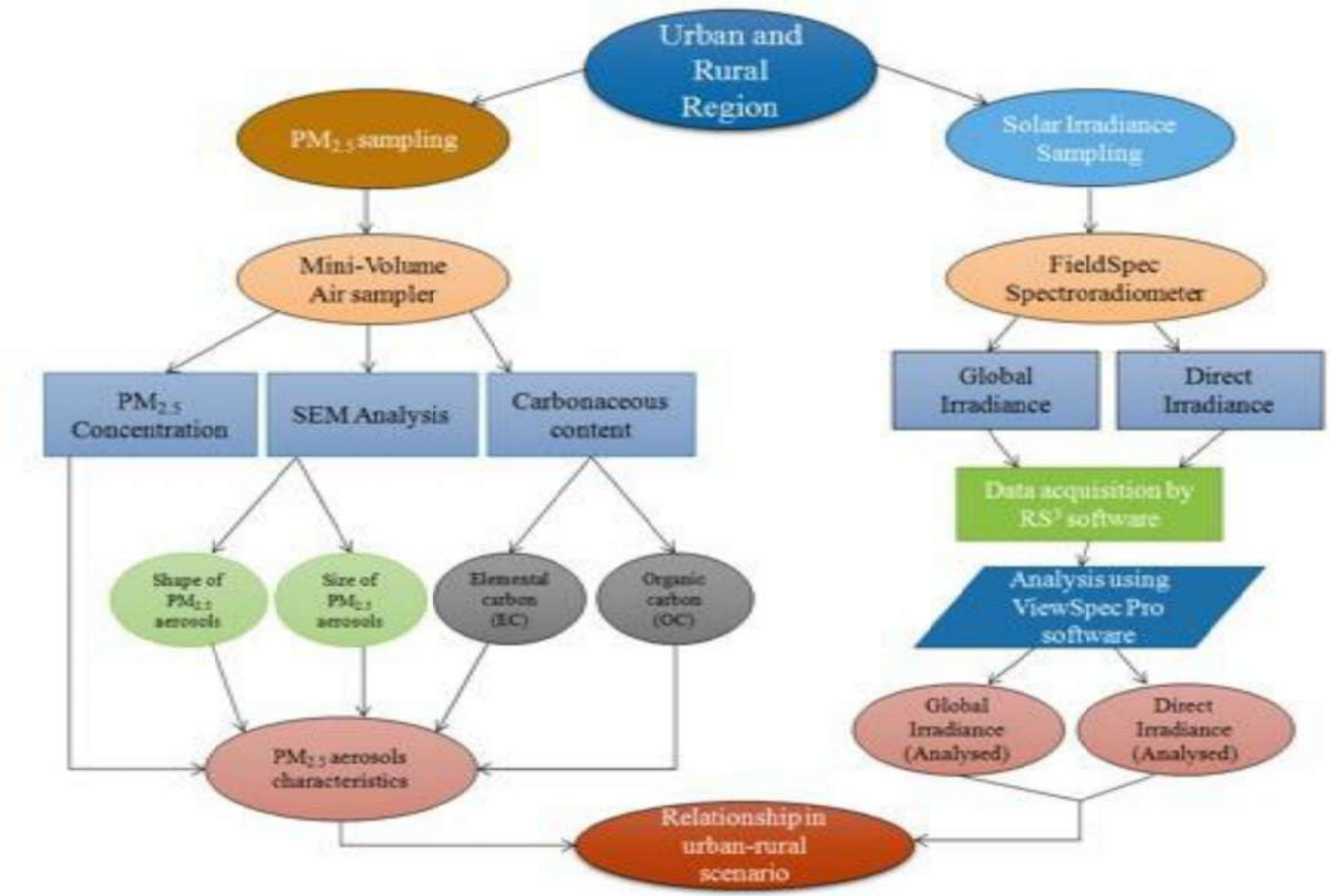

Figure 2.6 Flowchart of the Methodology.

CHAPTER – III

RESULTS AND DISCUSSION

3.1 $PM_{2.5}$ Characteristics

As $PM_{2.5}$ dominates the fine mode aerosols, it's monitoring on local and regional scale is very important for the air quality assessment and human health studies. In order to gain an insight into various properties of $PM_{2.5}$ aerosols such as concentration, shape, size and carbonaceous (elemental and organic) content, $PM_{2.5}$ aerosol sampling was carried out at two locations viz., Shahdara (urban) and Sampla (rural) in Delhi-NCR in Summer, Post- Monsoon (PoM) and winter seasons. PoM season has been studied as the two separate cases of September-October (SO) and November (N) months for the shape, size and EC-OC analysis at the Shahdara and Sampla sites.

3.1.1 $PM_{2.5}$ Concentration

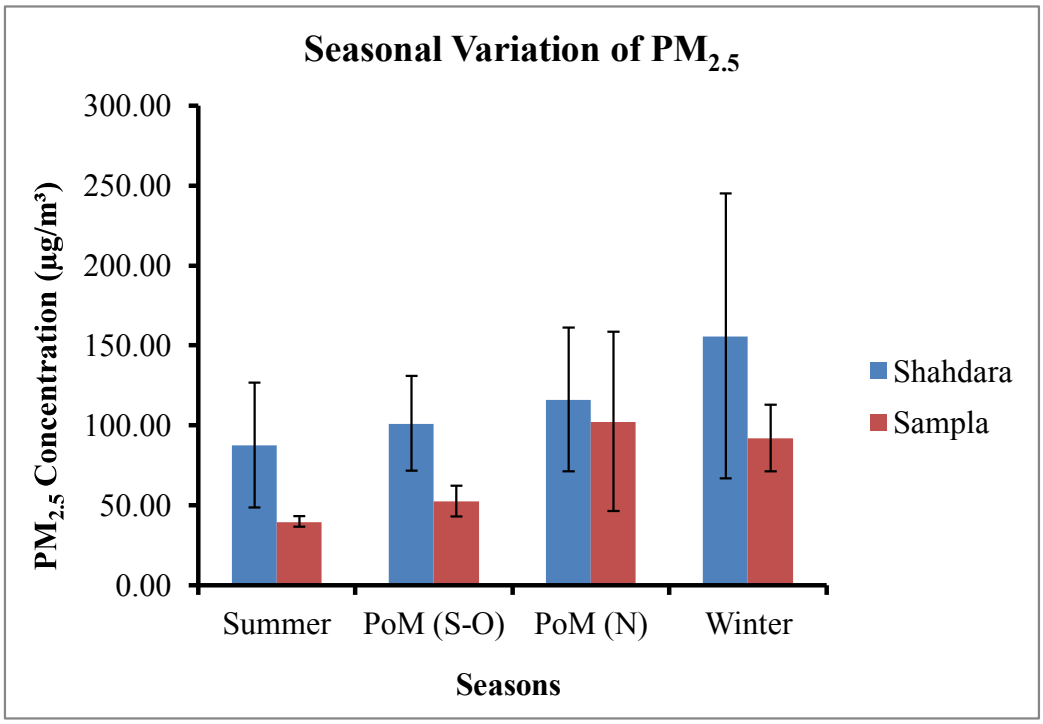

Fig. 3.1. Seasonal variation of $PM_{2.5}$ concentration at urban and rural sites.

Figure 3.1 shows the seasonal variation of the average $PM_{2.5}$ concentrations with standard deviation (SD) at the Shahdara and Sampla sites. There is an increasing seasonal trend observed in the concentrations at both the Shahdara and Sampla sampling sites. However, the

average concentration of $PM_{2.5}$ at the urban (Shahdara) site was found to be relatively higher as compared to the rural site (Sampla) in all the seasons. The average $PM_{2.5}$ concentration in the urban site was measured to be 87.33μg/m^3, 108.30 μg/m^3 and 155.56μg/m^3 and in rural was 39.46μg/m^3, 75.53μg/m^3, and 91.62μg/m^3 in the summer, post-monsoon and winter seasons respectively. The average daily concentrations at both the sites exceeded the 24 hourly average levels of Central Pollution Control Board (CPCB)-NAAQS $PM_{2.5}$ level (60 μg/m^3), WHO guidelines (25 μg/m^3) & US-EPA standards (35 μg/m^3) except in the summer season at the rural site which were below the prescribed 24 hourly CPCB-NAAQ Standards but exceeded those of US-EPA and WHO standards. The average, minimum, maximum concentrations and standard deviation at urban and rural locations in summer, post-monsoon and winter seasons respectively are listed in Table 1.

The sources of $PM_{2.5}$ aerosols in the rural region may include the dust, both wind-blown from nearby Thar Desert region and re-suspended from vast open agricultural fields, bi-annual agricultural waste burning (during April-May & October-December), use of bio-fuels (wood and cow-dung cakes) for cooking purposes, transport of pollutants by wind from the nearby industrial areas and brick kilns. At the urban site, the major sources of $PM_{2.5}$ may include emissions from road traffic, thermal power plants, industries and large scale construction activities.

During the summer season, proper dispersion of the pollutants takes place as a result of high atmospheric boundary layer and strong surface winds therefore, leading to less concentration at both the rural and urban sites as compared to the concentration in other seasons. The average temperature, relative humidity (RH in %) and wind speed during the summer sampling duration over Delhi were reported to be 34.33 ºC, 41.75% and 2.64 m/s respectively (www.wunderground.com).

The Post-Monsoon season witnesses the change in the weather indicating the transition from summer to winter season in the month of October. The average temperature, RH and wind speed during the month of October & November are 30ºC, 51.5% and 1.81 m/s & 19.57 ºC, 50.42% and 1.31 m/s respectively. Slightly foggy and cooler conditions could be observed during the early morning time in this period, which could help in the accumulation of the

pollutants during this time. The months of October-November are important for the air quality studies as during these months large amount of agricultural waste is burned openly by the farmers to clear the fields for sowing the next crops. These events affect the air quality of not only the immediate area but have a great impact on the surrounding regions as well.

$PM_{2.5}$ concentrations during winter in the Delhi-NCR were observed to be the maximum at both the sites. The $PM_{2.5}$ aerosol concentrations are also affected by meteorological conditions (calm or no winds and lower inversion height). The average temperature, RH and wind speed during the sampling duration were 10.33 ºC, 92.33% and 1.99 m/s. Under these conditions, aerosols generated by various anthropogenic emissions tend to accumulate near the surface thereby increasing the concentration during the winter season.

Table 3.1. The average, minimum and maximum $PM_{2.5}$ concentration (all in $\mu g/m^3$) at Shahdara and Sampla in different seasons. (Standard Deviation (S.D) is given in parenthesis).

Location	**Summer**			**Post-Monsoon**						**Winter**		
				Sept-October			**November**					
	Avg. (SD)	Min.	Max.	Avg. (SD)	Min.	Max.	Avg. (SD)	Min.	Max.	Avg.	Min.	Max.
Shahdara (Urban)	87.36 (39.04)	41.66	152.70	100.85 (29.59)	55.56	152.78	115.74 (45.01)	69.44	208.33	155.56 (89.14)	69.40	263.88
Sampla (Rural)	39.46 (3.26)	33.33	41.67	52.26 (9.60)	40.82	65.36	102.12 (56.10)	41.67	204.08	91.62 (20.87)	70.92	125.0

3.1.2 Particle shape

Particle size and shape was analysed using the SEM technique in different seasons viz. summer, post-monsoon and winter at both the urban (Shahdara) and rural (Sampla) sampling sites as described below. Figure 3.2 shows the SEM images of the blank quartz fibre filter. The long tube-like structures represent the quartz filter fibres in all the SEM images.

Blank Quartz fiber filter

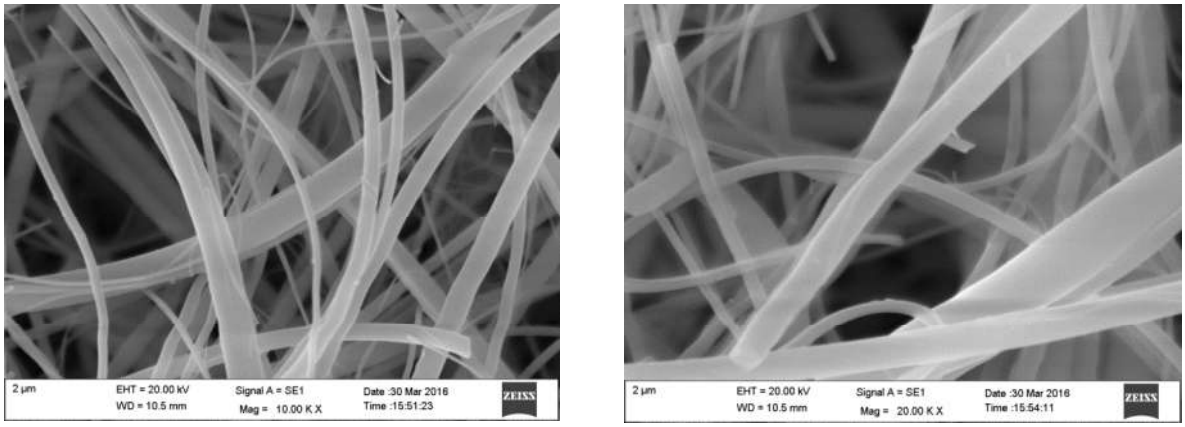

(a) (b)

Fig.3.2. SEM micrographs for the blank quartz fibre filters.

The seasonal variation in the morphology of the particles at Shahdara and Sampla sampling sites is described below. The SEM results show a clear difference between the morphological properties at both the urban and rural sites during the summer, post-monsoon and winter seasons.

I. Summer Season:

Figure 3.3 below shows the SEM images of the $PM_{2.5}$ aerosols at the urban and rural site during the summer season. A stark contrast between the urban and rural samples could be observed. The SEM results show that the rural area samples (3.3- b, d, f) were relatively cleaner as compared to the urban area samples which is in agreement with the $PM_{2.5}$ concentrations levels at both the urban and rural sites. During the summer season, the strong convective winds and high temperatures in Delhi-NCR increases the height of boundary layer,

allowing the proper dispersion of the pollutants. Even then, the high pollution levels could be observed at the urban site as compared to the rural site as is evident from the Summer SEM images as well. The flaky, free, aggregated and irregular shaped particles were found to dominate at the urban site during the summer season (Figure 3.3 a, c, e). However, ultrafine and spherical shaped particles were found to be present in the rural samples during the summer season but not in the significant amount. Urban area samples were clearly found to be dominated by the soot-like aggregates in the summer season indicating the presence of large amount of anthropogenic emissions from the vehicular, industrial and coal based combustion processes. Soot aggregates are often irregular shaped agglomerates of smaller particles (figures 3.3- c and e). A few crystalline particles could be observed in the rural samples (figure 3.3 - d and f) which could be due to the presence of dust/silica. During this season, Delhi-NCR is affected by the severe dust storm events which increase the amount of dust particles in the atmosphere. Rural area, in addition to dust storms, is also affected by the wind-blown dust from the large open dry agricultural fields which also add up to the amount of dust in the atmosphere. Soot aggregates in smaller amounts were also observed in the rural area which could be due to the consumption of the bio-fuels (woods and cow-dung cakes) in the households throughout the year for cooking purposes in the morning and evening times. Also, at the end of April or beginning of May, agricultural waste of wheat crop is burned to clear away the fields for sowing the rice crop.

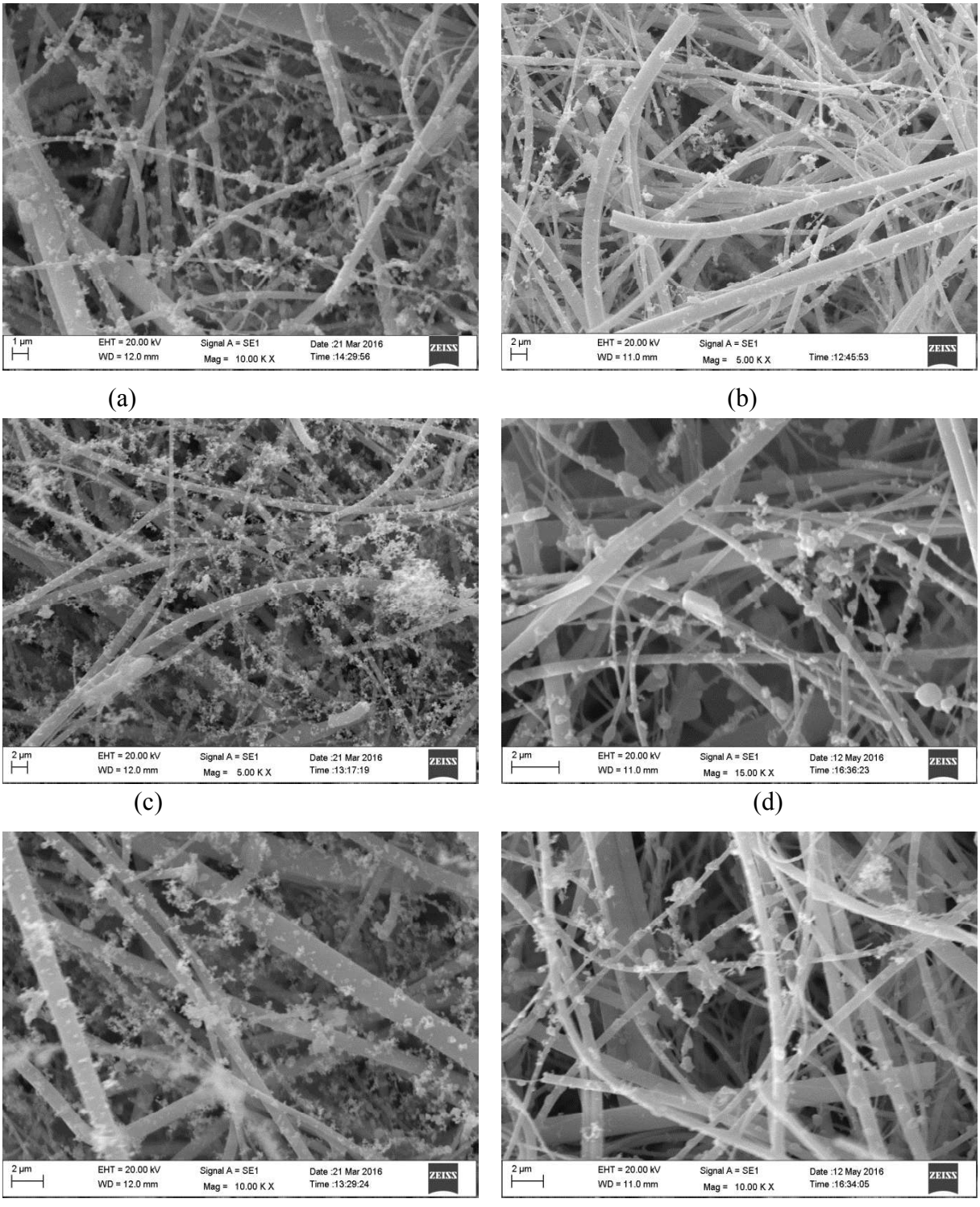

Fig.3.3. SEM micrographs for the summer season at two sites Shahdara (a, c, e) and Sampla (b, d, f).

II. Post-Monsoon Season

The post-monsoon season comprises of the September, October and November months. The shapes of the particles have been studied separately at both the urban and rural sites as described below:

PoM (S-O)

Figure 3.4 shows the $PM_{2.5}$ aerosol particles at the Shahdara (Figure 3.4 - a, c, e) and Sampla (Figure 3.4 – b, d, f) sites during the PoM (S-O). During the months of September – October also, the urban area samples were heavily loaded as compared to the rural area ones. However, the nature of the particles and deposition changed slightly at both the sites. Unlike summer season, where mostly soot-like particles were present, the urban site recorded the small aggregates of the $PM_{2.5}$ aerosols in addition to the soot particles. This may be due to the beginning of the seasonal change over this region from summer to fall season when the days are still warm but nights start to become cooler. The small aggregates of ultrafine particles were observed in abundance at the urban site whereas at rural site, small round and crystalline shaped (Fig. 3.4 - f) particles were observed. A few large particles such as the perfectly spherical/round shaped soot particles of size approximately up to 10μm (Fig 3.4 – c) along with the other smaller aggregates could also be seen in the urban area samples whereas at rural site fluffy particles (Fig 3.4 – d) were observed which could be soot particles. However, SEM images could not tell whether the round/spherical particles were hollow or solid from inside.

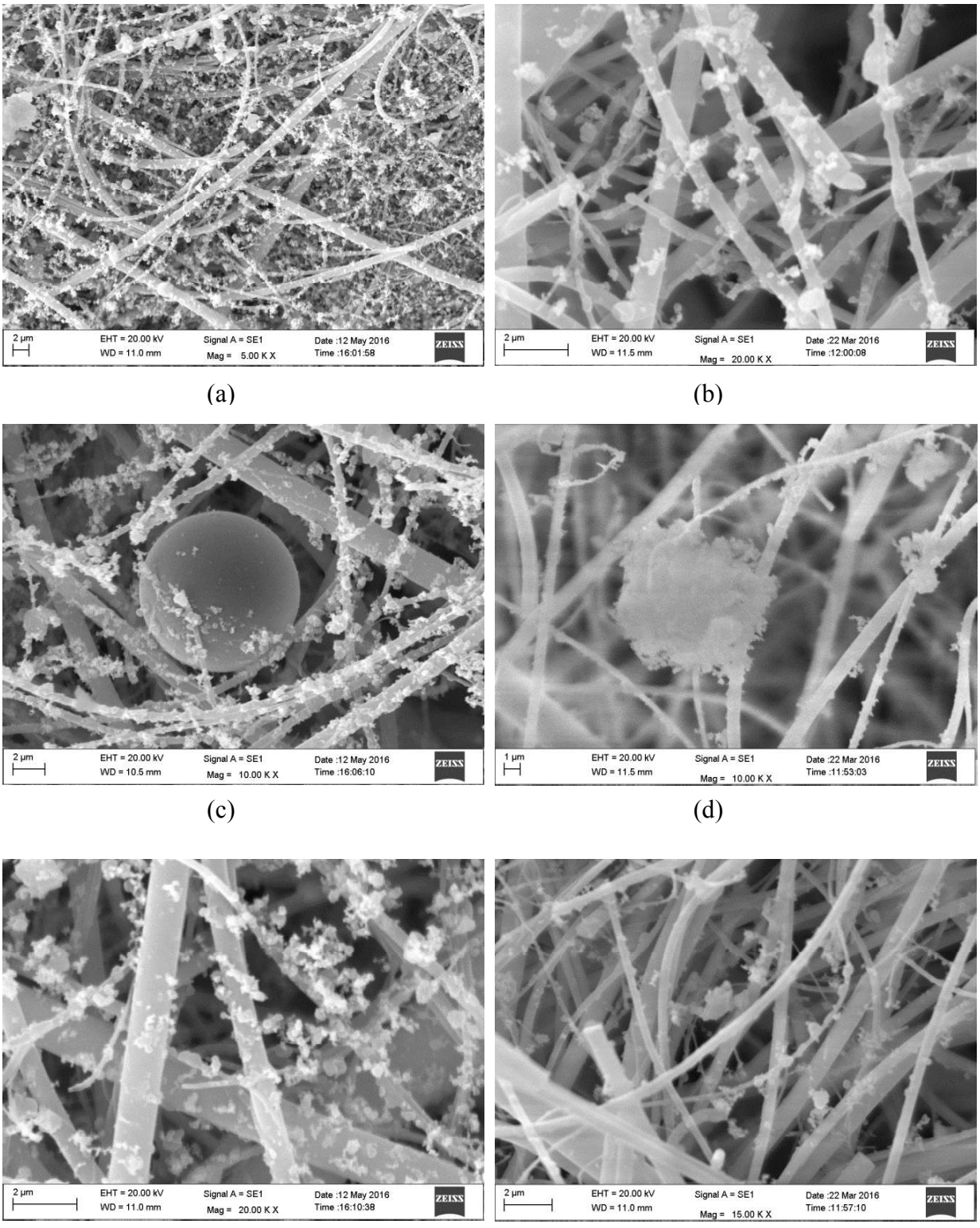

Fig.3.4. SEM micrographs for the PoM (S-O) months at the two sites viz. Shahdara (a, c, e) and Sampla (b, d, f).

PoM(N)

Figure 3.5 shows the $PM_{2.5}$ aerosol particles at the Shahdara (Figure 3.5- a, c, e) and Sampla (Figure 3.5 – b, d, f) sites during the month of November. The variability in the aerosols shapes and sizes could easily be noticed. Urban site samples recorded the abundance of aggregates of ultrafine particles, spherical, round and irregular shaped particles. On the other hand, rural area samples were found to be dominated by spherical and spindle or bead shaped particles (Figure 3.5 – d). This month also witnessed the Deepawali festival on the 11th November 2015. Burning of fire crackers continued for three-four days even after Deepawali festival. Soot particles were again commonly found in the urban area samples. Different processes of particle formation result in different morphologies of the particles. Coagulation processes also result in irregular particles in the fine mode fraction. Breed et al. (2002) reported contribution of combustion processes more to the fine mode fraction. The month of November is one of the most important months in the year as far as air quality and aerosol characteristics studies are concerned. This month marks the event of open biomass burning on a large scale in the northern Indian states especially in Haryana and Punjab. During this season, the transition of crops from Kharif to Rabi takes place and in order to do so, farmers burn the residual agricultural waste of Kharif crops to clear the fields for the sowing of the next crop. This is an economical method for the farmers to get rid of the large amount of crop residues fairly quickly. Burning of the crops usually starts in the late afternoon and is sometimes continued in the night as well.

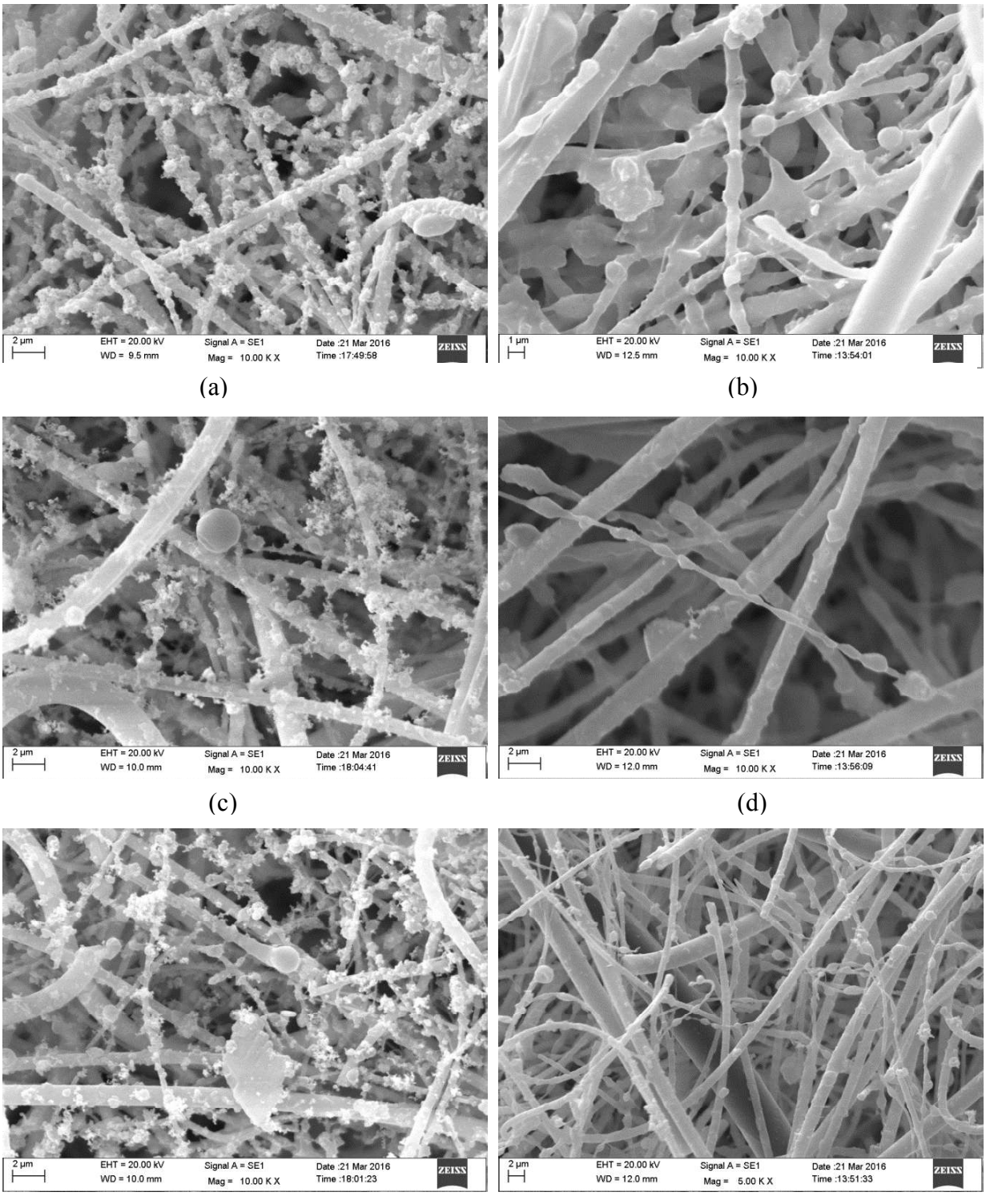

Fig.3.5. SEM micrographs for the PoM (N) season at two sites Shahdara (a, c, e) and Sampla (b, d, f).

III. Winter Season

Figures 3.6 shows the $PM_{2.5}$ aerosols morphology in the Shahdara (Figure 3.6 - a, c, e) and Sampla (Figure 3.6 – b, d, f) sampling sites during the winter season. During this season, the round, aggregated and irregular shaped particles were found to be dominating at both the urban and rural sites. However, at the rural site, the individual irregular, spherical and spindle shaped particles, though embedded in filter fibres, were more prominently observed as compared to the urban site where particles were observed to be in a highly concentrated/aggregated form on the fibre filter strands making it difficult to ascertain their shape and size properly. Very few particles could be observed individually at the urban site. The morphology of the particles in this season at both the sites indicate the presence of combustion sources which could be vehicular, industrial, coal combustion, dry leaves or garden waste in the urban areas, bio-fuel consumption for both cooking and heating purposes and biomass burning during winter season. At the urban site, during winters, high amount of $PM_{2.5}$ aerosols from various sources under low temperatures and calm or no winds may undergo the process of aggregation. Soot was again observed as the major component of $PM_{2.5}$ particles especially in the urban area. The meteorological conditions as well play a great role during this season. As discussed above, low temperatures and development of low inversion layer during this season result in the accumulation of the particles near the surface thereby increasing the concentrations of the aerosols.

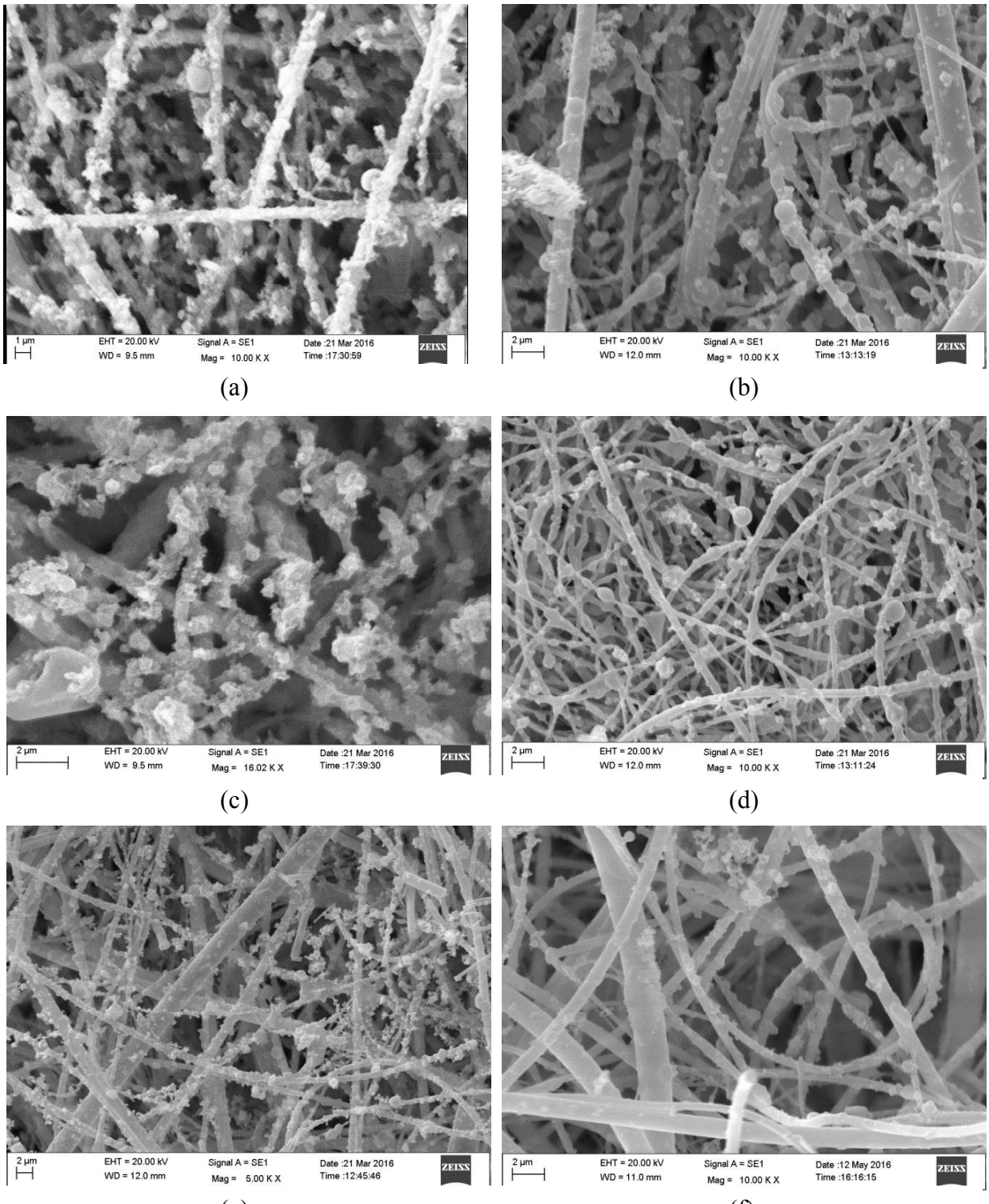

Fig.3.6. SEM micrographs for the Winter season at two sites Shahdara (a, c, e) and Sampla (b, d, f).

Discussion

The urban site samples were always found to be more heavily loaded than those of rural ones which is in agreement with the measured concentration and SEM images. High concentrations at the urban site may have resulted in the aggregation of the $PM_{2.5}$ particles especially during the Post-monsoon and winter season. Aggregation processes often results in the formation of irregular shaped particles of different sizes (Rodriguez et al. 2009). Whereas the rural site SEM images still showed the particles to be present in the independent/individual state. The sources of the $PM_{2.5}$ particles were observed almost identical in the urban and rural areas with exceptions to their number and season (such as biomass burning event). High temperature combustion processes are generally associated with the production of spherical shaped and smooth surfaced particles (Tasic et al. 2006), such as biomass burning and wood/coal combustion observed in the November and winter season. Spherical shape of the particles is an important consideration in the study of solar attenuation by various atmospheric models (Buseck et al. 2000). Certain particles such as Soot can cause "heating" of the atmosphere by absorbing the incoming solar radiation (Tiwari et al. 2015). Though the SEM analysis is a powerful tool to determine the shape and size of the $PM_{2.5}$ particle but it still has some limitations. For example, the SEM analysis, cannot tell the presence of the hollow spherical particles. Given the complex fibre structure of the quartz fibre filter, manual SEM analysis of the collected particles is often limited by the heavily loaded samples which makes it difficult for the individual particles to be analyzed effectively (Casuccio et al. 2004).

3.1.3 Particle Size Distribution:

The size distribution of the $PM_{2.5}$ aerosols at the urban and rural site in three seasons is compared below. Approximately 300-400 particles from 5-11 images from each season at both the sites, Shahdara and Sampla, were analyzed to measure the diameter. The distribution curves have been plotted. The red line indicates the log-normal distribution fit. The seasonal size distribution at both the sites has been discussed below:

I. Summer:

The particle size distribution at both the urban and rural site (Figure 3.7) was observed to be skewed to the right. The geometric mean (μ_g) and geometric standard deviation (σ_g) of the particles size at both the sites were 0.58, 1.7 and 0.58, 2.0 respectively. As is observed from the two sites distribution curves, the geometric mean diameter is comparable but the spread of the distribution curve is more at the Sampla site than the Shahdara site. At the urban site, the dominant size range is the 0.2 - 1.4 μm whereas at the rural site 0.1 – 2.0 μm indicating the presence of coarse mode particles such as dust or crystalline particles in good amount at the rural site. Rural distribution clearly indicates the dominance of particles in both the Accumulation and aitkin mode whereas at urban site aitkin mode could be found to be the dominant one. This indicated the presence of vehicular and industrial emission sources in the urban area which generally contribute to the fine mode fraction of the aerosols. In rural area particles with size >1 μm were observed in large amount compared to the urban area which could be due to the presence of large number of coarser particles such as dust or crystalline particles. As is seen above, urban area samples during the summer season were largely influenced by the soot fluffy, mesh-like aggregates making it difficult to discern their sizes. The accumulation mode particles generally result from the burning of the bio-fuel (wood, cow-dung cakes) for various cooking purposes in the households (Sienfeld and Pandis, 2006).

Summer Season

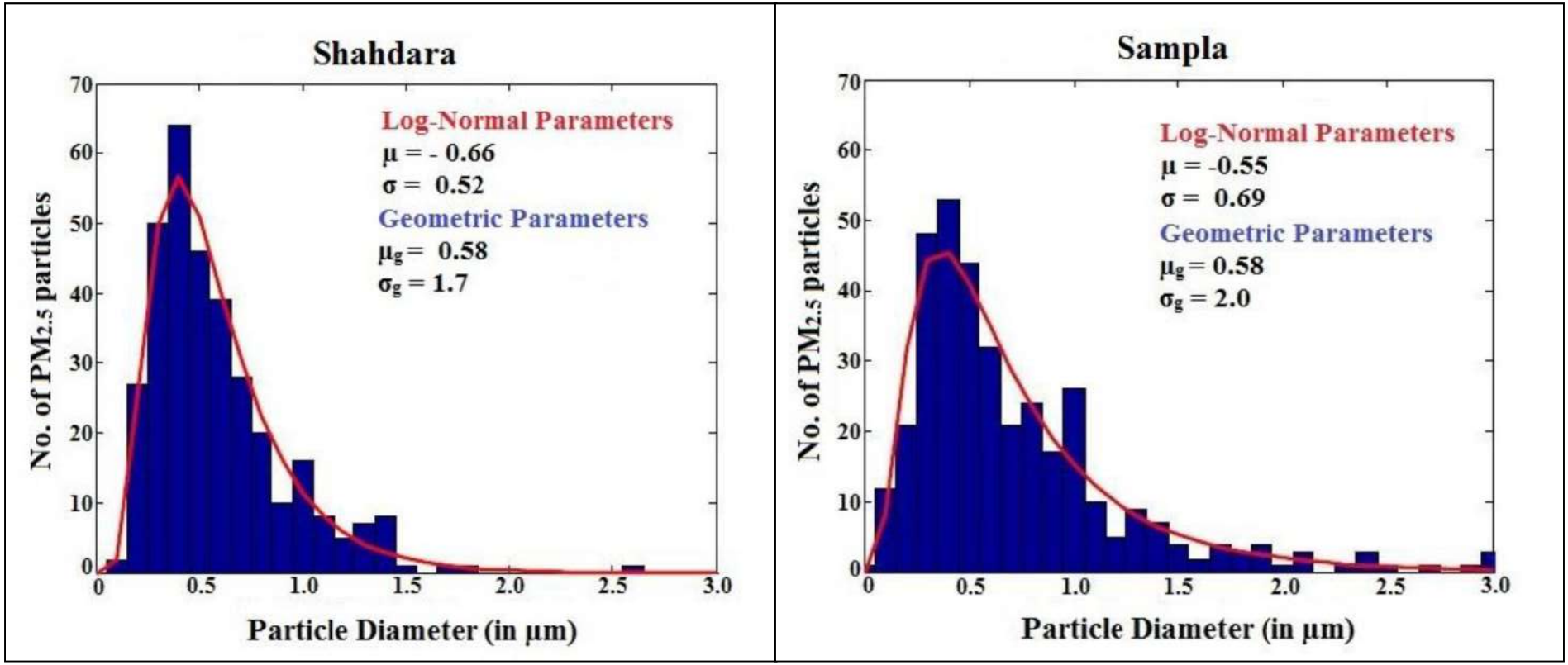

Fig. 3.7. The size distribution of $PM_{2.5}$ particles at the Shahdara and Sampla site during the Summer season.

II. Post-Monsoon:

PoM(S-O)

The figure 3.8 shows the particles diameter distribution at the Shahdara and Sampla site PoM (S-O) season. The particle size distribution at both the urban and rural site was observed to be skewed to the right. The geometric mean (μ_g) and geometric standard deviation (σ_g) of the particles size at both the sites were 0.47; 1.8 and 0.59; 1.8 respectively.

The size distribution curve at the urban site shows a maximum around 0.40 μm size aerosols whereas at the rural site maximum is observed around 0.4 - 0.5 μm particles. The geometric mean diameter of particles is observed to be higher in the rural area than the urban area. But the spread of the distribution curve is almost similar at both the urban and rural sites. The rural site was observed to be dominated by the particles in the size range 200- 900 nm and particles in the size range 200 -700 nm dominated at the urban site. This curve again shows the dominance of accumulation and aitkin mode particles in both the urban and rural areas indicating the presence of anthropogenic emission sources in both the urban and rural areas. However, since the distribution curve in the rural area contains particle larger than 1 micrometer as well, fine dust aerosols could also be present in the rural samples.

Post-Monsoon (September-October):

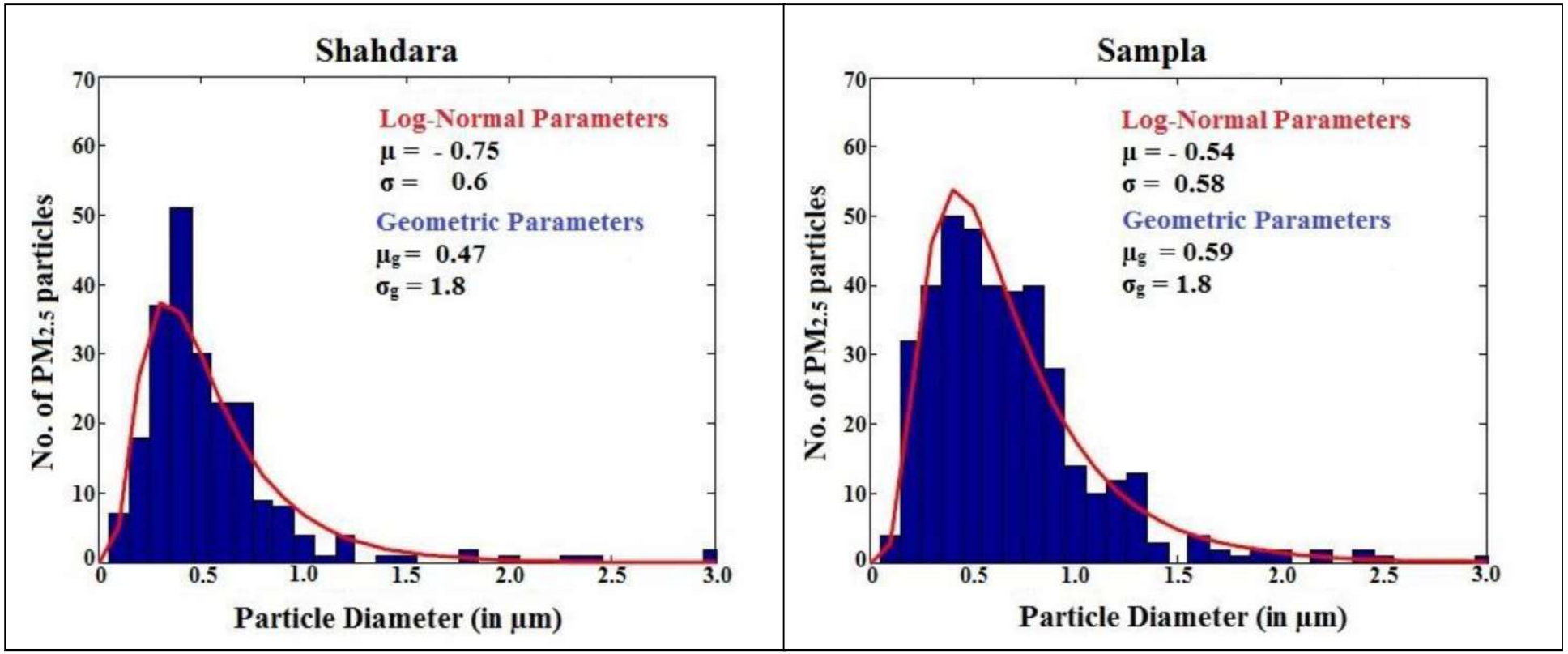

Fig. 3.8. The size distribution of $PM_{2.5}$ particles at the Shahdara and Sampla site during the Post-Monsoon (S-O) season.

PoM(N)

The size distribution observed at both the urban and rural site is log-normal (Figure 3.9). The distribution curve at the urban site (Shahdara) is dominated by the particles of the size less than 1 micro-meter indicating the dominance of accumulation mode whereas at the rural distribution curves indicates the dominance of the accumulation as well as coarse mode particles (diameter >1 μm). The geometric mean and geometric standard deviation at both the urban and rural site are 0.58, 2.1; 1.3, 1.7 respectively. The urban aerosols were observed to be dominant in the 0.1-1μm size range (fine mode particles) and rural samples were found to be dominant in the range 0.5- 2.0 μm (fine + coarse mode). This indicates that the urban area particles are more influenced by the vehicular and industrial emissions whereas the rural area particles could be influenced by the particles originating from agricultural biomass burning activities, combustion of wood and coal for household chores in addition to dust particles. Biomass burning activities generally produces particles in the accumulation mode (Sienfeld and Pandis). As mentioned above, the rural site witnessed the biomass burning activities during the sampling duration. The larger particles than the accumulation mode size were also observed at the rural site. This could be due to the aggregation of fine particles (external mixing) or the deposition of the particles melted at high temperatures which could result in the larger size particles at the rural site.

Post-Monsoon (November)

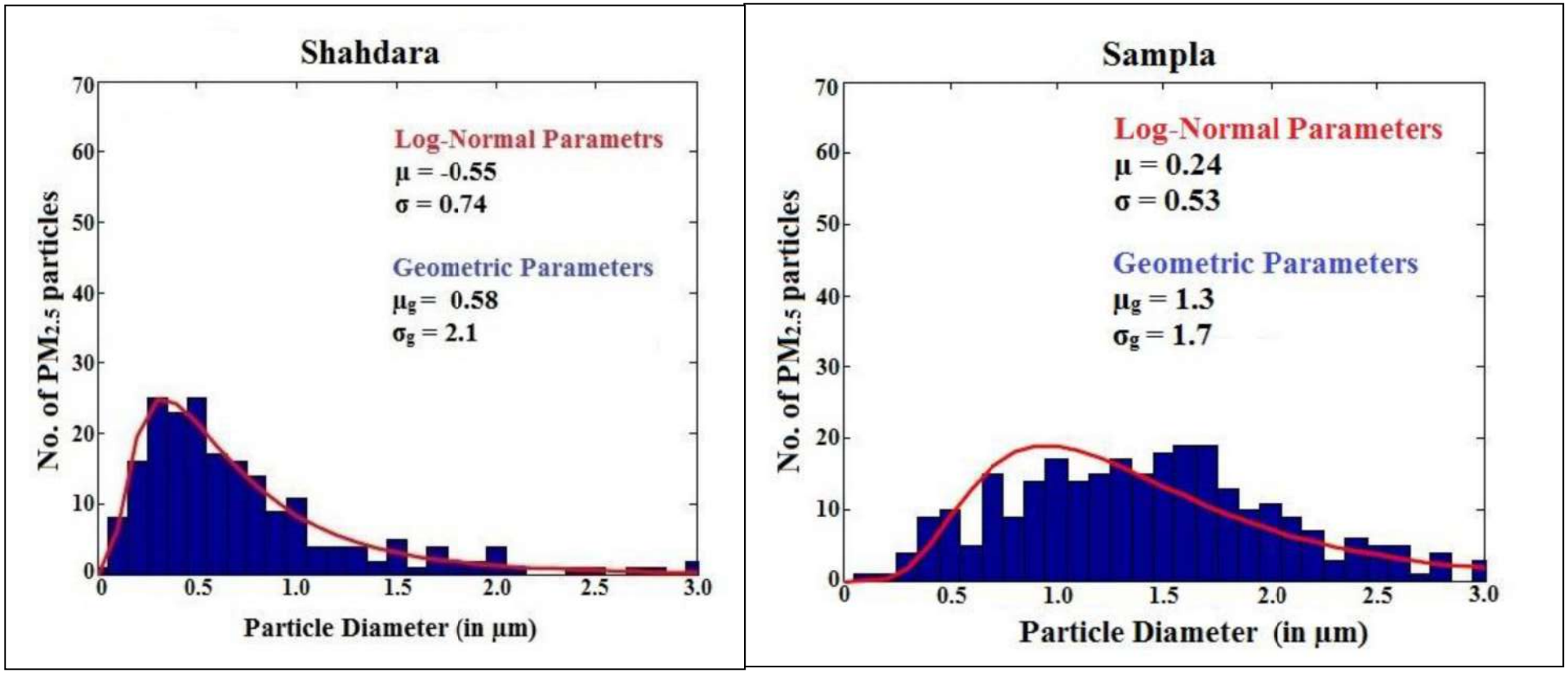

Fig.3.9. The size distribution of $PM_{2.5}$ particles at the Shahdara and Sampla site during the Post-Monsoon (N) season.

III. Winter:

The size distribution curve observed in the urban and rural areas is skewed to the right giving the log-normal distribution (Figure 3.10). At the urban site, the particles were observed to be in the size range of 0.4 – 2.0 μm size range and at the rural site, the particles were observed in the 0.2 – 2.0 μm. Distribution curve in the urban area has a peak around the size range of approximately 0.5-1.2 μm whereas in the rural area, distribution shows two peaks from 0.5-0.7 and 0.9-1.4 μm size range. The geometric mean and geometric standard deviation at both the urban and rural site are (0.93; 1.7), (0.95; 1.9) respectively. As can be seen, the mean geometric diameter comparable at both the urban and rural site but the spread of the distribution is curve is more at the rural site than the urban site. This may be due to the presence of the large number of the individual particles at the rural site as compare to the urban site where particles were mainly in the agglomerated form during the winter season. During the winter season also, the rural site was dominated by the fine mode as well as coarse mode particles indicating the emission from the automobiles, factories, wood and coal burning in addition the dust aerosols may be responsible for this size range aerosols. Urban areas particles were mainly dominated by the fine mode aerosols with size less than 1 micro-meter showing the dominance of vehicular and industrial emissions which contribute mainly to the fine mode fractions than the coarse mode fraction.

Winter Season

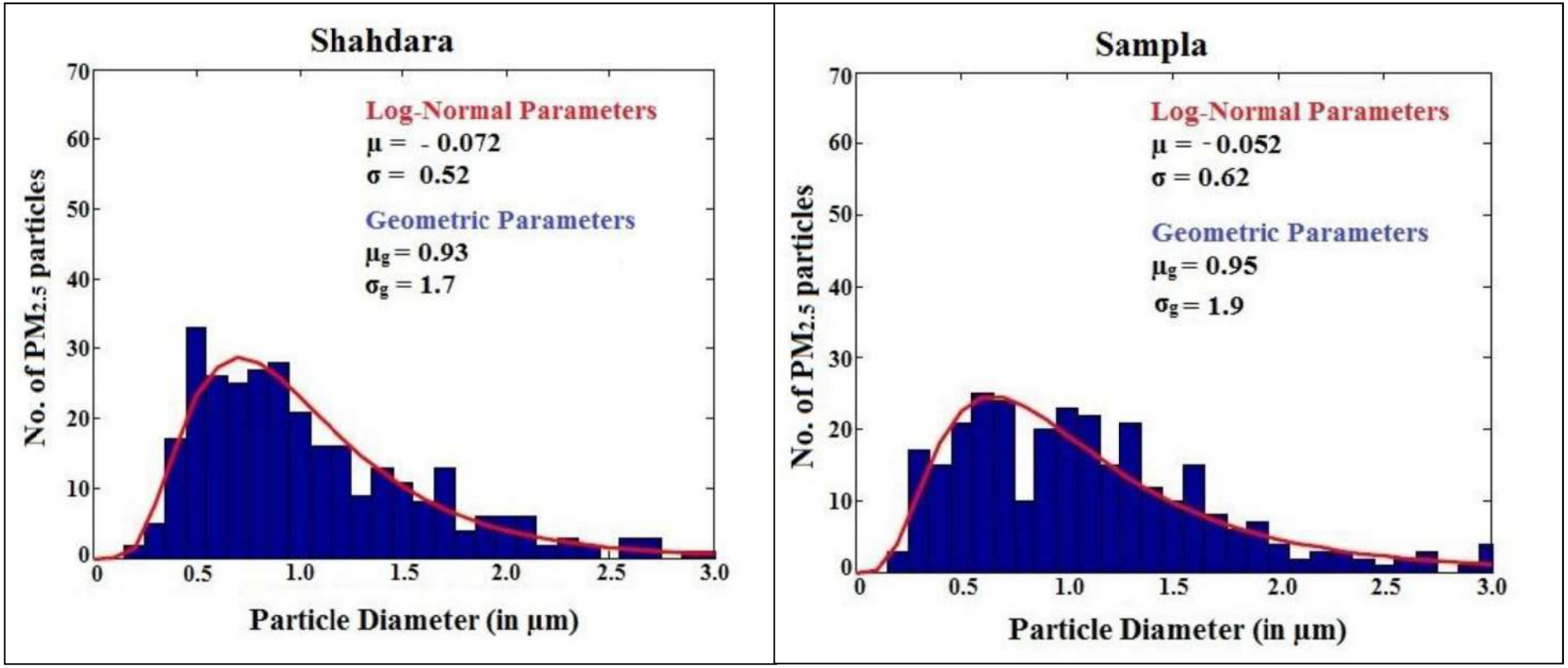

Fig. 3.10. The size distribution of $PM_{2.5}$ particles at the Shahdara and Sampla site during the winter season.

3.1.4 Seasonal Comparative study of urban and rural particle Size Distribution

To understand the various interaction processes of aerosols in the atmosphere, it is imperative to understand their size distribution in the atmosphere. As $PM_{2.5}$ aerosols include particles of diameters ≤ 2.5 μm, it is important to estimate their size distribution as particles of different sizes interact differently in the atmosphere. As can be seen from the above particle diameter distribution, majority of the particles at the Shahdara and Sampla site were distributed within the 0-1.5 μm size range except in the month of November in Sampla where particles were observed to be distributed throughout the 2.5 μm spectrum. These distribution curves indicate the dominance of fine mode aerosols in both the urban and rural site in all the seasons except during the month of November in rural area where coarse mode aerosols (size > 1μm) also seem to dominate. Agricultural waste burning activities during the month of November may be responsible for the presence of large particles (due to agglomeration) in the size distribution at the rural site. Dominance of fine mode aerosols indicate the presence of anthropogenic emissions such as wind-blown or re-suspended dust, vehicular, industrial and biomass burning at both urban and rural sites. As discussed in the chapter 1, the sizes of the particles play a crucial role in determining the kind of scattering (Rayleigh, Mie or Optical) exhibited by the aerosols. These scattering processes help in determining the kind of forcing that these aerosols exert at the surface or TOA or in the atmosphere over a particular region, in turn, affecting the local/regional climate system.

3.1.5 Carbonaceous content

The carbonaceous content such as OC and EC and their ratio (OC/EC) were analysed seasonally at Shahdara and Sampla site.

Summer season:

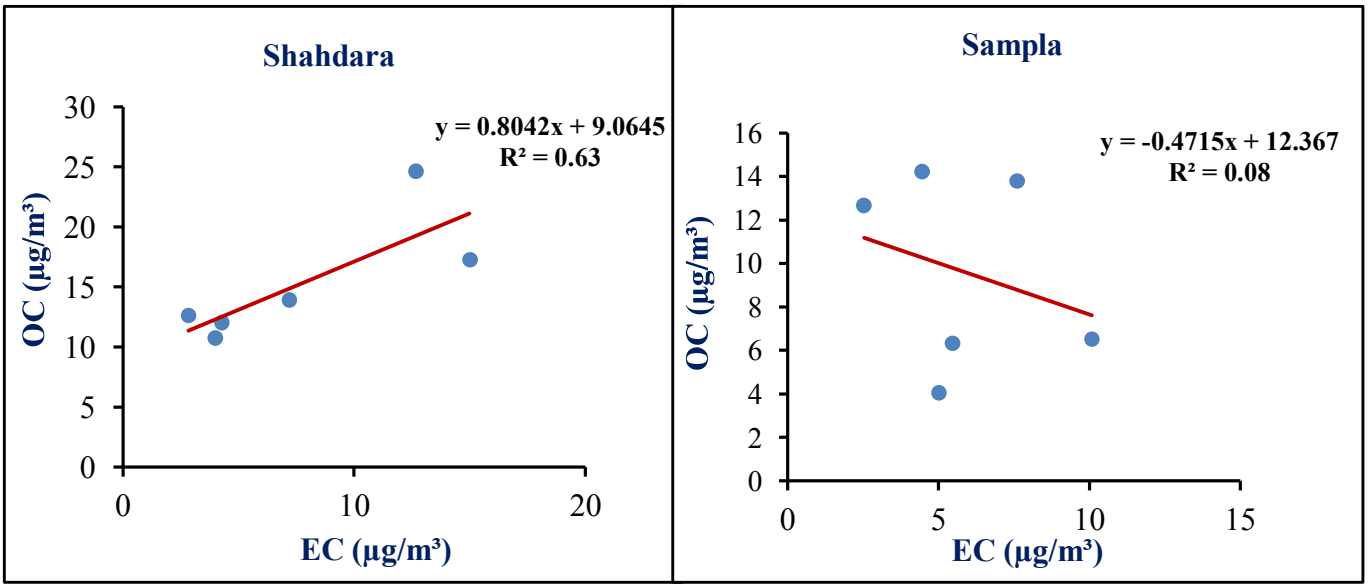

(a) (b)

Fig.3.11. Relationship between OC and EC during summer season at two sites Shahdara (a) and Sampla (b).

The OC and EC concentrations were found to be higher at the Shahdara site than Sampla site. The OC values ranged from 10.76 - 24.64 µg/m^3 at Shahdara and 4.06-14.23 µg/m^3 at Sampla sites during the summer season. On the other hand, EC values were observed to be varying from 2.82 – 14.99 µg/m^3 and 2.53 – 10.09 µg/m^3 at the Shahdara and Sampla sampling sites respectively. A significant relation (R^2 = 0. 63) could be seen between OC and EC at the Shahdara site (Figure 3.11 a) depicting an increasing/positive trend between the OC and EC values indicating the presence of common sources of OC and EC emissions in the urban area. The average OC and EC concentrations with standard deviation at the urban and rural sites are 15.22 ± 5.13 µg/m^3, 7.65± 5.05 µg/m^3; 9.60 ± 4.46 µg/m^3, 5.86 ± 2.64 µg/m^3 respectively. The respective average OC/EC ratio (with standard deviation) at the Shahdara and Sampla site

are 2.51±1.14, 2.10 ± 1.70. In rural area, however, the trend is opposite to that observed at the urban site. A negative slope/decreasing trend with poor association (R^2= 0.08) between EC and OC has been observed at the rural sampling site during the summer season (Figure 3.11 b). The poor correlation between the EC and OC at rural site indicates the presence of different sources of emission which could be the presence of dust particles in the atmosphere in the rural area as a result of dust storms which was witnessed during the sampling period. There is no direct relation observed between the OC and EC values observed at the rural sampling site. For some days, for the given values of EC, OC shows higher values whereas for other days almost similar concentration of EC and OC could be observed. Not much significant differences between the OC and EC concentrations at the Shahdara and Sampla sites could be observed during the summer season. Since, OC/EC >1 at both the urban and rural sites, indicate the influence of anthropogenic emissions during the summer season.

Post-Monsoon

PoM (S-O)

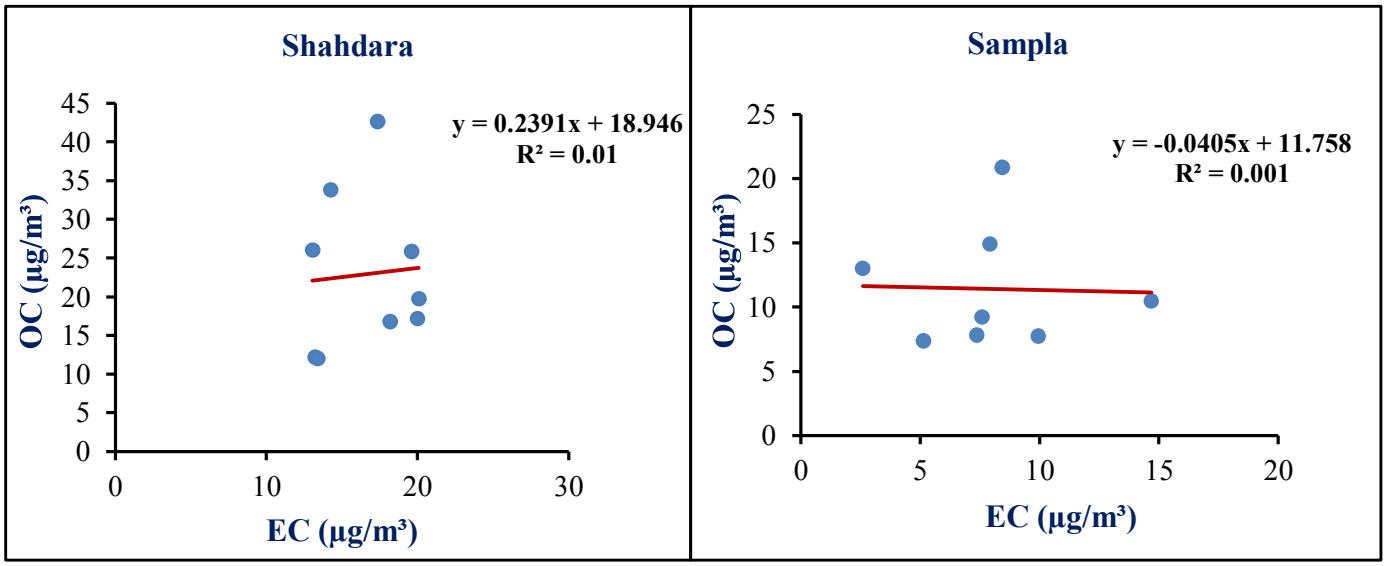

(a) (b)

Fig. 3.12. Relationship between OC and EC during September-October months at two sites Shahdara (a) and Sampla (b).

The average OC and EC concentrations (± SD) at the urban and rural site were observed to be 22.91 ± 10.24, 16.56 ± 3.07; 11.43± 4.67, 7.96 ± 3.52 µg/m^3 respectively. The OC and EC values at both the urban (R^2 = 0.01) and rural (R^2 = 0.001) sites were found to be poorly correlated (Figure 3.12 a-b) indicating the other emissions sources than the usual for EC and OC in the urban and rural areas. However, the variation between OC and EC showed a positive trend as compare to the rural site which depicted a negative variation between the OC and EC concentrations. Even though the OC and EC concentrations measured were higher at urban site than the rural sampling site, the average OC/EC ratio at the urban and rural site are 1.41± 0.67 and 1.82 ± 1.42 respectively. The OC and EC concentrations at the urban site were measured to be varying from 12.02 – 42.62 and 20.08 – 13.05 µg/m^3 respectively whereas at the rural site respective OC and EC values were found to be varying from 7.38 – 20.88 and 2.59 – 14.69 µg/m^3. No direct relation could be observed at the rural site between the OC and

EC values. The OC/EC ratio during this period was observed to be lower than the summer season at both the Shahdara and Sampla sampling sites. These months are relatively cleaner than other months after the monsoon period is over. The season starts a transitioning from summer to autumn which witnesses a slight fall in temperature. Nights and mornings start to become cooler and a slight fog also starts to develop during the early morning hours. Also at the end of September - October, the post harvesting agricultural waste burning just begins which may contribute to the higher OC and EC concentrations than summer season during these months.

PoM (N)

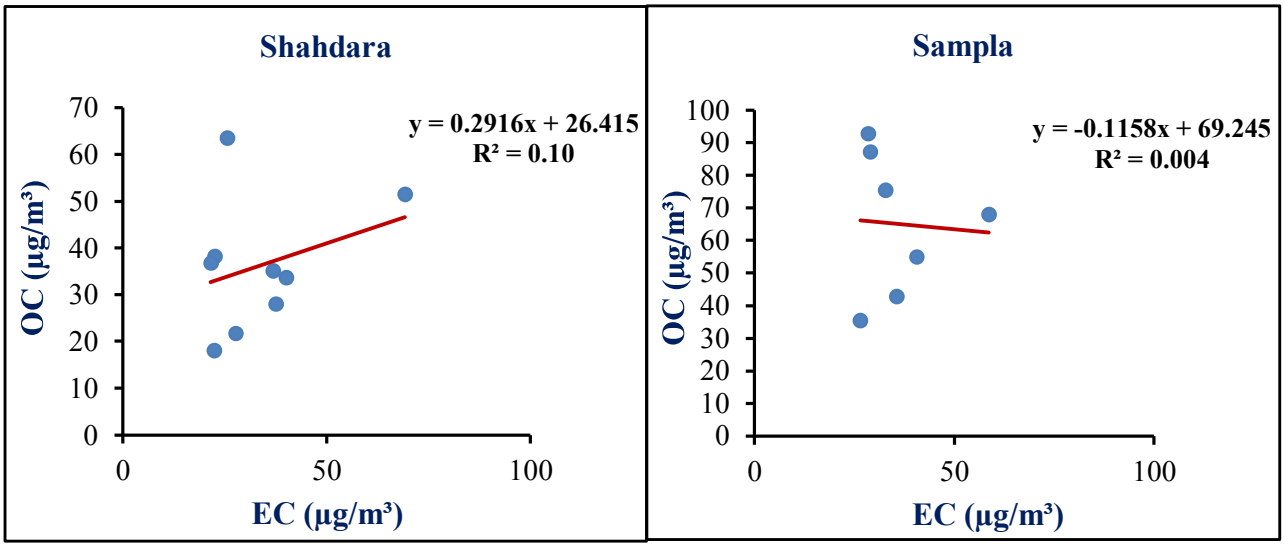

(a) (b)

Fig.3.13. Relationship between OC and EC during November month at two sites Shahdara (a) and Sampla (b).

The average OC and EC values with standard deviation at the Shahdara and Sampla site were 36.22 ± 14.13 µg/m^3, 33.63 ±15.12 µg/m^3; 65.08 ± 21.79 µg/m^3, 35.96 ± 11.12 µg/m^3 respectively. The average OC/EC ratio at the Shahdara and Sampla sites are 1.20± 0.60 and 1.94 ±0.90 respectively. At the Shahdara sampling site, the OC varied from 17.99 - 63.46 µg/m^3 and EC from 21.49- 69.15 49 µg/m^3. The rural site saw the variation in the OC from 35.29 – 92.64 µg/m^3 and EC from 26.50 - 58.69 µg/m^3 during the month of November. Both

the sites observed a poor correlation (Urban, R^2= 0.1; Rural, R^2= 0.004) between OC and EC during this month indicating the presence of EC and OC sources in both the urban and rural area (Figure 3.13). The average EC values were observed to be higher (but not significantly) at Sampla than the Shahdara during the month of November indicating the presence of combustion sources such as large scale biomass burning in addition to other local sources such as wood and coal combustion in the households. The rural site also observes a very high OC content than the urban sampling site which might be due to the formation of higher amount of secondary organic carbons in the rural atmosphere where the solar irradiance reaching the surface is still more as compare to the urban area (next section). The higher OC and EC values in the rural area showed that the biomass burning activity has affected rural area more than the urban area even though the sources of pollution are more in the urban area as is evident from the $PM_{2.5}$ concentrations during this season. The OC and EC showed a negative association at the rural site as compared to urban site which observed a positive trend despite the poor association between the OC and EC concentrations.

Winter

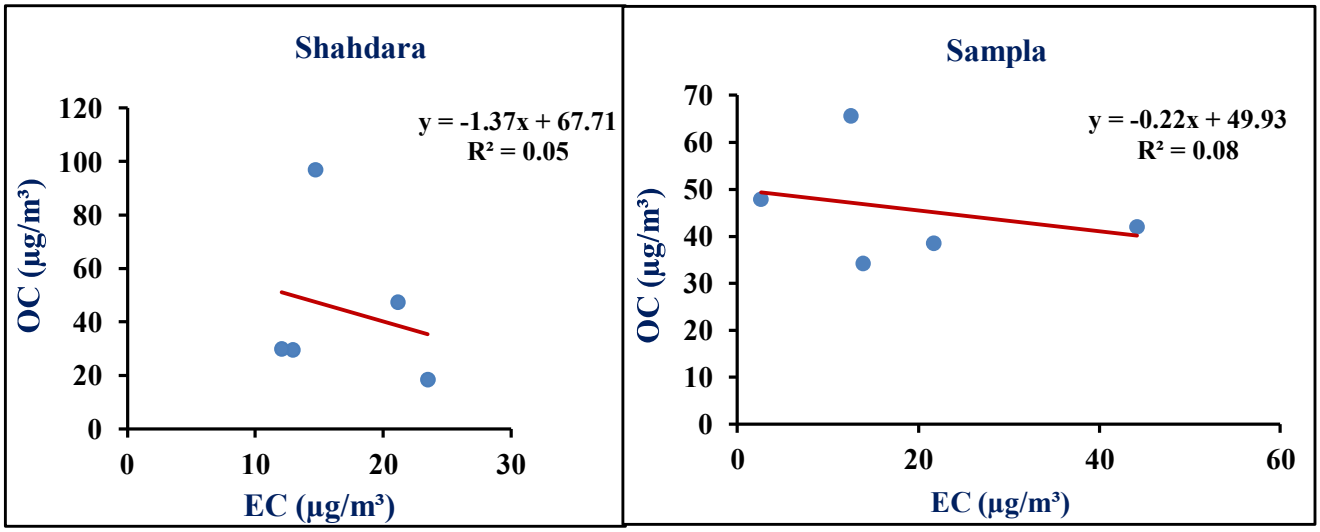

(a) (b)

Fig.3.14. Relationship between OC and EC during winter season at two sites Shahdara (a) and Sampla (b).

During the winter season, the average OC and EC concentrations (± SD) at the urban and rural sites are 44.55 ± 31.08µg/m^3, 16.85± 5.13µg/m^3; 45.70 ± 12.24µg/m^3, 18.98± 15.63 µg/m^3 respectively. During the winter season as well, a poor association between the concentrations of OC and EC could be seen (Figure 3.14 a and b) at both the urban and rural sites. Also, the OC and EC relation has a negative slope at both the Shahdara and Sampla sampling sites. The OC and EC concentrations varied from 18.57 – 96.98 µg/m^3 and 12.04 – 23.47 µg/m^3 respectively at the urban site whereas at the rural site, they ranged from 34.26 – 65.68 µg/m^3 and 2.60 – 44.16 µg/m^3 respectively. The average (± SD) OC/EC ratio at both the urban and rural site are 2.89 ± 2.19 and 5.77 ± 7.25 respectively.

The average OC concentrations at both the urban and rural sites were observed to be comparable and EC concentrations at the rural site were found to be slightly higher than the urban site. High EC concentrations at the rural area might be due to the burning of biomass (agricultural waste) and a good amount of wood/coal burning for the cooking and heating

purposes in the vicinity of sampling site by the people during this season in addition to the emissions from diesel powered vehicles like trucks and tractors used for agricultural purposes and the nearby industries and factories.

Whereas in the urban area, the burning of garden waste cuttings, dry leaves by the road side, wood/coal burning by the poor people in order to keep themselves warm during the harsh winter season in addition to the vehicular, industrial, emissions from the coal-based thermal power plants could also contribute to the EC and OC concentrations. The formation of the secondary organic carbons in the presence of sunlight could also contribute to the high OC concentrations at the rural site. The low temperatures (coupled with the low inversion layer and calm winds during this season also lead to the aerosol accumulation near the surface. The boundary layer/height becomes very low during this season which doesn't allow the particles to disperse properly.

3.1.6 Seasonal variation for the urban and rural EC and OC

Table 3.2 summarizes the average values of EC and OC along with their standard deviations and standard error during the seasons viz. summer, PoM (S-O), PoM (N) and winter.

A positive association between the OC and EC values has been observed in the urban area except during the winter season whereas at the rural site, a negative association between OC and EC is observed during the entire study period. Also the association was observed to be poor in almost all the seasons at both urban and rural sites except during the summer season at urban site which showed a relatively good association among the OC and EC values. The poor association indicated the contribution of other sources in addition to combustion processes. The OC and EC values were observed to high in the urban area than the rural area during the summer and September-October months of Post-Monsoon season. However, in the month of November and winter season, the OC and EC concentrations were found to higher in the rural area than the urban area.

The percentage contribution of OC to the $PM_{2.5}$ at the urban site is 17. 43%, 22.72%, 31.29% and 28.64% during the summer, PoM (S-O), PoM (N) and winter seasons respectively. At the

Table 3.2. The average values of EC, OC (all in μg/m^3), standard deviation (S.D) and standard error (SE) in parenthesis at Shahdara and Sampla in different seasons.

Seasons		**Urban (μg/m^3)**			**Rural (μg/m^3)**		
		OC (± SD; SE)	**EC (± SD; SE)**	**OC/EC (± SD; SE)**	**OC (± SD; SE)**	**EC (± SD; SE)**	**OC/EC (± SD; SE)**
Summer		15.22 (±5.13; 2.06)	7.65 (±5.05; 2.06)	2.51 (±1.14; 0.47)	9.60 (±4.46; 1.99)	5.86 (±2.64; 1.18)	2.10 (±1.70; 0.76)
Post-Monsoon	September - October	22.91 (±10.24; 3.41)	16.56 (±3.07; 1.02)	1.41 (±0.67; 0.22)	11.43 (±4.67; 1.65)	7.96 (±3.52;1.24)	1.82 (±1.42; 0.50)
	November	36.22 (±14.13; 4.71)	33.63 (±15.12; 5.04)	1.20 (±0.60; 0.21)	65.08 (±21.79; 8.90)	35.96 (±11.12; 4.54)	1.94 (±0.90; 0.37)
Winter		44.55 (±31.08; 13.90)	16.85 (±5.13; 2.30)	2.89 (±2.19; 0.98)	45.70 (±12.24; 5.47)	18.98 (±15.63; 6.99)	5.77 (±7.25; 3.24)

rural site OC contributed to about 24.32%, 21.87%, 63.73% and 49.88% to the $PM_{2.5}$ in the summer, PoM (S-O), PoM (N) and winter seasons respectively.

The EC contribution in the summer, PoM (S-O), PoM (N) and winter seasons was observed to be 8.76%, 16.42%, 29.06% and 10.83% respectively in the urban area and 14.85%, 15.23%, 35.21% and 20.72% respectively in the rural area.

At the urban site, a gradual seasonal increase in the OC concentrations could be seen (see Table 3.2). The seasonal trend followed by OC values at the urban site is Winter > PoM (N) > PoM (SO) > Summer whereas at the rural site it is PoM (N) > Winter > PoM (SO) > Summer. OC concentrations were 2 times (approx.) higher at the Shahdara site than Sampla during the summer and PoM (SO) whereas in the month of November they were 2 times higher at Sampla site than Shahdara. OC concentrations were comparable in the winter season.

At both the sites, EC concentrations were found to be increasing from summer till Post-Monsoon season but decreased in the winter season. The increasing trend followed by the EC concentrations at both urban and rural sites is PoM (N) > Winter > PoM (SO)> Summer. Very high EC concentrations were observed during the month of November at both the urban and rural sites which may be due to the large scale agricultural residue burning activities in the neighbouring states of Haryana and Punjab in addition to the local sources already present at the two sites.

At the urban site, not much significant variation in the OC/EC ratio could be observed at urban site. At the Shahdara site, the OC/EC ratio in summer and winter (maximum) is almost comparable whereas in the PoM (S-O) and PoM (N) they were lowest as well as not much variable (Table 3.2). At the Sampla OC/EC ratio increased from summer to winter by a factor of ~ 3. OC/EC ratio at rural site was maximum in Winter and minimum in PoM (SO). However, during the PoM season, like urban, were lowest and not much variable. On comparing the two sites, the OC/EC ratios, except during the summer season, were observed to be higher in the rural area than urban area in both PoM and winter seasons. OC/EC ratio

was slightly higher at the urban site than rural site during the summer season. During the winter season, rural OC/EC ratio was approximately 2 times higher than the urban ratio.

However, the result did not indicate a significant variation in the urban and rural carbonaceous content as expected. This may be due to the close proximity of the two sites (~ 60 kms). The transport of aerosols by air may affect the concentrations of carbonaceous content at the two sites. Table 3.3 provides the minimum and maximum values of EC, OC and OC/EC ratio at Shahdara and Sampla in different seasons.

Table 3.3. The minimum and maximum values of EC, OC (all in μg/m^3) and OC/EC ratio at Shahdara and Sampla in different seasons.

Seasons		**Urban** (μg/m^3)						**Rural** (μg/m^3)					
		OC		EC		OC/EC		OC		EC		OC/EC	
		Min.	Max.	Min.	Max.	Max.	Min.	Min.	Max.	Min.	Max.	Min.	Max.
Summer		10.76	24.64	2.82	14.99	1.15	4.48	4.06	14.23	2.53	10.09	0.65	5.01
Post-Monsoon	September-October	12.02	42.62	13.05	20.08	0.86	2.46	7.38	20.88	2.59	14.69	0.71	5.02
	November	17.99	63.46	21.49	69.15	0.74	2.49	35.29	92.64	26.50	58.69	1.16	3.25
Winter		18.57	96.98	12.04	23.47	0.79	6.61	34.26	65.68	2.60	44.16	0.95	18.41

3.1.7 Secondary Organic Carbons (SOCs):

Table 3.4 below gives the seasonal concentrations of the secondary organic carbons along with their standard deviations and percentage contribution to the organic carbon at the Shahdara and Sampla sampling sites. The secondary organic carbons (SOCs) were calculated using the measured concentrations of OC and EC (Previous section). EC tracer method is used for the SOC estimation using the minimum OC/EC ratio in different seasons. Further details regarding this method can be found in various literatures (Turpin and Huntzicker 1995; Castro et al. 1999; Ram et al. 2008). The minimum OC/EC ratios are different (Table 3.2) in different seasons as the major sources of carbonaceous aerosols are also different. Rastogi et al. (2016) have also reported SOC estimation using different minimum OC/EC ratios. Therefore, the estimated contribution of SOCs from this method can be considered as approximate values only.

Table 3.4 Secondary organic carbon (SOCs) concentrations with standard deviation (SD) and their % contribution to organic carbon (OC) at Shahdara and Sampla sites in different seasons.

Season		Urban		Rural	
		SOC (± SD)	%contribution to OC	SOC (± SD)	%contribution to OC
Summer		6.42 (±3.58)	45.50	5.79 (±5.20)	48.95
Post-Monsoon	September-October	8.66 (±10.39)	27.85	5.78 (±5.36)	44.25
	November	11.33 (±15.04)	25.89	23.37 (±25.97)	29.27
Winter		31.24 (±32.25)	57.41	27.67 (±21.76)	56.99

As can be inferred from the Table 3.4, the % contribution of SOCs in the urban area is less as compare to the rural area except during the winter season where the contribution is almost comparable. During the summer season, the SOCs contributed 45.50 % to OC content in the urban area as compare to the 48.95% in the rural area. However, the SOC contribution is lowest (25.89%) in the month of November and the maximum (56.99%) contribution is observed in the winter season over the urban area indicating that the combustion sources were the main contributor to the OC concentrations during PoM (N). Similarly, in the rural area, the maximum contribution is observed in the winter season and lowest in the month of November. The seasonal trend in the SOCs contribution observed at both the Shahdara and Sampla sites is Winter > summer> Post-monsoon.

3.2 Solar irradiance studies over Delhi-NCR

This chapter describes the seasonal variation of the Global and Direct irradiance components of the incoming solar radiation over the urban and rural regions in the Delhi-NCR. The measurement of the solar irradiance gives an insight into the attenuation of the incoming solar radiation over a region and the level of pollution present in the atmosphere. The seasonal variation in the solar irradiance over Shahdara and Sampla sampling site is described below:

3.2.1 Global Irradiance Observations:

Summer Season

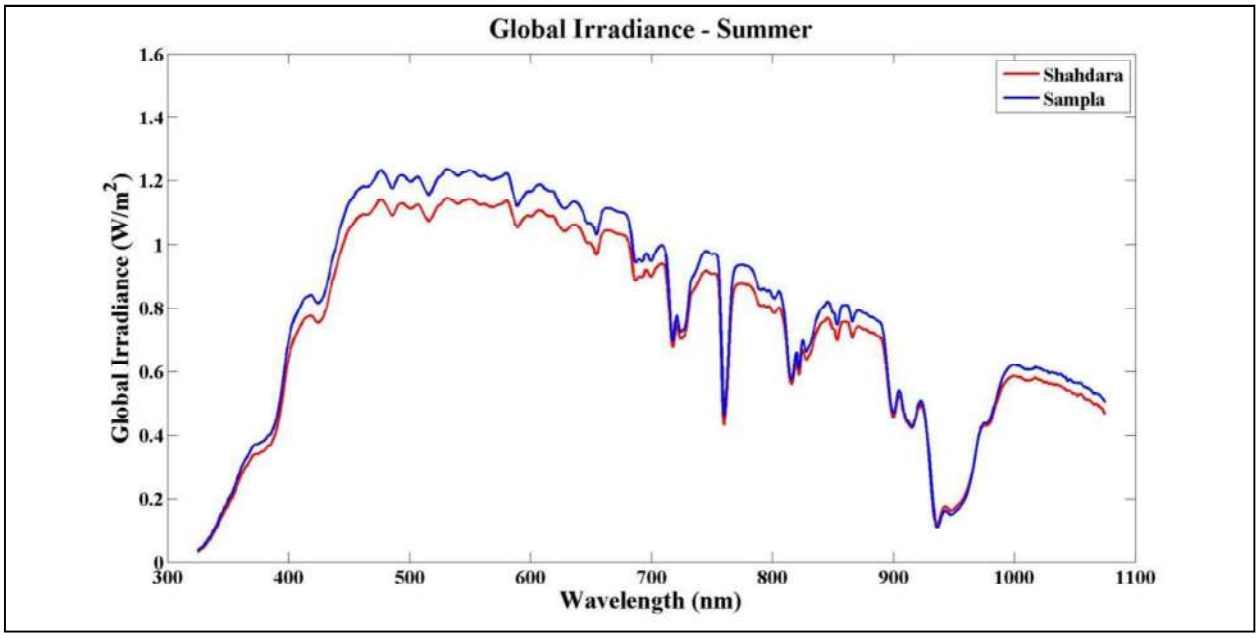

Figure 3.15. Variation of Global Irradiance at Shahdara and Sampla during Summer season.

Figure 3.15 shows the variation of the average global irradiance over two sites in Delhi-NCR in summer. The average global solar irradiance was found to be higher at Sampla (maximum=1.24 Wm^{-2} at 531 nm) than Shahdara (maximum=1.15 Wm^{-2} at 531 nm) in summer season. As observed there was no shift in the maxima at the two sites. Global irradiance for the two sampling sites shows a maximum variation in the visible region (VR) followed by slight variation in the near infrared region (NIR) of the solar spectrum. Latha and

Badrinath (2005) also reported similar variations in global irradiance over Hyderabad. But at shorter and longer wavelengths there is not much variation in the global solar irradiance at the two sampling sites.

Post-Monsoon Season (September-October)

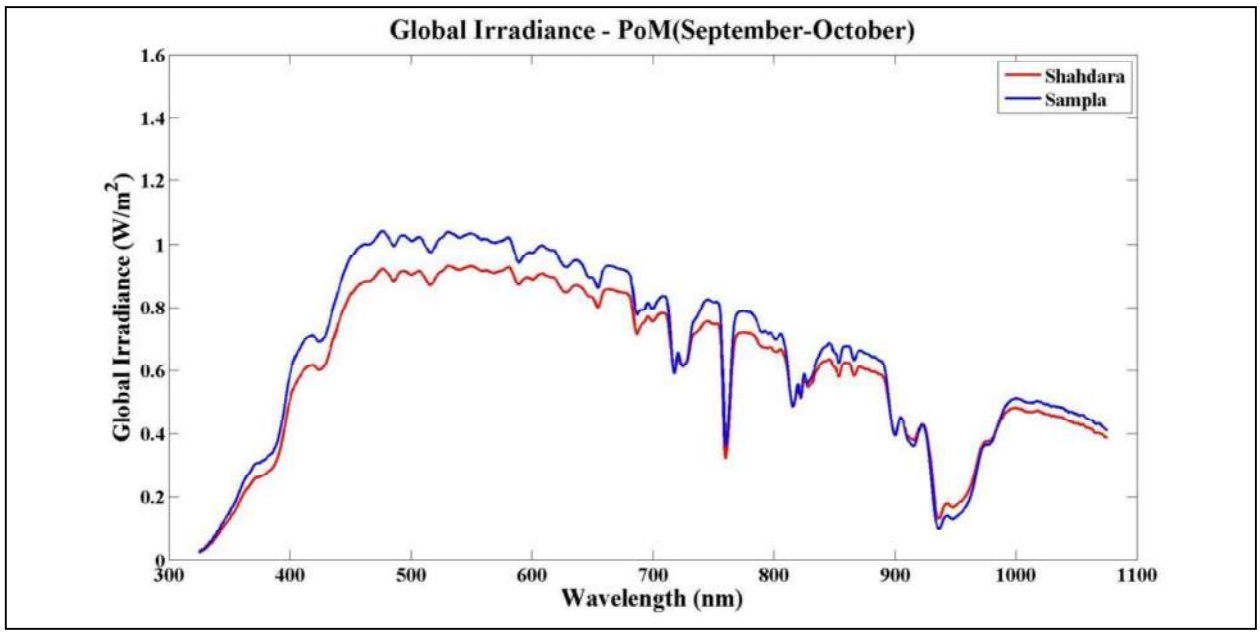

Figure 3.16. Variation of Global Irradiance at Shahdara and Sampla during PoM (Sept-October) season.

Figure 3.16 shows the variation of the average global irradiance over Delhi-NCR in PoM (Sept-October) season. The average global solar irradiance was observed to be higher at Sampla (maximum=1.04 Wm^{-2} at 477 nm) than Shahdara (maximum=0.93 Wm^{-2} at 531 nm) in summer season. A shift in the maxima at the two sites can be observed. A good variation in the average global irradiance can be observed between the Shahdara and Sampla sites in the visible region (VR) and near infrared region (NIR) of the solar spectrum. But at shorter and longer wavelengths there is a poor variation in the global solar irradiance between the two sampling sites.

Post-Monsoon (November)

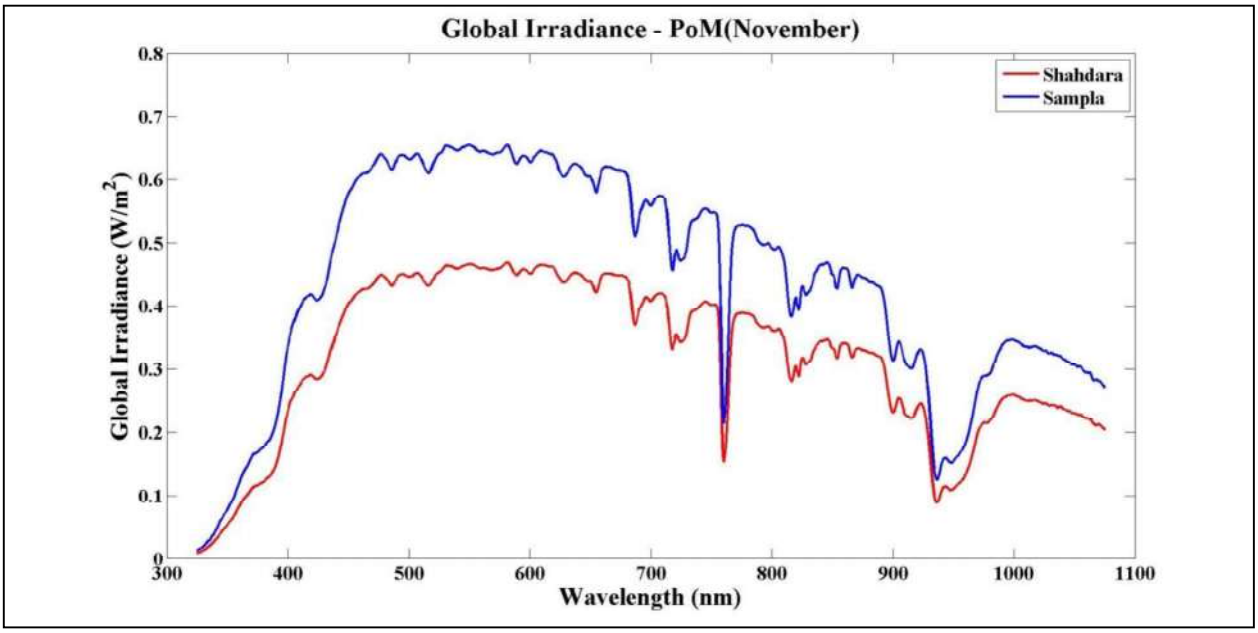

Figure 3.17. Variation of Global Irradiance at Shahdara and Sampla during PoM (November) season.

Figure 3.17 shows the variation of the average global irradiance at the Shahdara and Sampla sampling sites in the month of November in the post-monsoon season. The average global solar irradiance was found to be higher at Sampla (maximum= 0.65 Wm^{-2} at 581 nm) than Shahdara (maximum= 0.47 Wm^{-2} at 581 nm) in the month of November. No shift in the maxima is observed between the two sites. Global irradiance at the two sampling sites shows a significant variation throughout the entire solar spectrum.

Winter Season

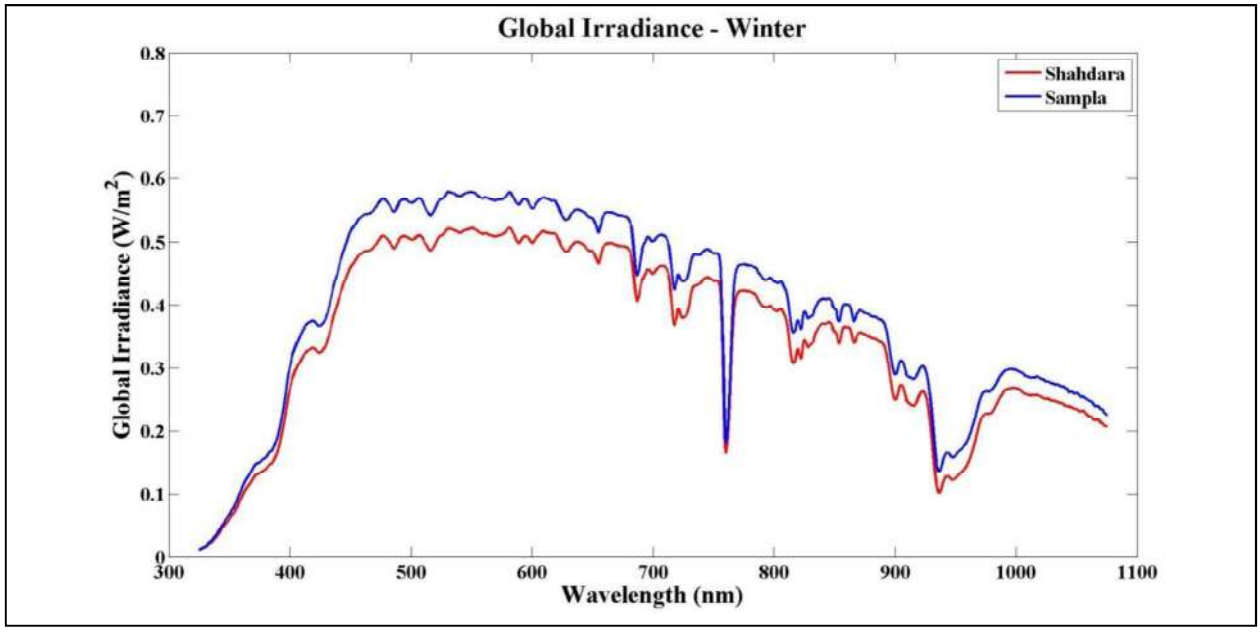

Figure 3.18. Variation of Global Irradiance at Shahdara and Sampla during Winter season.

The variation of the average global irradiance at the Shahdara and Sampla sites in winter is shown in Figure 3.18. The average global solar irradiance was observed to be higher at Sampla (maximum=0.58 Wm^{-2} at 531 nm) than Shahdara (maximum=0.52 Wm^{-2} at 581 nm) in winter season. This may be on account of high pollution levels at the urban site compare to rural site during this season. The variation in the visible and near infrared region could be observed. However, in the UV region not much variation in the global irradiance values could be observed.

3.2.2 Direct Irradiance Observations:

Summer Season

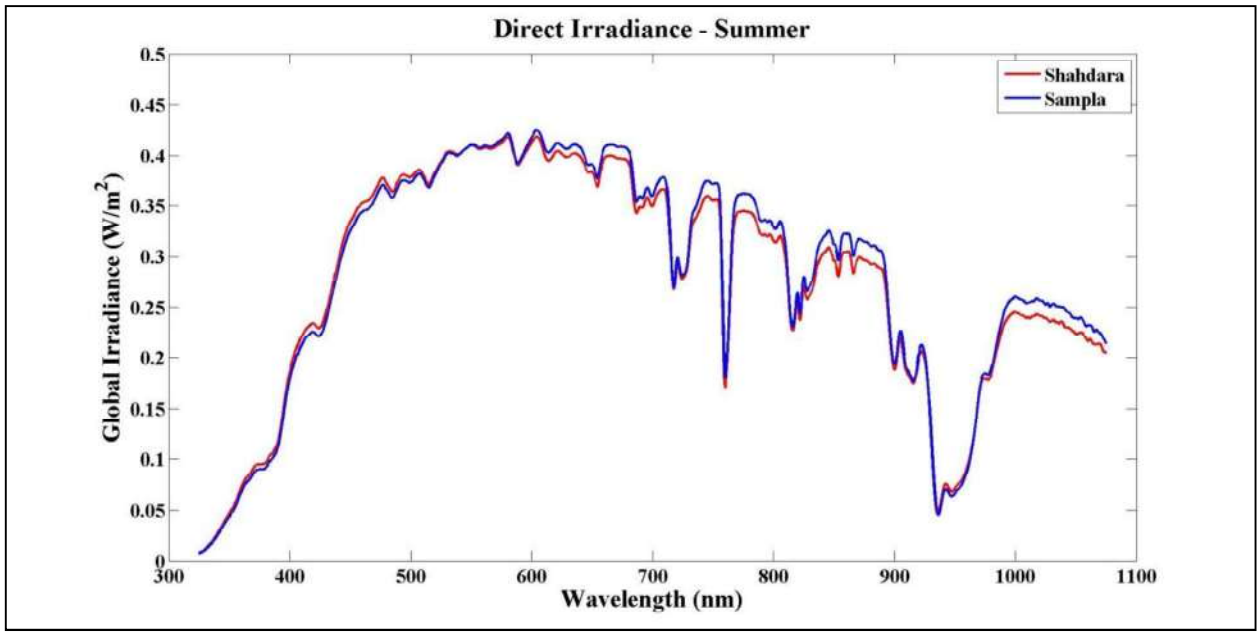

Figure 3.19. Variation of Direct Irradiance at Shahdara and Sampla during Summer season.

Figure 3.19 shows the variation of the average direct irradiance at the Shahdara and Sampla sites in Delhi-NCR respectively, in summer season. The observed direct irradiance values were similar at the two sites during the summer season. The average direct irradiance was observed in Sampla with maximum = 0.424 Wm^{-2} at 604nm and Shahdara with maximum = 0.428 Wm^{-2} at 604nm. However, a slight, though not very significant, variation in the near infrared region of the spectrum could be seen. The comparable direct irradiances at the urban and rural sites could be due to the presence of dust aerosols which scatters the incoming solar radiation, on account of dust storms and wind-blown dust from the vast agricultural fields during this season.

Post-Monsoon Season (September-October)

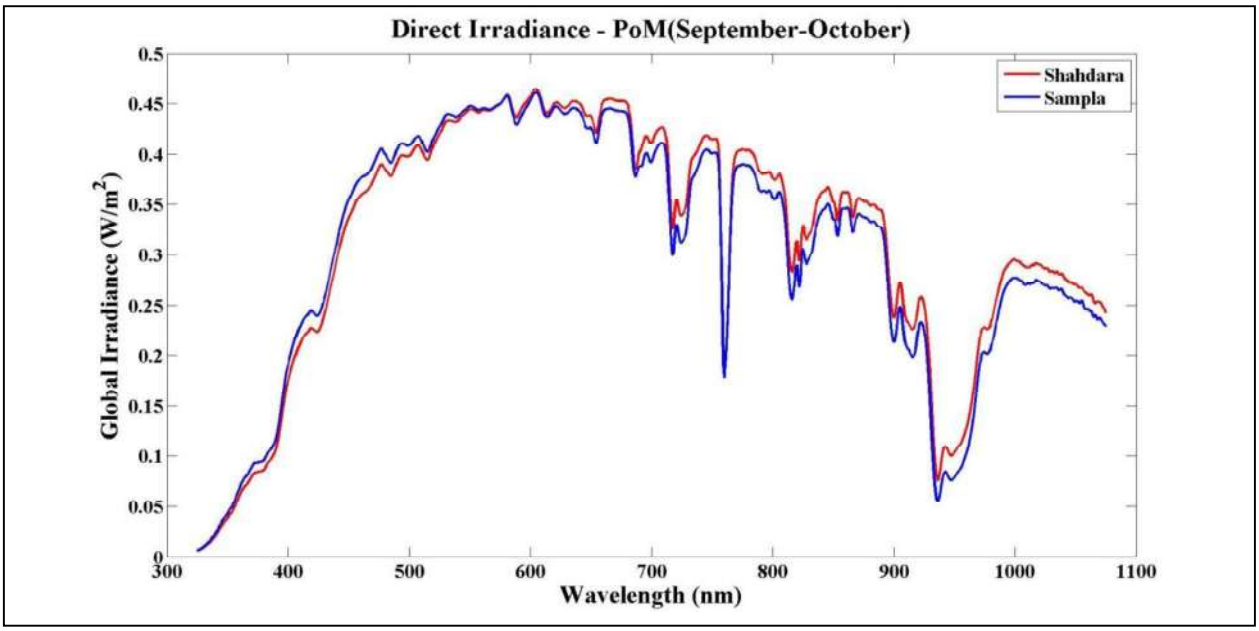

Figure 3.20. Variation of Direct Irradiance at Shahdara and Sampla during PoM (Sept-October) season.

Figure 3.20 shows the variation of the average direct irradiance at the Shhadara and sampla sites during the PoM (S-O) season. The average direct irradiance was found to be slightly lower in Sampla with (maximum=0.461 Wm^{-2} at 605nm) than Shahdara (maximum=0.465 Wm^{-2} at 604 nm). Direct irradiance did not show much variation in the VR and NIR of the solar spectra; however, slight variation can be seen in the longer wavelengths of the solar spectrum. Such negligible variation in the direct irradiances during this season could be due to the presence of high altitude clouds which are not otherwise visible to the naked eye.

Post-Monsoon (November)

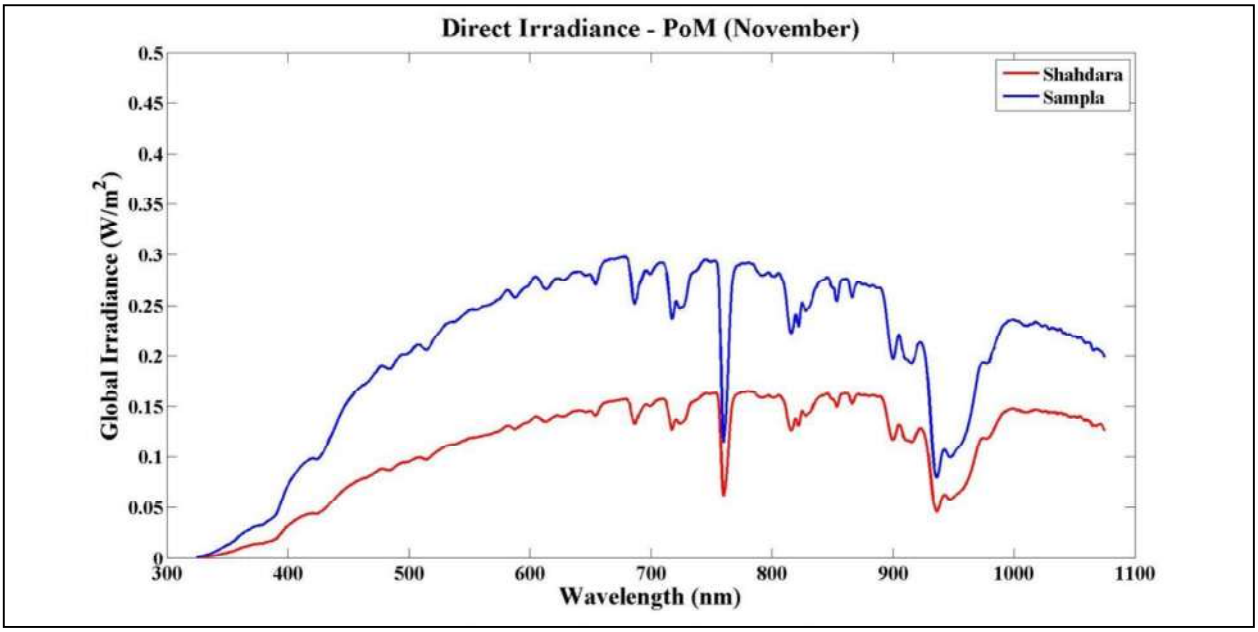

Fig. 3.21. Variation of Direct Irradiance at Shahdara and Sampla during PoM (November) season.

Figure 3.21 gives the variation of the average direct irradiance over Delhi-NCR sites in November. A significant variation in the direct irradiances at the Shahdara and Sampla sampling sites could be observed in the PoM (N). The average direct irradiance was found to be higher in Sampla with (maximum = 0.30 Wm^{-2} at 678nm) than Shahdara (maximum= 0.17 Wm^{-2} at 780nm) in PoM (N).

Winter Season

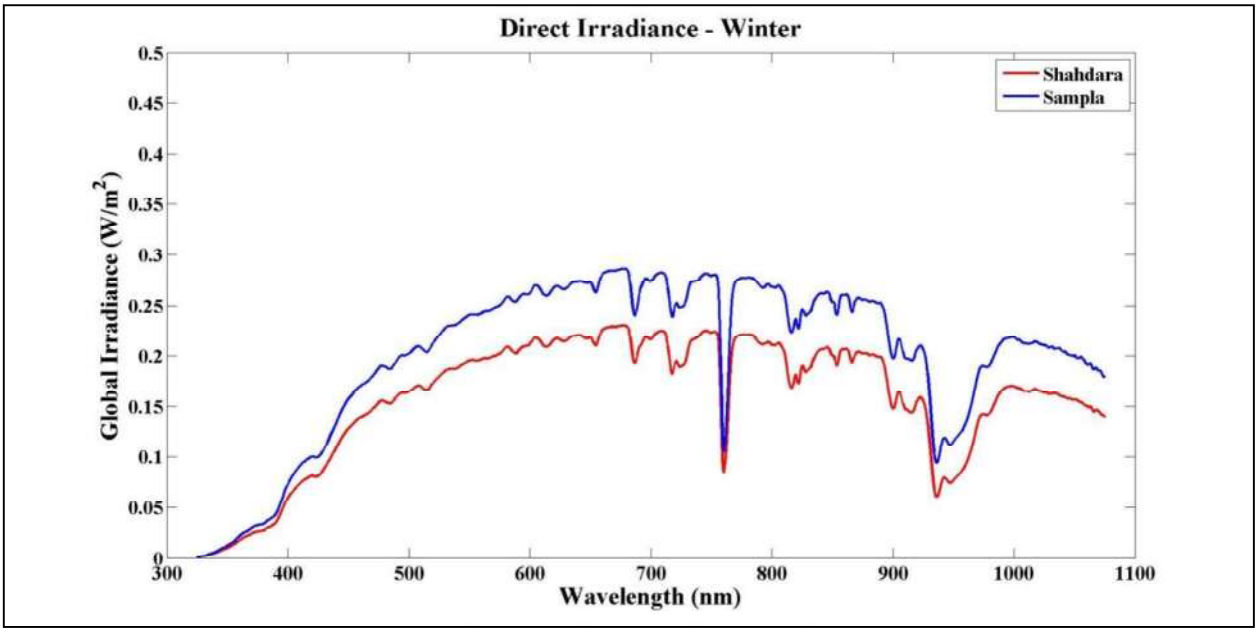

Fig.3.22. Variation of Direct Irradiance at Shahdara and Sampla during Winter season.

Figure 3.22 shows the variation of the average direct irradiance over Delhi-NCR respectively, in winter. The average direct irradiance was found to be higher in Sampla with (maximum=0.29 $Wm^{-2}nm^{-1}$ at 678nm) than Shahdara (maximum=0.23 $Wm^{-2}nm^{-1}$ at 678nm) in summer 2015. There is no shift in the maximum at the urban and rural site. Direct irradiance is found to be varying considerably in the VR and NIR of the solar spectra.

3.2.3 Global and Direct irradiances averaged over 325-1075nm wavelength band:

The global and direct irradiance for the entire wavelength band 325-1075 nm have been observed (Table3.5). From Table (3.5) it can be observed that the global and direct insolation decreased from summer (maximum) to winter. The global insolation was found o be the minimum during the PoM (N) at the urban site indicating the greater attenuation of solar irradiance at the urban site during this period. Again, the solar irradiance (both global and direct) was observed to be increasing from the PoM (N) to winter season at the urban site indicating the effect of the aerosols on the solar radiation. But at the rural site it was found to be comparable in both the PoM (N) and winter seasons.

Table 3.5 The global and Direct Irradiance (Wm^{-2}) value for the 325-1075 nm wavelength band

		Global Irradiance (Wm^{-2})		Direct Irradiance (Wm^{-2})	
		Shahdara	Sampla	Shahdara	Sampla
Summer		559.01	595.88	208.19	211.91
Post-Monsoon	Sept-Oct	459.72	498.34	232.02	231.45
	November	238.87	294.06	84.50	155.07
Winter		262.94	293.96	118.88	150.51

Discussion

As can be seen from the solar radiance studies over Delhi and Haryana, both global and direct irradiances have been consistently low over the urban site showing a "dimming" effect over the urban area, as compare to the rural site in almost all the seasons viz. summer, PoM and winter seasons. These studies show that the effect of air pollution is more pronounced in the urban area as compared to the rural area. As is indicated by the $PM_{2.5}$ concentration levels in the previous section, the concentration level increased from summer to winter. Correspondingly, the average global irradiance values at the urban site observed a shift in the maximum from summer (531 nm) to more polluted PoM (N) & winter season (both at 581 nm) towards the longer wavelengths. Similar shift in the maximum global irradiance from clean to polluted days towards the longer wavelengths have been observed in other studies by (Lorente et al. 1993; Jacovides et al. 2000). Similar shift have been observed for the direct irradiance maximum as well. However, at the rural area, shift in the maximum values of global and direct irradiances from summer season (less polluted) occurs in the PoM (N) and Winter seasons (most polluted) only. This may be due to the large scale agricultural residue burning during this month by the farmers. Attenuation processes such as scattering and absorption by the aerosols may cause a change in the solar radiation under the absence of cloud in the atmosphere.

3.3 Urban-Rural aerosol characteristics and Solar Insolation Relationship

The figures 3.23 shows the association between the difference in $PM_{2.5}$ concentrations ($PM_{2.5\ (Diff.)}$) between the two sites and integrated global solar irradiance at the Shahdara and Sampla sampling sites during the summer, post-monsoon and winter seasons. Similarly, figure 3.24 shows the $PM_{2.5\ (Diff.)}$ and direct irradiance association during the three seasons at the Shahdara and Sampla sampling sites.

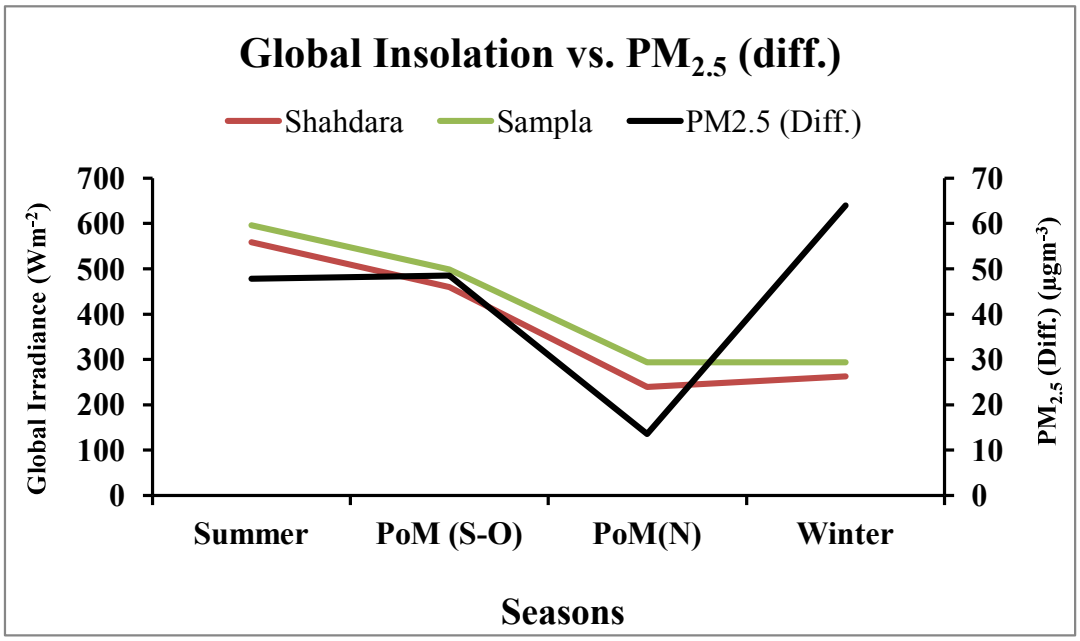

Figure 3.23. Seasonal associations of the $PM_{2.5}$ (difference) concentration and global solar irradiance at the Shahdara and Sampla.

Table 3.6 shows the variation of the difference in $PM_{2.5}$ concentration and Global and Direct irradiances at the Shahdara and Sampla sites. Global irradiance is always higher at the Sampla site than the Shahdara site in all the seasons. During the summer season, the difference in $PM_{2.5}$ concentration is high (47.84 $\mu g/m^3$) and global irradiance is high at both the sites (around 500 Wm^{-2}). In the PoM (S-O), the concentration difference increases slightly, the global irradiance also decreases at both the sites. The difference in the $PM_{2.5}$ concentrations is lowest in the month of November at the two sites and the global irradiance is also lowest during this month. As during the PoM (N), extensive biomass burning activities greatly increases the amount of aerosols in the atmosphere which may lower the amount of

solar irradiance reaching the Earth's surface. But in the winter season, even though the concentration difference increases from November (and is maximum), there is a slight increase in the global irradiance at both the sites.

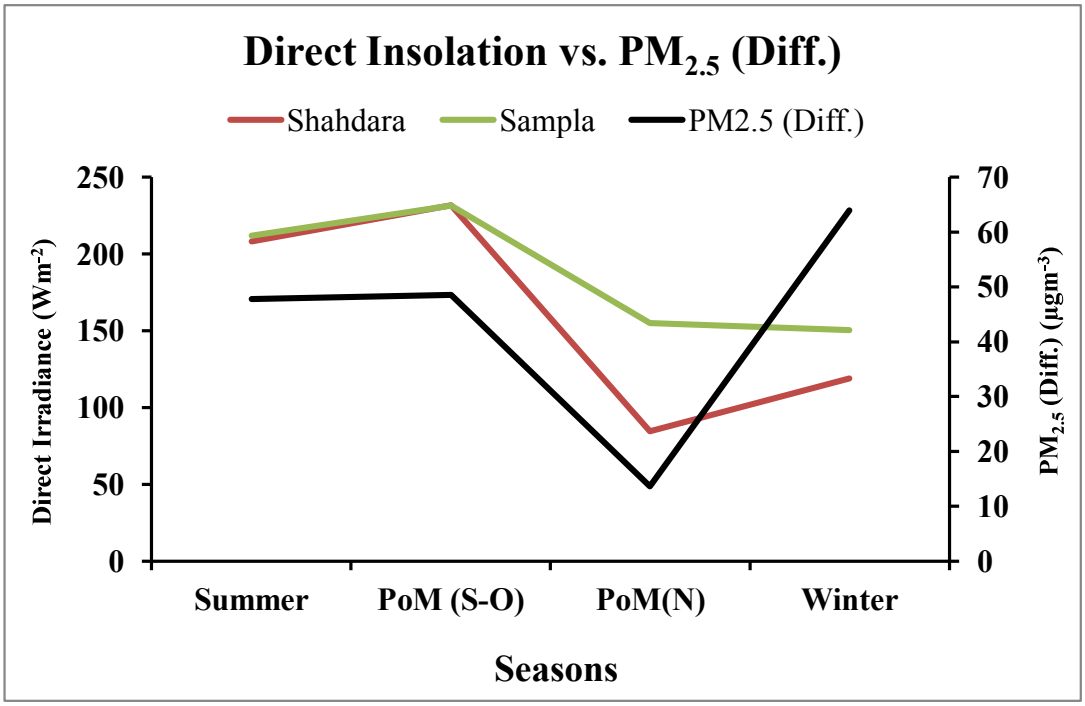

Figure 3.24. Seasonal associations of the $PM_{2.5}$ (difference) concentration and direct solar irradiance at the Shahdara and Sampla.

From figure 3.24, the direct solar irradiance is comparable at both the Shahdara and Sampla site in the summer season. During the post-monsoonal months of September-October, there is a slight increase in the $PM_{2.5}$ concentration difference, but the direct irradiance is higher in the Shahdara site as compared to the Sampla site. Again in the month of November, the difference in the concentration is the minimum but there is a sharp dip in the direct irradiance over Shahdara site (64.03 Wm^{-2}) from the PoM (S-O) compare to the Sampla site (155.07 Wm^{-2}). Further, during the winter season, the concentration difference is maximum, the direct irradiance increases (84.50 to 118.88 Wm^{-2}) significantly over Shahdara site but at the Sampla site there is a slight decrease in the direct irradiance values (155.07 to 150.51 Wm^{-2}).

Table 3.6 Seasonal variations of the $PM_{2.5}$ concentration difference, Global and Direct Irradiance at Shahdara and Sampla sites.

		$PM_{2.5}$ Concentration (Difference) ($\mu g/m^3$)	Global Irradiance (Wm^{-2})		Direct Irradiance (Wm^{-2})	
			Shahdara	Sampla	Shahdara	Sampla
Summer		47.84	559.01	595.88	208.19	211.91
Post-Monsoon	Sept-Oct	48.60	459.72	498.34	232.02	231.45
	November	13.62	238.87	294.06	84.50	155.07
Winter		63.93	262.94	293.96	118.88	150.51

3.3.1 Carbonaceous aerosols and solar irradiance

This section deals with the seasonal association of the carbonaceous aerosols- elemental and organic carbon with the global and direct solar irradiances at the wavelength of 550nm at the Shahdara and Sampla sites.

Figures 3.25 and 3.26 show the association between the organic carbon and solar irradiances at 550 nm wavelength at the Delhi and Haryana site respectively. Figure 3.27 and 3.28 show the association between the elemental carbon (EC) and direct and global irradiance at 550 nm wavelength at the Delhi and Haryana sites respectively.

3.3.2 Organic Carbon (OC) and Solar irradiance association

As can be seen from the figure 3.25 and 3.26, there is a negative association between the OC and solar irradiance at Shahdara and Sampla sampling sites.

At Shahdara Site

Figure 3.25 shows the seasonal association of the organic carbon and solar irradiance (global and direct) at Shahdara site. During the summer and PoM (S-O), the OC content is low but the global irradiance is high but direct irradiance is low. But during the PoM (N), the OC content increases on account of biomass burning in the surrounding rural area and the local pollution levels during that period, both direct and global irradiance take a sharp dip from the PoM (S-O). However, during the winter season, OC is maximum in Delhi but direct and global irradiances increases slightly from the PoM (N). Even though the pollution level was observed to be higher during this season, sky was generally clear during the sampling duration. This could be the reason for an increase in direct solar irradiance from the month of November during the winter season.

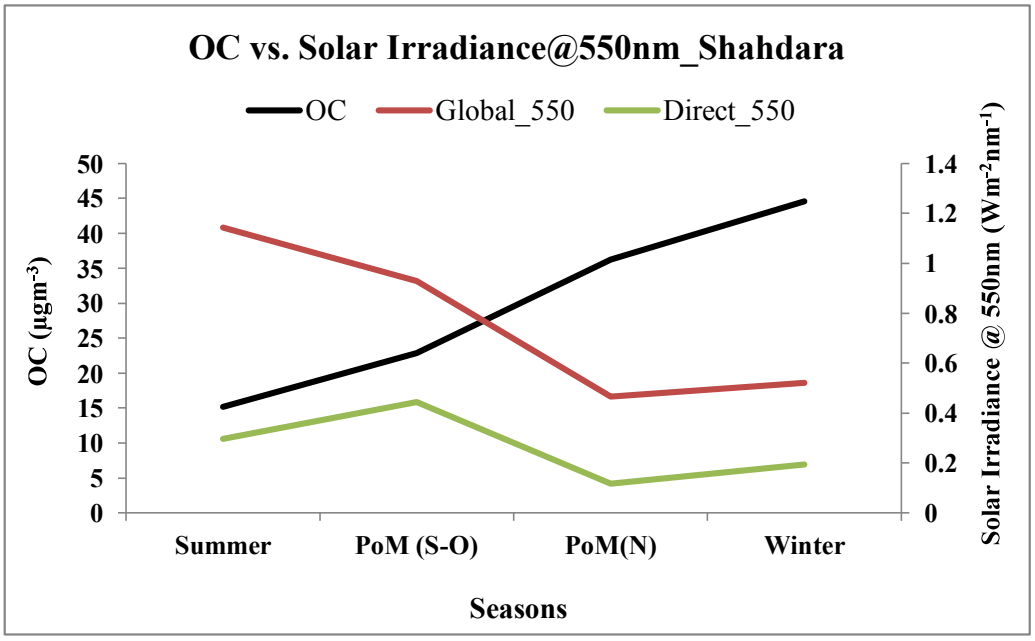

Figure 3.25 The seasonal association of the organic carbon (OC) and solar irradiance (global and direct) at Shahdara site.

At Sampla site

Similar pattern has also been observed in the Sampla (rural site) (figure 3.26). During the Summer and PoM (S-O), the OC levels are low, global and direct irradiances are also high but during the PoM (N), solar irradiances are minimum, when the OC is maximum. The OC levels drop sharply during the winter but the direct and global irradiances increases slightly from the PoM (N) levels. This shows the effect of aerosols on the solar irradiance produced during the biomass burning activities in the PoM (N) season.

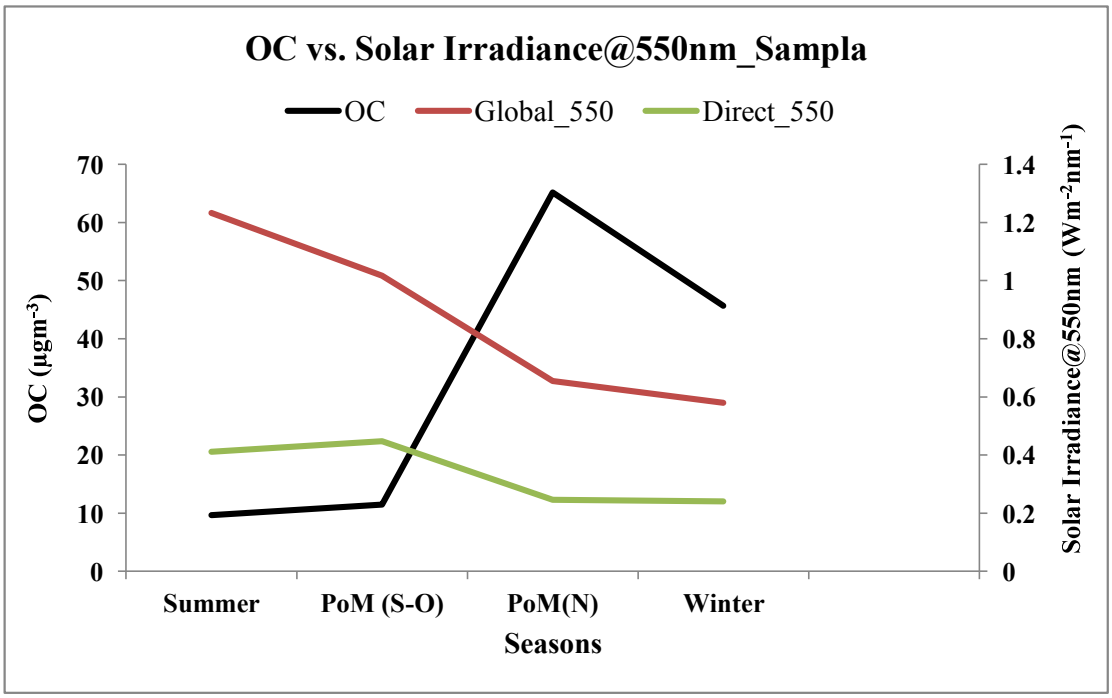

Figure 3.26 The seasonal association of the organic carbon (OC) and solar irradiance (global and direct) at Sampla site.

3.3.3 Elemental carbon (EC) and Solar Irradiance Association

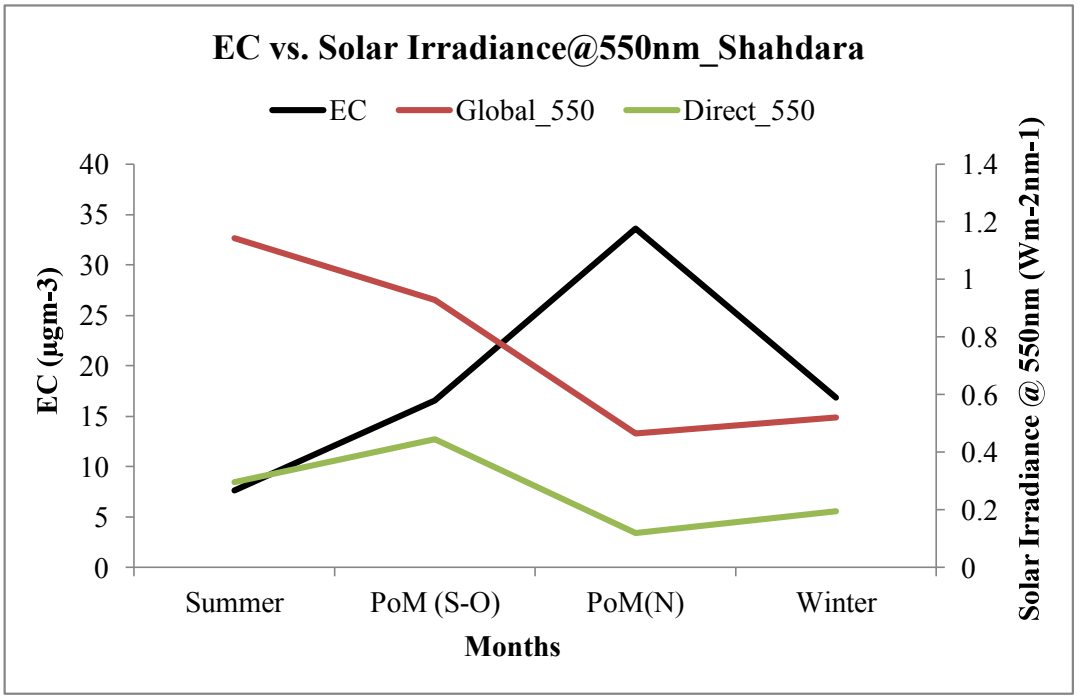

Figure 3.27 The seasonal association of the elemental carbon (EC) and solar irradiance (global and direct) at Shahdara site.

The association of EC is observed to be similar to that of OC with the solar irradiances at the Shahdara site (Figure 3.27). During the summer season, EC is minimum in the Delhi with a high global and low direct irradiance values. But in the PoM (S-O) season, the direct irradiance is maximum but global irradiance decreases from summer in Shahdara. From June to November there is sharp and steady increase in the EC values. However, during the month of November, direct irradiance is minimum when the EC is maximum. In the winter season, the EC values observe a sharp dip from the November with an increase in the global and direct irradiances.

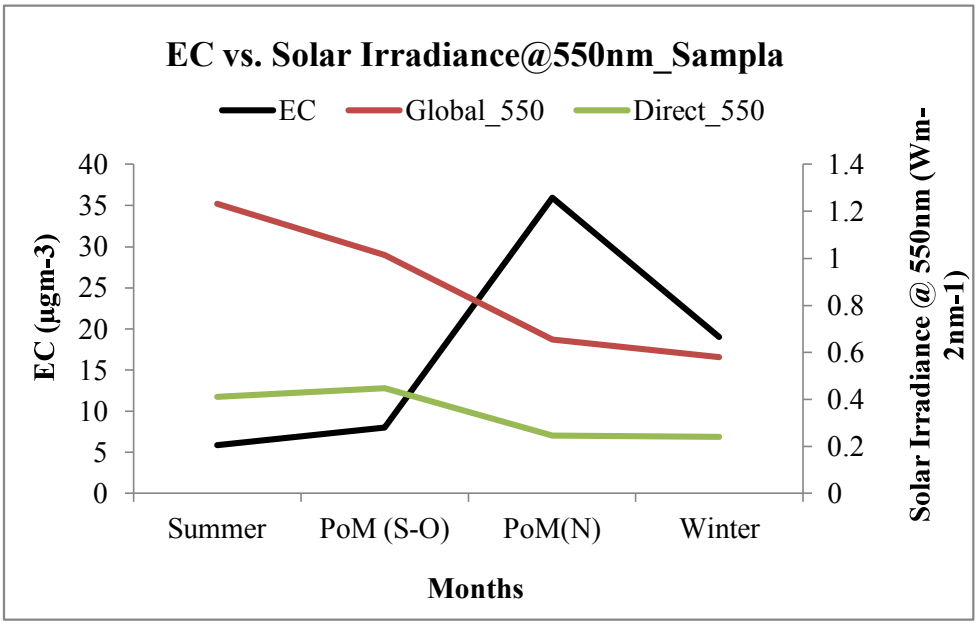

Figure 3.28 The seasonal association of the elemental carbon (EC) and solar irradiance (global and direct) at Sampla site.

Similar association has been observed at the rural site (Figure 3.28). As the EC values increase from the Summer (minimum) to Winter with PoM (N) showing the maximum value, the solar irradiance values - both global and direct, decreases gradually from summer (maximum) to winter season with a minimum in PoM (N) season. At the Sampla site as well, a slight increase in the solar irradiances is observed in the winter season from PoM (N) season.

3.4 Radiative Forcing

Figures 3.31, 3.32, 3.33 and 3.34 shows the variation of the CERES measured outgoing shortwave fluxes at surface (SRF) and at top of the atmosphere (TOA) and co-located MODIS-Aqua observed aerosol optical depth (AOD) at 550nm for the April-May-June (AMJ) months comprising Pre-Monsoon (PrM), September-October-November (SON) as Post-Monsoon (PoM) and December-January-February (DJF) as winter (W) seasons over Delhi and Haryana sampling sites. Table 3.7 and 3.8 list the radiative forcing efficiency (η, in $Wm^{-2}AOD^{-1}$) and clear sky fluxes at SRF and TOA over Delhi and Haryana sites in PrM, PoM and W seasons, respectively. The calculated aerosol radiative forcings and associated errors/uncertainties are shown in Table 3.9 and 3.10 at SRF, TOA and in the atmosphere over Delhi and Haryana respectively.

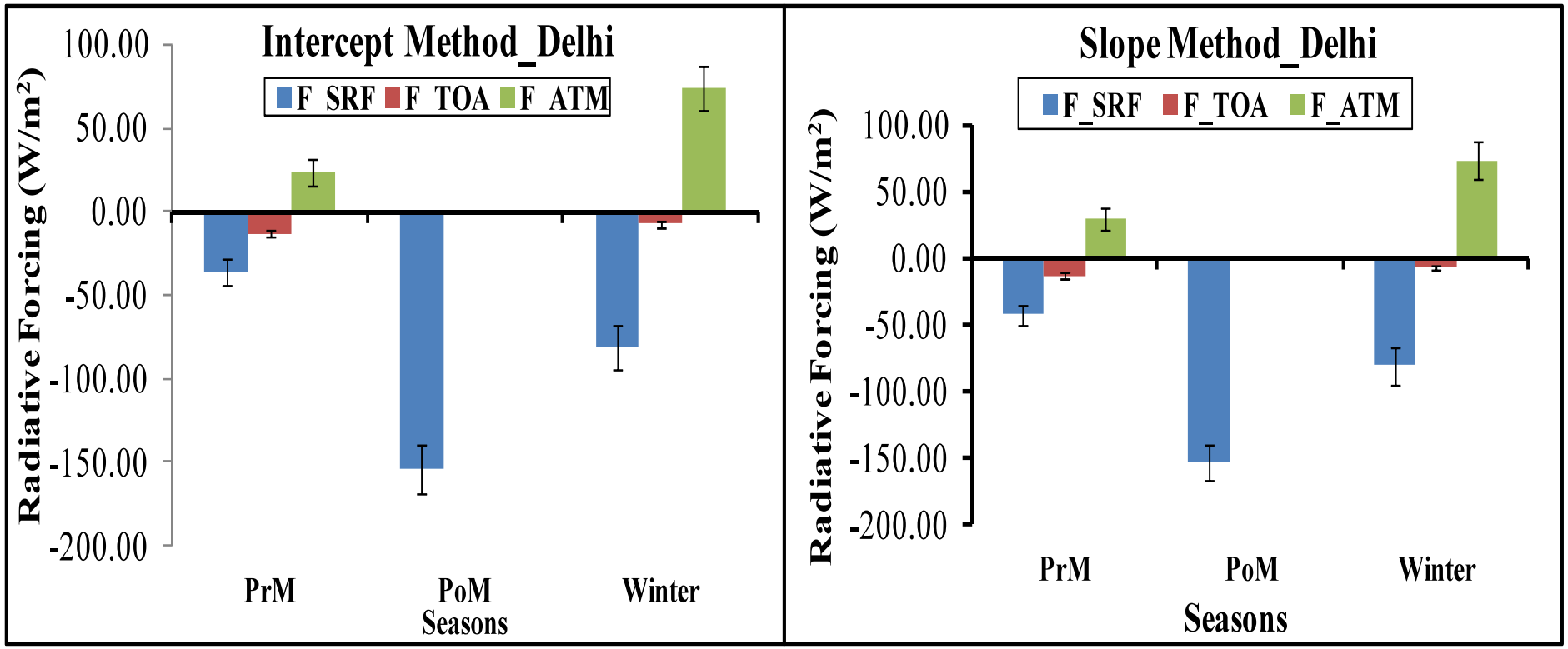

Figure 3.29. The Radiative Forcing over Delhi using Intercept and Slope Methods in Pre-monsoon (PrM), Post-monsoon (PoM) and Winter (W) season.

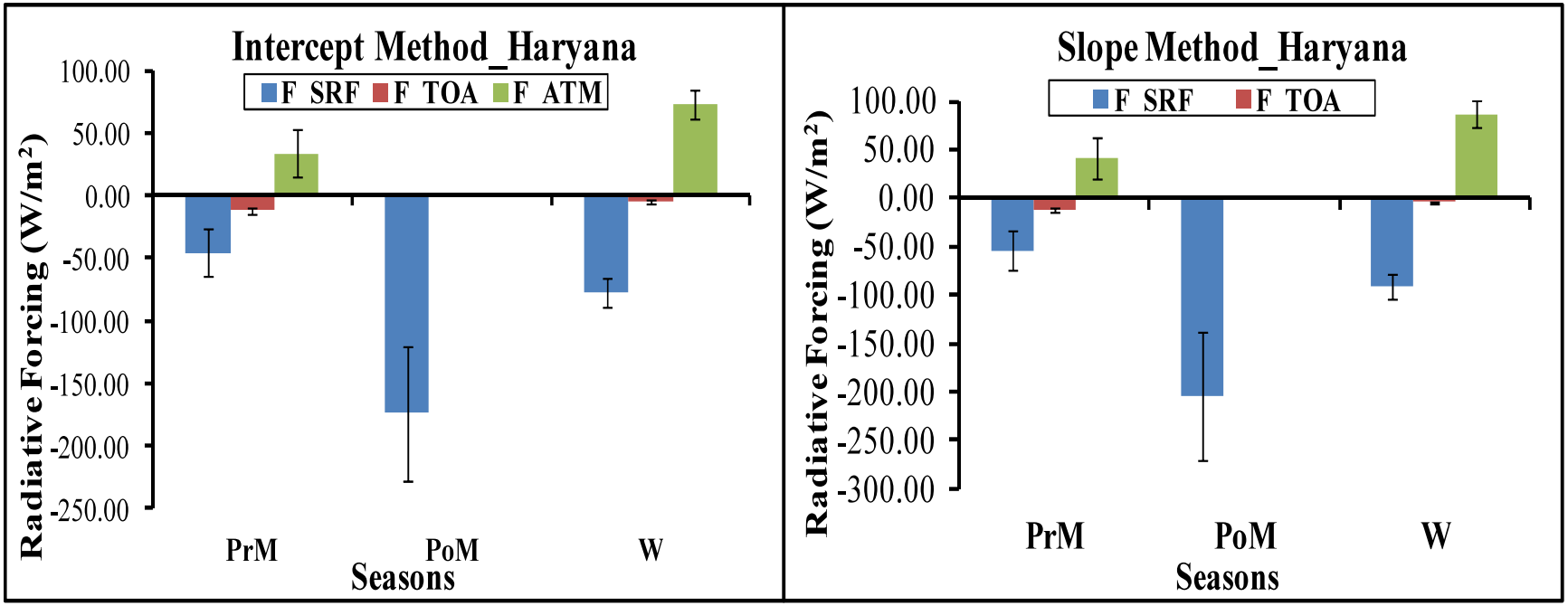

Figure 3.30. The radiative forcing over Haryana using Intercept and Slope Methods in Pre-monsoon (PrM), Post-monsoon (PoM) and Winter (W)seasons.

The aerosols properties such as AOD, single scattering albedo (SSA) and Angstrom exponent (AE) are listed in the Table 3.11.

The aerosol radiative forcing over Delhi and Haryana sites have been calculated using the slope and intercept method as explained in chapter 2. All the regression analyses were within 95% significant level ($p<0.05$) except in the PoM at TOA in Delhi which was below the 95% significant level. Hence the aerosol radiative forcing at TOA over Delhi in PoM has been excluded from the analysis. The TOA analysis over Haryana for the PoM season was also not performed because of the excessive cloud contamination in the data.

Aerosols short wave radiative forcing efficiency, η (in $Wm^{-2}AOD^{-1}$), represents the change in the short wave aerosol radiative forcing per unit change in AOD. The magnitude of η is given by the slope of the regression equations between AOD and fluxes at SRF and TOA respectively. However, its sign varies in both the cases. The sign of η at SRF is same as that of the slope in the regression equations but in the case of TOA, it is opposite to that of the slope of regression equations (Chapter 2). The radiative forcing efficiency in the atmosphere will be estimated by the difference between the η at the SRF and TOA.

The flux at SRF decreases with the increasing AODs indicating a negative association in all the three seasons. This negative association indicates the attenuation of the incoming solar radiation at the surface in all the three seasons over both Delhi and Haryana (Figure 3.31 & 3.22). The instantaneous radiative forcing efficiencies over Delhi are -47.908 $Wm^{-2}AOD^{-1}$ ($r = -0.31$), -219.19 $Wm^{-2}AOD^{-1}$ ($r = -0.65$), and -122.42 $Wm^{-2}AOD^{-1}$ ($r = -0.45$) during the PrM, PoM and W seasons, respectively. Similarly, over Haryana, the instantaneous radiative forcing efficiencies are -63.93 $Wm^{-2}AOD^{-1}$ ($r = -0.4$), -285.24 $Wm^{-2}AOD^{-1}$ ($r = -0.74$) and -134.7 $Wm^{-2}AOD^{-1}$ ($r = -0.48$) during the PrM, PoM and W seasons, respectively. The seasonal variability in the η values maybe due the seasonal variation in the aerosol composition. The observed η values were lower than the reported η values in other studies during the pre-monsoon season. Singh et al., 2005 reported -136.30 $Wm^{-2}AOD^{-1}$ during April- June 2003, Gautam et al., 2010 during the April-June (2006-2007) reported very high value of η (-188.00 $Wm^{-2}AOD^{-1}$) at the surface over Kanpur.

In contrast to the association of surface fluxes with the AOD, TOA fluxes have a positive association with the AOD. The TOA fluxes were observed to be increasing with the increasing AOD values in the PrM and W seasons over Delhi and Haryana (Figure 3.33 & 3.34). This increase in the fluxes at the TOA with the increasing AODs may indicate towards the backscattering of the incoming solar radiation by the aerosols thereby leading to cooling at the TOA. The instantaneous shortwave TOA radiative forcing efficiencies over Delhi are -15.22 $Wm^{-2}AOD^{-1}$ (r = 0.36) and -9.49 $Wm^{-2}AOD^{-1}$ (r = 0.30) during the PrM and W seasons respectively over Delhi. Similarly, over Haryana, the instantaneous radiative forcing efficiencies are -14.55 $Wm^{-2}AOD^{-1}$ (r = 0.40) and -6.44 $Wm^{-2}AOD^{-1}$ (r = 0.23) during the PrM and W seasons respectively. The relatively weak association of the outgoing shortwave fluxes at TOA with AOD could be due to the increased surface albedo. The average surface albedo over Delhi and Haryana during all the seasons, however, was observed to be constant 0.151 and 0.149 respectively.

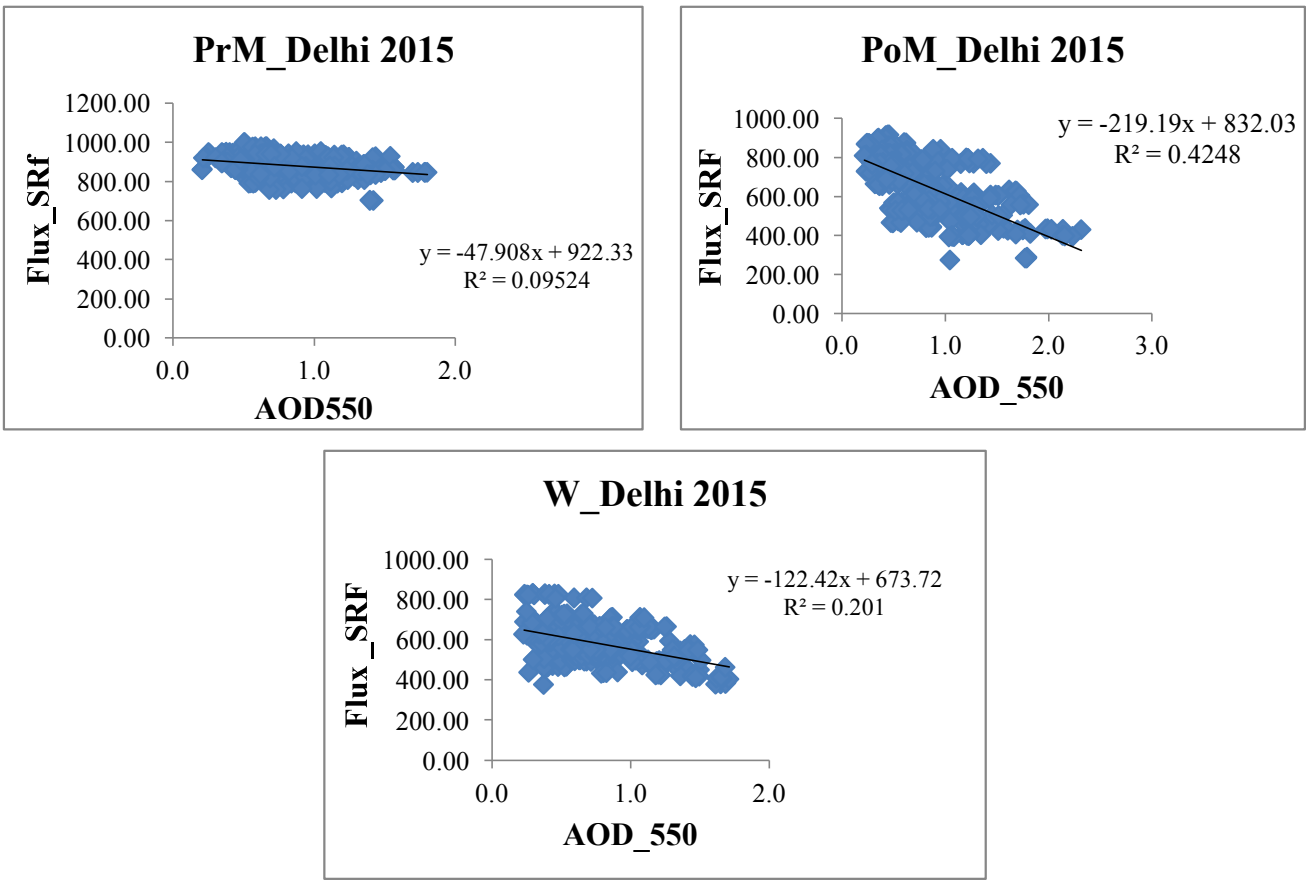

Figure 3.31. Variation of surface (SRF) solar fluxes in PrM, PoM and W seasons at Delhi site.

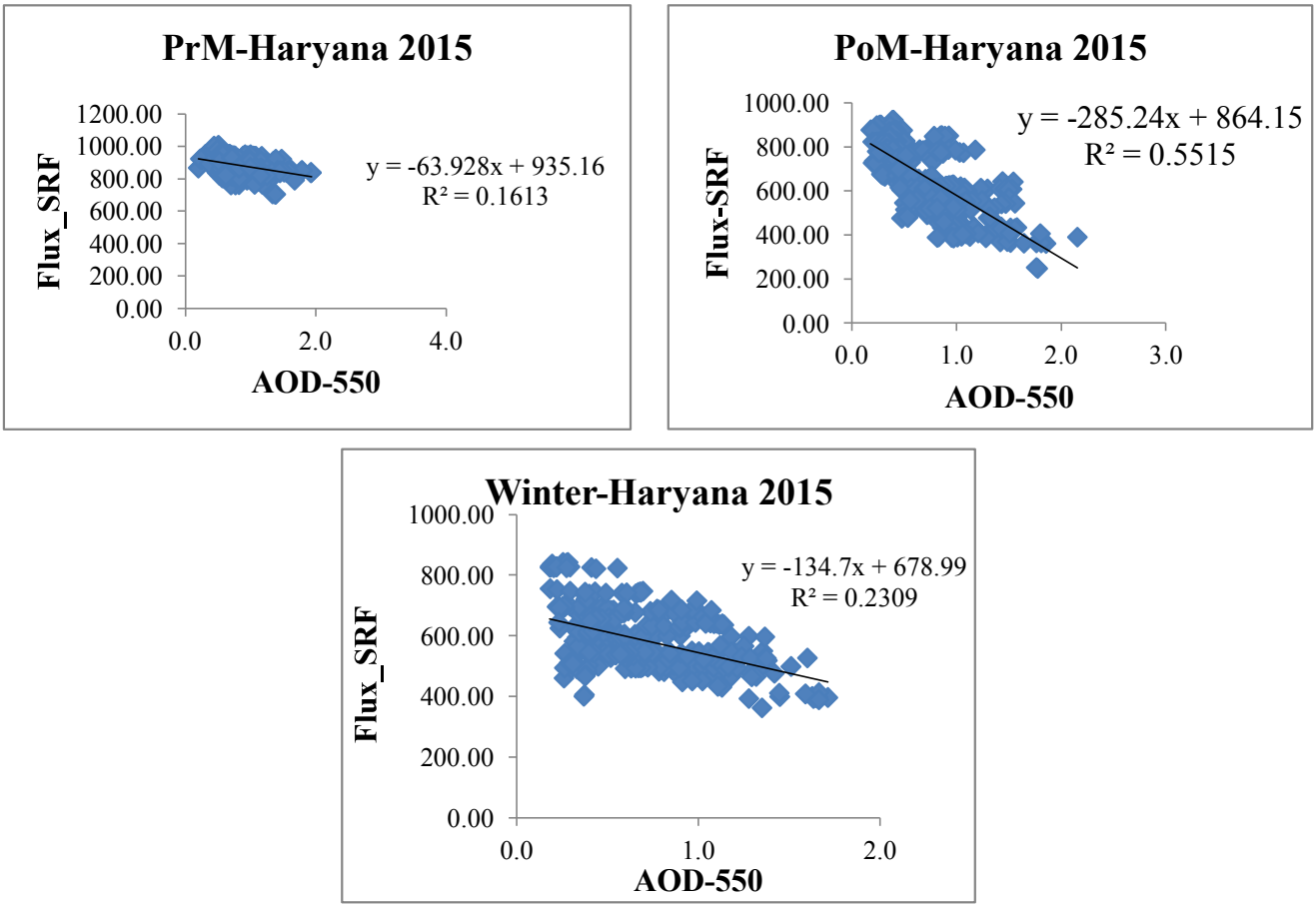

Figure 3.32 Variation of surface (SRF) solar fluxes in PrM, PoM and W seasons at Haryana site.

This simultaneous decrease in surface fluxes and increase in TOA fluxes with the AOD indicate the increase in both the absorption and scattering of the solar radiation by the aerosols. The aerosol forcing efficiencies at TOA during the PrM and W seasons were 3-4 times lower than the aerosol forcing efficiencies at the SRF. Their differences (+ 32.69 $Wm^{-2}AOD^{-1}$ in PrM and +112.93 $Wm^{-2}AOD^{-1}$ in W) over Delhi and over Haryana (+ 49.374 $Wm^{-2}AOD^{-1}$ in PrM and + 128.26 $Wm^{-2}AOD^{-1}$ in W) implies the significant warming in the atmosphere with per unit increase in the AOD over these two sites.

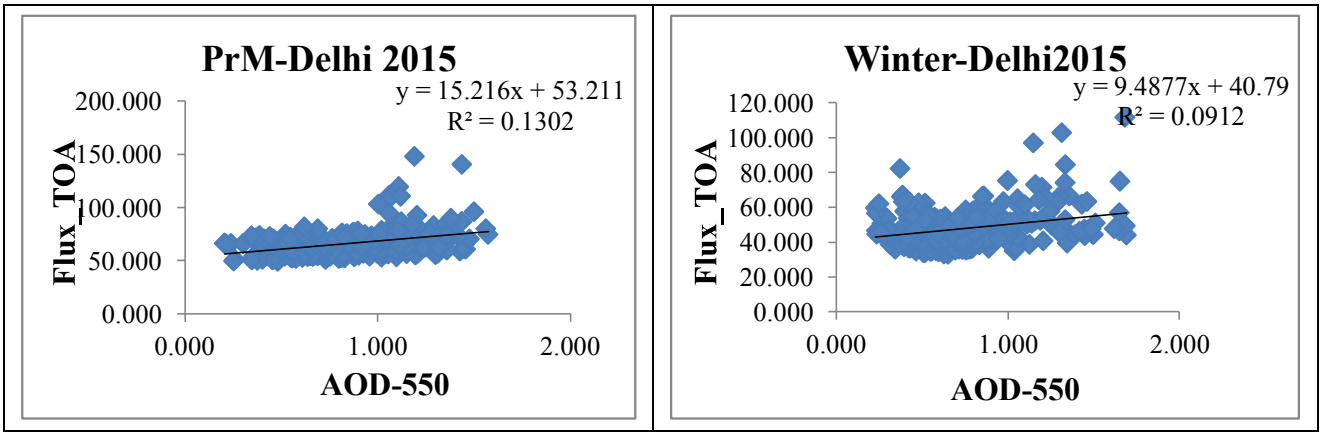

Figure 3.33 Variation of top of the atmosphere (TOA) fluxes with AOD_{550} in PrM and W seasons at Delhi site.

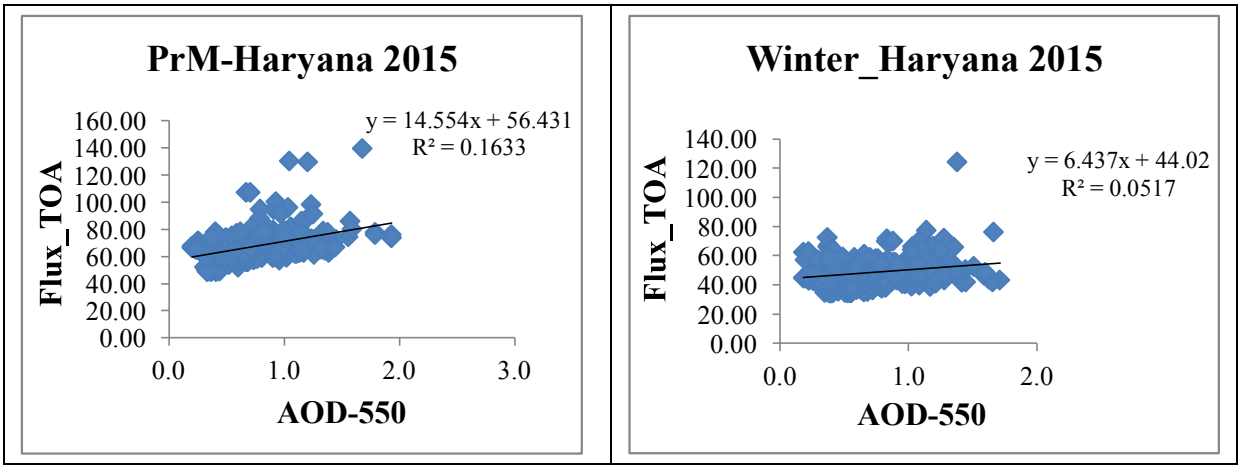

Figure 3.34 Variation of top of the atmosphere (TOA) fluxes with AOD_{550} in PrM and W seasons at Haryana site.

Table 3.7. The seasonal radiative forcing efficiency (η) and Clear sky flux (F^o) variation at surface (SRF) and top of the atmosphere (TOA) over Delhi.

	SRF			TOA		
	PrM	PoM	W	PrM	PoM	W
η	-47.908	-219.19	-122.42	-15.216	-	-9.4877
F^o	922.33	832.03	673.72	53.211	-	40.79

Table 3.8. The seasonal radiative forcing efficiency (η) and Clear sky flux (F^o) variation at surface (SRF) and top of the atmosphere (TOA) over Haryana.

	SRF			TOA		
	PrM	PoM	W	PrM	PoM	W
η	-63.928	-285.24	-134.7	-14.554	-	-6.437
F^o	935.16	864.15	678.99	56.431	-	44.02

Delhi

Table 3.9. Radiative Forcing over Delhi using slope and intercept methods with errors in Pre-Monsoon, Post-Monsoon and Winter seasons.

	INTERCEPT METHOD (±error)			**SLOPE METHOD** (±error)		
	PrM	PoM	W	PrM	PoM	W
F_{SRF}	-36.16 (±7.73)	-153.98 (±14.90)	-80.78 (±12.99)	-42.59 (±7.75)	-153.98 (±13.54)	-80.78 (±13.69)
F_{TOA}	-13.04 (±2.07)	-	-7.21 (±1.55)	-13.04 (±2.29)	-	-7.21 (±1.85)
F_{ATM}	23.12 (±8.06)	-	73.57 (±13.12)	29.54 (±8.08)	-	73.57 (±13.81)

Haryana

Table 3.10. Radiative Forcing over Haryana using slope and intercept methods with errors in Pre-Monsoon, Post-Monsoon and Winter seasons.

	INTERCEPT METHOD (±error)			**SLOPE METHOD** (±error)		
	PrM	PoM	W	PrM	PoM	W
F_{SRF}	-45.72 (±19.10)	-173.88 (±53.99)	-77.77 (±11.50)	-53.72 (±20.94)	-204.32 (±65.32)	-91.39 (±13.35)
F_{TOA}	-11.90 (±1.87)	-	-4.32 (±1.34)	-11.90 (±1.98)	-	-4.32 (±1.61)
F_{ATM}	33.82 (±19.19)	-	73.45 (±11.58)	41.83 (±21.04)	-	87.07 (±13.45)

Table 3.11. The seasonal single scattering albedo (SSA), (AE) and Aerosol Optical Depth (AOD) variations over Delhi and Haryana.

	Delhi			Haryana		
	PrM	PoM	W	PrM	PoM	W
AOD	0.86	0.83	0.77	0.85	0.73	0.68
SSA	0.96	0.95	0.96	0.95	0.95	0.96
AE	1.22	1.35	1.61	1.25	1.34	1.55

Tables 3.9 and 3.10 compare the radiative forcing at the SRF, TOA and in the atmosphere (ATM) by using the intercept and slope methods as explained in chapter 2 over Delhi and Haryana sampling sites respectively in the PrM, PoM and W seasons for the year 2015. In Delhi (Table 3.9), similarities in some of the radiative forcing values from the two methods were observed. The F_{SRF} values were found to be similar in the PoM and winter seasons, whereas, F_{TOA} and F_{ATM} values were observed to be similar in the winter season only. However, in the PrM, except F_{TOA} (13.04 W/m^2), both F_{SRF} and F_{ATM} values were observed to be slightly different by the slope and intercept methods, however within the error range. In Delhi, the radiative forcing at the SRF was observed to be higher in PoM and W compare to PrM season. Maximum forcing was observed in the PoM at the SRF. SRF radiative forcing followed the trend PrM<W<PoM. However, the trend for F_{TOA} was found to be PrM>W but for F_{ATM} it was observed to be PrM<W.

In Haryana (Table 3.10), similarities in the radiative forcing values from the two methods were observed at the TOA only during the PrM and W season. F_{SRF} and F_{ATM} values were observed to be different in all the seasons by the intercept and slope methods. Similar trends were observed for the radiative forcing over Haryana with SRF radiative forcing following the trend PrM<W<PoM. The trend for F_{TOA} was found to be PrM>W and for F_{ATM} it was observed to be PrM<W. The F_{ATM} values indicate the warming in the atmosphere whereas the F_{SRF} and F_{TOA}

indicate cooling at the SRF and TOA, respectively. In Haryana also, the maximum forcing was observed in the PoM at the surface.

Positive aerosol atmospheric forcing from PrM (23.12 W/m^2) to W (73.57 W/m^2) could be observed over Delhi site with the associated with negative aerosol radiative forcing at SRF and TOA (cooling), indicating the presence of higher concentration of aerosols during the winter season as is indicated by the higher $PM_{2.5}$ concentration level (Chapter 3). Similar pattern of the atmospheric forcing was observed in the Haryana region as well. However, the aerosol atmospheric forcing was observed more in the Haryana region (33.82 – 41.83 W/m^2) as compared to the Delhi (23.12 – 29.54 W/m^2) during the PrM season. This might be due to the presence of large amount of dust aerosols (coarser mode) on account of dust storms and wind-blown dust from the vast open dry agricultural fields during the summer season than Delhi where fine mode aerosols dominate even during the summer season. Slope method observed the higher winter season atmospheric forcing (+87.07W/m^2) over Haryana site than the Delhi site, whereas intercept method reported a comparable atmospheric forcing over the two sites. Not much significant difference in the atmospheric forcing values during the winter season could be observed at both Delhi and Haryana sites. Also, the single scattering albedo (SSA) has been observed to be constant over the Delhi and Haryana region (Table 3.11) and its higher values shows the dominance of scattering aerosols. Also, in all the seasons, at both Delhi and Haryana sites, the AE > 1 indicating the presence of coarser mode particles (For example, dust) to a large extent as compare to finer mode particles. The variation in the AOD also was not observed to be very significant at both Delhi and Haryana in PrM, PoM and W seasons respectively. Since the region around the Delhi is rapidly urbanizing and the close proximity of the two sampling sites (approx. 60 kms) could be the reason for the similar aerosol properties and hence the atmospheric radiative forcing over the Delhi- and Haryana sampling site.

CHAPTER – IV

CONCLUSIONS

The $PM_{2.5}$ aerosol physical properties such as their shape and size as well as chemical properties like concentration and carbonaceous content (organic and elemental carbon) were monitored and studied in the summer, post-monsoon and winter seasons over an urban and rural location in Delhi-NCR.

The $PM_{2.5}$ concentrations were observed to be consistently higher at the urban site than the rural site in all the studied seasons. However, the rural site observed exceptionally high $PM_{2.5}$ concentration during the month of November in the Post-Monsoon season which could be due to the post-harvesting biomass burning events taking place during this month. The concentration trend observed at the urban site was Winter > PoM(N) > PoM (S-O) > Summer and at the rural site was PoM (N)> Winter > PoM(S-O) > Summer.

The shape and size of the particles were analysed with the help of SEM technique. At the urban site, in the summer season, flaky, fluffy irregular shaped agglomerates dominated at the urban site. In the September-October months of post-monsoon season, the small agglomerates of ultrafine particles were observed in abundance along with a few individual spherical large particles. The November month in the post-monsoon season observed the large number of spherical, round, irregular shaped and agglomerates of ultrafine particles whereas, in the winter season the urban site was mainly dominated by the aggregates/agglomerates of the smaller particles. The number of individual particles observed at the urban site during the winter season was very less as compared to the other seasons. The SEM analysis has shown that soot was observed to be the major component of $PM_{2.5}$ aerosols at the urban site in all the seasons indicating the dominance of anthropogenic sources.

In the summer season ultrafine spherical and irregular shaped particles were observed at the rural site. The presence of crystalline particles of different shapes was also observed indicating the presence of dust during this period. Small aggregates of the soot were also observed at the rural site which could be due to biomass burning in the households for cooking purposes. But overall

the rural site was observed to be relatively cleaner than the urban site. In the Post-Monsoon (S-O) season, the rural site observed round, crystalline and fluffy (soot) particles. PoM (N) period was found to be dominated by spindle/bead shaped as well as few round particles. Winter season was found to be dominated by soot agglomerates, spherical, spindle/bead like and irregular shaped particles. The number of individual particles could be observed more at the rural site than those at urban site. The particle morphology indicated the presence of both natural (dust) and anthropogenic sources.

The size distribution curves showed a log-normal size distribution at both the urban and rural site in all the seasons. During the summer season, the geometric mean (μ_g) was observed to be similar at the two sites but the spread of the distribution curve (σ_g) was more at rural site than the urban site. At the urban site, the dominant size range is the 0.2 - 1.4μm whereas at the rural site 0.1 – 2.0 μm indicating the presence of coarse mode particles such as dust or crystalline particles in good amount at the rural site. In the PoM (S-O), the geometric mean was observed to be higher at the rural site than the urban site but the spread of the distribution curve was similar at both the sites. The rural site was observed to be dominated by the particles in the size range 200- 900nm (maximum at 0.4 - 0.5 μm) and particles in the size range 200 -700nm (maximum at 0.40 μm) dominated at the urban site. PoM (N) showed that the urban aerosols were observed to be dominant in the 0.1-1μm size range (fine mode particles) and rural samples were found to be dominant in the range 0.5- 2.0 μm (fine + coarse mode). The geometric mean was observed to be higher at rural site than the urban site but the spread of the distribution was more at urban site. During the winter season, at the urban site, the particles were observed to be in the size range of 0.4 – 2.0 μm size range whereas at the rural site, the particles were observed in the 0.2 – 2.0 μm size range. Distribution curve in the urban as well as rural site observed a peak around the size range of approximately 0.5-1.4 μm. Urban and rural site were dominated mainly by the $PM_{2.5}$ particles in the size range up to 1.0 μm with peak values around 0.5 μm in all the seasons except PoM (N) at the rural site. Rural site in PoM (N) was found to be dominated by the coarser mode particles (size > 1μm).

Carbonaceous content (EC and OC) was found to be highly variable at both the urban and rural sites during the studied seasons. OC/EC ratios were observed to be similar at both the urban and rural sites during the summer, PoM (S-O) and PoM (N). In winter OC/EC ratio at the rural site, was 2 times higher than that observed at the urban site. In seasonal comparison at rural site, the OC/EC ratio in winter was approximately 3 times higher than that observed in summer. Very high EC (35.96µg/m³) and OC (65.08µg/m³) concentrations were observed at rural site during the month of November on account of biomass burning activities. At urban site, OC concentrations followed the trend: Winter > PoM (N)> PoM (SO) > Summer whereas EC showed a trend: PoM (N) > Winter > PoM (SO) > Summer. At rural site, for both OC and EC concentration, the trend observed was PoM (N) > Winter > PoM (SO) > Summer. The secondary organic carbons contribution was observed to be maximum during the winter season at both the sites followed by summer, PoM (S-O) and PoM(N) season.

The global solar irradiances were observed to be higher at the rural site in all the seasons. The Direct irradiances were observed to be comparable at both sites during summer and PoM (S-O) seasons but were significantly higher at the rural site in PoM (N) and winter seasons than the urban site. Further, the solar irradiance studies over the urban and rural site have shown a dimming effect over Delhi.

The association between the OC, EC and solar irradiance showed an inverse relation in almost all the seasons. The association between the $PM_{2.5}$ (Diff.) and global and direct irradiances were also observed to be negative. The estimated radiative forcing over Delhi and Haryana (NCR) site was observed to be higher in winter as compare to summer season.

REFERENCES

References:

Aldabe, J., Elustondo, D., Santamaría, C., Lasheras, E., Pandol, M., Alastuey, A., Santamaría, J. M. (2011). Chemical characterisation and source apportionment of PM2 . 5 and PM10 at rural , urban and traffic sites in Navarra (North of Spain). *Atmospheric Research*, *102*, 191–205.

Alpert, P., & Kishcha, P. (2008). Quantification of the effect of urbanization on solar dimming. *Geophysical Research Letters*, *35*(8).

Apte, J. S., Marshall, J. D., Cohen, A. J., & Brauer, M. (2015). Addressing Global Mortality from Ambient PM2.5. *Environmental Science and Technology*, *49*(13), 8057–8066.

Badarinath, K. V. S., Latha, K. M., Chand, T. R. K., & Gupta, P. K. (2009). Impact of biomass burning on aerosol properties over tropical wet evergreen forests of Arunachal Pradesh , India. *Atmospheric Research*, *91*(1), 87–93.

Badarinath, K. V. S., Sharma, A. R., Kaskaoutis, D. G., Kharol, S. K., & Kambezidis, H. D. (2010). Solar dimming over the tropical urban region of Hyderabad, India: Effect of increased cloudiness and increased anthropogenic aerosols. *Journal of Geophysical Research: Atmospheres*, *115*(D21).

Balakrishnan, K., Parikh, J., Sankar, S., Padmavathi, R., Srividya, K., Venugopal, V.,Pandey, V. L. (2002). Daily average exposures to respirable particulate matter from combustion of biomass fuels in rural households of Southern India. *Environmental Health Perspectives*, *110*(11), 1069–1075.

Beelen, R., Hoek, G., van den Brandt, P. A., Goldbohm, R. A., Fischer, P., Schouten, L. J., … Brunekreef, B. (2008). Long-term effects of traffic-related air pollution on mortality in a Dutch cohort (NLCS-AIR study). *Environmental Health Perspectives*

Behera, S. N., & Sharma, M. (2010). Reconstructing Primary and Secondary Components of PM 2.5 Composition for an Urban Atmosphere. *Aerosol Science and Technology*, *44*(11), 983–992.

Bergstrom, R. W. (1972). Predictions of the spectral absorption and extinction coefficients of an urban air pollution aerosol model. *Atmospheric Environment (1967)*, *6*(4), 247-258.

Bergstrom, R. W., Russell, P. B., & Hignett, P. (2002). Wavelength Dependence of the Absorption of Black Carbon Particles: Predictions and Results from the TARFOX Experiment and Implications for the Aerosol Single Scattering Albedo. *Journal of Atmospheric Sciences*, 567–577.

Bhattacharya, A. B., Kar, S. K., & Bhattacharya, R. (1996). Diffuse solar radiation and associated meteorological parameters in India. *Annals of Geophysics*, *14*, 1051–1059.

Bilbao, J., Román, R., Yousif, C., Pérez-Burgos, A., & De, M. A. (2014). Global, diffuse, direct, and ultraviolet solar irradiance recorded in Malta and atmospheric component influences. *Energy Procedia*, *57*, 1206–1210.

Blackburn, G., & Vignola, F. (2012). Spectral Distributions of Diffuse and Global Irradiance for Clear and Cloudy Periods. *World Renewable Energy Forum (WREF)*.

Bond, T. C., & Bergstrom, R. W. (2006). Light Absorption by Carbonaceous Particles: An Investigative Review. *Aerosol Science and Technology*, *40*(1), 27–67.

Buseck, P. R. (2010). Nature and Climate Effects of Individual Tropospheric Aerosol Particles. *Annual Review of Earth and Planetary Sciences*, *38*, 17–43.

Buseck, P. R., Jacob, D. J., Pósfai, M., Li, J., & Anderson, J. R. (2000). Minerals in the Air: An Environmental Perspective. *International Geology Review*, *42*(7), 577–593.

Castro, L. M., Pio, C. A., Harrison, R. M., & Smith, D. J. T. (1999). Carbonaceous aerosol in urban and rural European atmospheres: Estimation of secondary organic carbon concentrations. *Atmospheric Environment*, *33*(17), 2771–2781.

Casuccio, G. S., Schlaegle, S. F., Lersch, T. L., Huffman, G. P., Chen, Y., & Shah, N. (2004). Measurement of fine particulate matter using electron microscopy techniques. *Fuel Processing Technology*, *85*(6–7), 763–779.

Chameides, W. L., Yu, H., Liu, S. C., Bergin, M., Zhou, X., Mearns, L., Giorgi, F. (1999). Case study of the effects of atmospheric aerosols and regional haze on agriculture: an opportunity to enhance crop yields in China through emission controls? *Proceedings of the National Academy of Sciences of the United States of America*, *96*(24), 13626–13633.

Chengappa, C., Edwards, R., Bajpai, R., Shields, K. N., & Smith, K. R. (2007). Impact of

improved cookstoves on indoor air quality in the Bundelkhand region in India. *Energy for Sustainable Development*, *11*(2), 33-44.

Choudhury, N. K. D. (1963). Solar radiation at New Delhi. *Solar Energy*, *7*(2), 44-52.

Chow, J. C., Watson, J. G., Kuhns, H., Etyemezian, V., Lowenthal, D. H., Crow, D., … Green, M. C. (2004). Source profiles for industrial, mobile, and area sources in the Big Bend Regional Aerosol Visibility and Observational study. *Chemosphere*, *54*(2), 185–208.

Chung, S. H., & Seinfeld, J. H. (2002). Global distribution and climate forcing of carbonaceous aerosols. *Journal of Geophysical Research Atmospheres*, *107*(19).

Codato, G., Oliveira, A. P., Soares, J., Escobedo, J. F., Gomes, E. N., & Pai, A. D. (2008). Global and diffuse solar irradiances in urban and rural areas in southeast Brazil. *Theoretical and Applied Climatology*, *93*(1–2), 57–73.

Cohan, D. S., Xu, J., Greenwald, R., Bergin, M. H., & Chameides, W. L. (2002). Impact of atmospheric aerosol light scattering and absorption on terrestrial net primary productivity - art. no. 1090. *Global Biogeochemical Cycles*, *16*(4), 1090.

Colbeck, I., Nasir, Z. A., & Ali, Z. (2010). Characteristics of indoor/outdoor particulate pollution in urban and rural residential environment of Pakistan. *Indoor Air*, *20*(1), 40–51.

de la Campa, A. S., Pio, C., De la Rosa, J. D., Querol, X., Alastuey, A., & González-Castanedo, Y. (2009). Characterization and origin of EC and OC particulate matter near the Doñana National Park (SW Spain). *Environmental research*, *109*(6), 671-681.

DeLuisi, J. J., Furukawa, P. M., Gillette, D. A., Schuster, B. G., Charlson, R. J., Porch, W. M., ... & Weinman, J. A. (1976). Results of a comprehensive atmospheric aerosol-radiation experiment in the Southwestern United States Part I: size distribution, extinction optical depth and vertical profiles of aerosols suspended in the atmosphere. *Journal of applied meteorology*, *15*(5), 441-454.

Duan, J., Tan, J., Cheng, D., Bi, X., Deng, W., Sheng, G., … Wong, M. H. (2007). Sources and characteristics of carbonaceous aerosol in two largest cities in Pearl River Delta Region, China. *Atmospheric Environment*, *41*(14), 2895–2903.

Elminir, H. K. (2007a). Relative influence of weather conditions and air pollutants on solar

radiation - Part 2: Modification of solar radiation over urban and rural sites. *Meteorology and Atmospheric Physics*, *96*(3–4), 257–264.

Elminir, H. K. (2007b). Relative influence of weather conditions and air pollutants on solar radiation – Part 2 : Modification of solar radiation over urban and rural sites. *Meteorology and Atmospheric Physics*, *264*, 257–264.

Feng, Y., Chen, Y., Guo, H., Zhi, G., Xiong, S., Li, J., … Fu, J. (2009). Characteristics of organic and elemental carbon in PM2.5 samples in Shanghai, China. *Atmospheric Research*, *92*(4), 434–442.

Gadhavi, H., & Jayaraman, A. (2010, January). Absorbing aerosols: contribution of biomass burning and implications for radiative forcing. In *Annales Geophysicae* (Vol. 28, No. 1, pp. 103-111). Copernicus GmbH.

Gauderman, W. J., Avol, E., Lurmann, F., Kuenzli, N., Gilliland, F., Peters, J., & McConnell, R. (2005). Childhood asthma and exposure to traffic and nitrogen dioxide. *Epidemiology (Cambridge, Mass.)*, *16*(6), 737–43.

Gautam, R., N. C. Hsu, and K.-M. Lau (2010), Premonsoon aerosol characterization and radiative effects over the Indo-Gangetic Plains:Implications for regional climate warming, J. Geophys. Res., 115, D17208, doi:10.1029/2010JD013819.

Gautam, R., et al. (2011), Accumulation of aerosols over the Indo-Gangetic plains and southern slopes of the Himalayas: Distribution,properties and radiative effects during the 2009 pre-monsoon season, Atmos. Chem. Phys., 11, 12,841–12,863,doi:10.5194/acp-11-12841-2011.

Gharibzadeh, M., Alam, K., Bidokhti, A. A., Abedini, Y., & Masoumi, A. (2017). Radiative Effects and Optical Properties of Aerosol during Two Dust Events in 2013 over Zanjan, Iran. *Aerosol and Air Quality Research*, *17*(3), 888-898.

Grantz, D. A., Garner, J. H. B., & Johnson, D. W. (2003). Ecological effects of particulate matter. *Environment International*, *29*(2–3), 213–239.

Greenwald, R., Bergin, M. H., Xu, J., Cohan, D., Hoogenboom, G., & Chameides, W. L. (2006). The influence of aerosols on crop production: A study using the CERES crop model. *Agricultural Systems*, *89*(2), 390-413.

Harrison, R. M., Smith, D. J. T., Piou, C. A., & Castro, L. M. (1997). Comparative receptor modelling study of airborne particulate pollutants in Birmingham (United Kingdom), Coimbra (Portugal) and Lahore (Pakistan). *Atmospheric Environment*, *31*(20), 3309-3321

Hasselblad, V., Eddy, D. M., & Kotchmar, D. J. (1992). Synthesis of environmental evidence: nitrogen dioxide epidemiology studies. *Journal of the Air & Waste Management Association*, *42*(5), 662-671.

Hays, M. D., Cho, S. H., Baldauf, R., Schauer, J. J., & Shafer, M. (2011). Particle size distributions of metal and non-metal elements in an urban near-highway environment. *Atmospheric Environment*, *45*(4), 925–934.

Haywood, J., & Boucher, O. (2000). Estimates of the direct and indirect radiative forcing due to tropospheric aerosols: A review. *Reviews of Geophysics*, *38*(4), 513–543.

Huang, Y., Li, L., Li, J., Wang, X., Chen, H., Chen, J., … Chen, C. (2013). A case study of the highly time-resolved evolution of aerosol chemical and optical properties in urban Shanghai, China. *Atmospheric Chemistry and Physics*, *13*(8), 3931–3944.

Hueglin, C., Gehrig, R., Baltensperger, U., Gysel, M., Monn, C., & Vonmont, H. (2005). Chemical characterisation of PM2.5, PM10 and coarse particles at urban, near-city and rural sites in Switzerland. *Atmospheric Environment*, *39*(4), 637–651.

Husain, L., Dutkiewicz, V. A., Khan, A. J., & Ghauri, B. M. (2007). Characterization of carbonaceous aerosols in urban air. *Atmospheric Environment*, *41*(32), 6872–6883.

Iqbal, M. (2012). *An introduction to solar radiation*. Elsevier.

Jacobson, M. Z. (2001). Strong radiative heating due to the mixing state of black carbon in atmospheric aerosols. *Nature*, *409*(6821), 695–697.

Jacovides, C. P., Steven, M. D., & Asimakopoulos, D. N. (2000). Spectral solar irradiance and some optical properties for various polluted atmospheres. *Solar Energy*, *69*(3), 215-227.

Janhäll, S., Andreae, M. O., & Pöschl, U. (2010). Biomass burning aerosol emissions from vegetation fires: particle number and mass emission factors and size distributions.

Atmospheric chemistry and physics, *10*(3), 1427-1439.

Joon, V., Kumari, H., & Chandra, A. (2011). Predicting Exposure Levels of Respirable Particulate Matter (PM2.5) and Carbon monoxide for the Cook from Combustion of Cooking Fuels. *Ipcbee*, *10*, 229–232.

Kaskaoutis, D. G., & Kambezidis, H. D. (2009). The diffuse-to-global and diffuse-to-direct-beam spectral irradiance ratios as turbidity indexes in an urban environment. *Journal of Atmospheric and Solar-Terrestrial Physics*, *71*(2), 246–256.

Kaskaoutis, D. G., Kambezidis, H. D., & Tóth, Z. (2007). Investigation about the dependence of spectral diffuse-to-direct-beam irradiance ratio on atmospheric turbidity and solar zenith angle. *Theoretical and Applied Climatology*, *89*, 245–256.

Kaufman, Y. J., & Boucher, O. (2002). A satellite view of aerosols in the climate system. *Nature*, *419*(September), 215–223.

Kaushar, A. (2013). Spatio-Temporal Variation and Deposition of Fine and Coarse Particles during the Commonwealth Games in Delhi. *Aerosol and Air Quality Research*, 748–755.

Kaushar, A., Chate, D., Beig, G., Srinivas, R., Parkhi, N., Satpute, T., … Trivedi, D. K. (2013). Spatio-temporal variation and deposition of fine and coarse particles during the Commonwealth Games in Delhi. *Aerosol and Air Quality Research*, *13*(2), 748–755.

Khan, M. F., Shirasuna, Y., Hirano, K., & Masunaga, S. (2010). Characterization of PM2.5, PM2.5-10 and PM> 10 in ambient air, Yokohama, Japan. *Atmospheric Research*, *96*(1), 159–172.

Kulshrestha, A., Satsangi, P. G., Masih, J., & Taneja, A. (2009). Science of the Total Environment Metal concentration of PM 2 . 5 and PM 10 particles and seasonal variations in urban and rural environment of Agra , India. *Science of the Total Environment*, *407*(24), 6196–6204.

Kumar, R., Goel, N., Gupta, N., Singh, K., Nagar, S., & Mittal, J. (2013). Indoor Air Pollution and Respiratory Illness in Children from Rural India : A Pilot Study. *The Indian Journal of Chest Diseases & Allied Sciences*, 79–83.

Lam, J. C., & Li, D. H. W. (1996). Correlation between global solar radiation and its direct and

diffuse components. *Building and Environment*, *31*(6), 527–535.

Larson, T., Gould, T., Simpson, C., Liu, L. J. S., Claiborn, C., & Lewtas, J. (2004). Source apportionment of indoor, outdoor, and personal PM2.5 in Seattle, Washington, using positive matrix factorization. *Journal of the Air & Waste Management Association (1995)*, *54*(9), 1175–87.

Latha, K. M., & Badarinath, K. V. S. (2005). Spectral solar attenuation due to aerosol loading over an urban area in India. *Atmospheric Research*, *75*(4), 257–266.

Lelieveld, J., Evans, J. S., Fnais, M., Giannadaki, D., & Pozzer, A. (2015). The contribution of outdoor air pollution sources to premature mortality on a global scale. *Nature*, *525*(7569), 367–71.

Li, J., Song, Y., Mao, Y., Mao, Z., Wu, Y., Li, M., … Hu, M. (2014). Chemical characteristics and source apportionment of PM2.5 during the harvest season in eastern China's agricultural regions. *Atmospheric Environment*, *92*, 442–448.

Liou, K. N. (2002). *An Introduction to Atmospheric Radiation (Google eBook)*. *International Geophysics* (Vol. 84).

Liu, W., Wang, Y., Russell, A., & Edgerton, E. S. (2005). Atmospheric aerosol over two urban-rural pairs in the southeastern United States: Chemical composition and possible sources. *Atmospheric Environment*, *39*(25), 4453–4470.

Loeb, N. G., and S. Kato (2002), Top-of-atmosphere direct radiative effect of aerosols over the tropical oceans from the clouds and the Earth's Radiant Energy System (CERES) satellite instrument, J. Clim., 15, 1474–1484

Lorente, J., Redan, A., & De Cabo, X. (1994). Influence of urban aerosol on spectral solar irradiance. *Journal of Applied Meteorology*, *33*(3), 406-415.

Malm, W. C., Sisler, J. F., Huffman, D., Eldred, R. A., & Cahill, T. A. (1994). Spatial and seasonal trends in particle concentration and optical extinction in the United States. *Journal of Geophysical Research: Atmospheres*, *99*(D1), 1347-1370.

McGranahan, G., & Murray, F. (2003). Air pollution and health in rapidly developing countries. *Bulletin of the World Health Organization* (Vol. 81).

Meehl, G. A., Arblaster, J. M., & Collins, W. D. (2008). Effects of black carbon aerosols on the Indian monsoon. *Journal of Climate*, *21*(12), 2869–2882.

Meloni, D., di Sarra, A., Di Iorio, T., & Fiocco, G. (2005). Influence of the vertical profile of Saharan dust on the visible direct radiative forcing. *Journal of Quantitative Spectroscopy and Radiative Transfer*, *93*(4), 397–413.

Meng, Z. Y., Jiang, X. M., Yan, P., Lin, W. L., Zhang, H. D., & Wang, Y. (2007). Characteristics and sources of PM2.5 and carbonaceous species during winter in Taiyuan, China. *Atmospheric Environment*, *41*(32), 6901–6908.

Meywerk, J., & Ramanathan, V. (1999). Observations of the spectral clear- sky aerosol forcing over the tropical Indian Ocean. *Journal of Geophysical Research: Atmospheres*, *104*(D20), 24359-24370.

Mishra, S. K., Agnihotri, R., Yadav, P. K., Singh, S., Prasad, M., Praveen, P. S., … Sharma, C. (2015). Morphology of atmospheric particles over semi-arid region (Jaipur, Rajasthan) of India: Implications for optical properties. *Aerosol and Air Quality Research*, *15*(3), 974–984.

Mukhopadhyay, R., Sambandam, S., Pillarisetti, A., Jack, D., Mukhopadhyay, K., Balakrishnan, K., … Smith, K. R. (2012). Cooking practices, air quality, and the acceptability of advanced cookstoves in Haryana, India: an exploratory study to inform large-scale interventions. *Global Health Action*, *5*(June), 1–13.

Myhre, G., Myhre, C. E. L., Samset, B. H., & Storelvmo, T. (2013). Aerosols and their relation to global climate and climate sensitivity. *Nature Education Knowledge*, *4*(7).

Nakajima, T., Takamura, T., Yamano, M., Shiobara, M., Yamauchi, T., Goto, R., … Atmosphere, U. (1986). T. Nakajima, T. Takamura, M. Yamano, M. Shiobara, T. Yamauchi, R. Goto and K. Murai. *Journal of the Meteorological Society of Japan*, *65*(5), 765–776.

Pachauri, T., Satsangi, A., Singla, V., Lakhani, A., & Maharaj Kumari, K. (2013). Characteristics and sources of carbonaceous aerosols in PM2.5 during wintertime in Agra, India. *Aerosol and Air Quality Research*, *13*(3), 977–991.

Pachauri, T., Singla, V., Satsangi, A., Lakhani, A., & Maharaj Kumari, K. (2013). SEM-EDX

characterization of individual coarse particles in Agra, India. *Aerosol and Air Quality Research*, *13*(2), 523–536.

Padma Kumari, B., Londhe, A. L., Daniel, S., & Jadhav, D. B. (2007). Observational evidence of solar dimming: Offsetting surface warming over India. *Geophysical Research Letters*, *34*(21).

Pandey, P., Kumar, D., Prakash, A., Masih, J., Singh, M., Kumar, S., … Kumar, K. (2012). A study of urban heat island and its association with particulate matter during winter months over Delhi. *Science of the Total Environment*, *414*, 494–507.

Pant, P., Shukla, A., Kohl, S. D., Chow, J. C., Watson, J. G., & Harrison, R. M. (2015). Characterization of ambient PM2.5 at a pollution hotspot in New Delhi, India and inference of sources. *Atmospheric Environment*, *109*, 178–189.

Pandithurai, G., Dipu, S., Dani, K. K., Tiwari, S., Bisht, D. S., & Devara, P. C. S. (2008). Aerosol radiative forcing during dust events over New Delhi , India. *Journal of Geophysical Research*, *113*(March), 1–13.

Paoletti, L., Diociaiuti, M., Berardis, B. De, Santucci, S., Lozzi, L., & Picozzi, P. (1999). Characterisation of aerosol individual particles in a controlled underground area. *Atmospheric Environment*, *33*, 3603–3611.

Patil, R. S., Kumar, R., Menon, R., Shah, M. K., & Sethi, V. (2013). Development of particulate matter speciation profiles for major sources in six cities in India. *Atmospheric Research*, *132*, 1-11.

Pinker, R. T., Zhang, B., & Dutton, E. . (2005). Do Satellites Detect Trends in Surface Solar Radiation ? *Climate Research*, *850*(2005), 850–855.

Pipal, A. S., Jan, R., Satsangi, P. G., Tiwari, S., & Taneja, A. (2014). Study of surface morphology, elemental composition and origin of atmospheric aerosols (PM2.5 and PM10) over Agra, India. *Aerosol and Air Quality Research*, *14*(6), 1685–1700.

Pipal, A. S., Kulshrestha, A., & Taneja, A. (2011). Characterization and morphological analysis of airborne PM2.5 and PM10 in Agra located in north central India. *Atmospheric Environment*, *45*(21), 3621–3630.

Platnick, S., M. D. King, S. A. Ackerman, W. P. Menzel, B. A. Baum, J. C. Riedi, and R. A. Frey (2003), The MODIS cloud products: Algorithms and examples from Terra, IEEE Trans. Geosci. Remote Sens., 41, 459–473, doi:10.1109/TGRS.2002.808301.

Pope III, C. A., Burnett, R. T., Thun, M. J., Calle, E. E., Krewski, D., & Thurston, G. D. (2002). to Fine Particulate Air Pollution. *The Journal of the American Medical Association*, *287*(9), 1132–1141.

Pöschl, U. (2005). Atmospheric aerosols: Composition, transformation, climate and health effects. *Angewandte Chemie - International Edition*, *44*(46), 7520–7540.

Putaud, J. P., Raes, F., Van Dingenen, R., Brüggemann, E., Facchini, M. C., Decesari, S., ... & Lorbeer, G. (2004). A European aerosol phenomenology—2: chemical characteristics of particulate matter at kerbside, urban, rural and background sites in Europe. *Atmospheric environment*, *38*(16), 2579-2595.

Putaud, J. P., Van Dingenen, R., Alastuey, A., Bauer, H., Birmili, W., Cyrys, J., … Raes, F. (2010). A European aerosol phenomenology - 3: Physical and chemical characteristics of particulate matter from 60 rural, urban, and kerbside sites across Europe. *Atmospheric Environment*, *44*(10), 1308–1320.

Quenzel, H. (1970). Determination of size distribution of atmospheric aerosol particles from spectral solar radiation measurements. *Journal of Geophysical Research*, *75*(15), 2915-2921.

Ram, K., Sarin, M. M., & Hegde, P. (2008). Atmospheric abundances of primary and secondary carbonaceous species at two high-altitude sites in India: Sources and temporal variability. *Atmospheric Environment*, *42*(28), 6785-6796.

Ram, K., & Sarin, M. M. (2010). Spatio-temporal variability in atmospheric abundances of EC, OC and WSOC over Northern India. *Journal of Aerosol Science*, *41*(1), 88–98.

Rastogi, N., Singh, A., Sarin, M. M., & Singh, D. (2016). Temporal variability of primary and secondary aerosols over northern India: Impact of biomass burning emissions. *Atmospheric Environment*, *125*, 396–403.

Remer, L. A., et al. (2005), The MODIS aerosol algorithm, products, and validation, J. Atmos. Sci., 62, 947–973, doi:10.1175/JAS3385.1.

Reist, P. C. (1984). *Introduction to aerosol science*. Macmillan publishing company.

Roderick, M. L. (1999). Estimating the diffuse component from daily and monthly measurements of global radiation. *Agricultural and Forest Meteorology*, *95*, 169–185.

Rodrguez, I., Gali, S., & Marcos, C. (2009). Atmospheric inorganic aerosol of a non-industrial city in the centre of an industrial region of the North of Spain, and its possible influence on the climate on a regional scale. *Environmental Geology*, *56*(8), 1551–1561.

Safaripour, M. H., & Mehrabian, M. A. (2011). Predicting the direct, diffuse, and global solar radiation on a horizontal surface and comparing with real data. *Heat and Mass Transfer/Waerme- Und Stoffuebertragung*, *47*(12), 1537–1551.

Sahu, S. K., Beig, G., & Parkhi, N. S. (2011). Emissions inventory of anthropogenic PM2.5 and PM10 in Delhi during Commonwealth Games 2010. *Atmospheric Environment*, *45*(34), 6180–6190.

Sarangi, C., Tripathi, S. N., Mishra, A. K., Goel, A., & Welton, E. J. (2016). Elevated aerosol layers and their radiative impact over Kanpur during monsoon onset period. *Journal of Geophysical Research: Atmospheres*, *121*(13), 7936–7957.

Seinfeld, J. H., & Pandis, S. N. (2006). *Atmospheric Chemistry and Physics: From Air Pollution to Climate Change*. *Atmospheric Chemistry and Physics*.

Shubhankar, B., & Ambade, B. (2016). Chemical characterization of carbonaceous carbon from industrial and semi urban site of eastern India. *SpringerPlus*, *5*(1), 1-17.

Singh, S., Nath, S., Kohli, R., & Singh, R. (2005). Aerosols over Delhi during pre- monsoon months: Characteristics and effects on surface radiation forcing. *Geophysical Research Letters*, *32*(13).

Singh, A., & Dey, S. (2012). Influence of aerosol composition on visibility in megacity Delhi. *Atmospheric Environment*, *62*, 367–373.

Singh, A., Rastogi, N., Sharma, D., & Singh, D. (2015). Inter and Intra-Annual variability in aerosol characteristics over northwestern Indo-Gangetic Plain. *Aerosol and Air Quality Research*, *15*(2), 376–386.

Slezakova, K., Pires, J. C. M., Martins, F. G., Pereira, M. C., & Alvim-Ferraz, M. C. (2011). Identification of tobacco smoke components in indoor breathable particles by SEM-EDS. *Atmospheric Environment*, *45*(4), 863–872.

Soriano, A., Pallarés, S., Pardo, F., Vicente, A. B., Sanfeliu, T., & Bech, J. (2012). Deposition of heavy metals from particulate settleable matter in soils of an industrialised area. *Journal of Geochemical Exploration*, *113*, 36–44.

Srimuruganandam, B., & Shiva Nagendra, S. M. (2012). Application of positive matrix factorization in characterization of PM 10 and PM 2.5 emission sources at urban roadside. *Chemosphere*, *88*(1), 120–130.

Srivastava, A., & Jain, V. K. (2007). Seasonal trends in coarse and fine particle sources in Delhi by the chemical mass balance receptor model. *Journal of Hazardous Materials*, *144*(1–2), 283–291.

Srivastava, A. K., Bisht, D. S., Ram, K., Tiwari, S., & Srivastava, M. K. (2014). Characterization of carbonaceous aerosols over Delhi in Ganga basin: Seasonal variability and possible sources. *Environmental Science and Pollution Research*, *21*(14), 8610–8619.

Streets, D. G., Wu, Y., & Chin, M. (2006). Two-decadal aerosol trends as a likely explanation of the global dimming/brightening transition. *Geophysical Research Letters*, *33*(15), 2–5.

Tasić, M., Đurić-Stanojević, B., Rajšić, S., Mijić, Z., & Novaković, V. (2006). Physico-Chemical Characterization of PM 10 and PM 2.5 in the Belgrade Urban Area. *Acta Chim. Slov*, *53*, 401–405.

Tanré, D., Devaux, C., Herman, M., Santer, R., & Gac, J. Y. (1988). Radiative properties of desert aerosols by optical ground- based measurements at solar wavelengths. *Journal of Geophysical Research: Atmospheres*, *93*(D11), 14223-14231.

Te Brake, W. H. (1975). Air pollution and fuel crises in preindustrial London, 1250-1650. *Technology and Culture*, 337-359.

Tiwari, S., Chate, D. M., Srivastava, M. K., Safai, P. D., Srivastava, A. K., Bisht, D. S., & Padmanabhamurty, B. (2012). Statistical evaluation of PM 10 and distribution of PM 1, PM 2.5, and PM 10 in ambient air due to extreme fireworks episodes (Deepawali festivals) in

megacity Delhi. *Natural Hazards*, *61*(2), 521–531.

Tiwari, S., Kumar, R., Tunved, P., Singh, S., & Panicker, A. S. (2016). Significant cooling effect on the surface due to soot particles over Brahmaputra River Valley region, India: An impact on regional climate. *Science of the Total Environment*, *562*, 504–516.

Tiwari, S., Pipal, A. S., Hopke, P. K., Bisht, D. S., Srivastava, A. K., Tiwari, S., … Pervez, S. (2015). Study of the carbonaceous aerosol and morphological analysis of fine particles along with their mixing state in Delhi, India: A case study. *Environmental Science and Pollution Research*, *22*(14), 10744–10757.

Tiwari, S., Srivastava, A. K., Bisht, D. S., Parmita, P., Srivastava, M. K., & Attri, S. D. (2013). Diurnal and seasonal variations of black carbon and PM2.5 over New Delhi, India: Influence of meteorology. *Atmospheric Research*, *125–126*, 50–62.

Tripathi, S. N., Dey, S., Tare, V., & Satheesh, S. K. (2005). Aerosol black carbon radiative forcing at an industrial city in northern India. *Geophysical Research Letters*, *32*(8), 1–4.

Tyagi, S., Tiwari, S., Mishra, A., Singh, S., Hopke, P. K., Singh, S., & Attri, S. D. (2017). Characteristics of absorbing aerosols during winter foggy period over the National Capital Region of Delhi: Impact of planetary boundary layer dynamics and solar radiation flux. *Atmospheric Research*, *188*, 1–10.

Unsworth, M. H., & Monteith, J. L. (1972). Aerosol and solar radiation in Britain. *Quarterly Journal of the Royal Meteorological Society*, *98*(418), 778–797.

Van Dingenen, R., Raes, F., Putaud, J. P., Baltensperger, U., Charron, A., Facchini, M. C., … Wåhlin, P. (2004). A European aerosol phenomenology - 1: Physical characteristics of particulate matter at kerbside, urban, rural and background sites in Europe. *Atmospheric Environment*, *38*(16), 2561–2577.

Viana, M., Kuhlbusch, T. A. J., Querol, X., Alastuey, A., Harrison, R. M., Hopke, P. K., … Hitzenberger, R. (2008). Source apportionment of particulate matter in Europe : A review of methods and results. *Journal of Aerosol Science*, *39*(3), 827–849.

Weart, S. (2015). Climate change impacts: The growth of understanding. *Physics today*, *68*(9), 46-52.

Wild, M., Gilgen, H., Roesch, A., Ohmura, A., Long, C. N., Dutton, E. G.,Tsvetkov, A. (2005). From Dimming to Brightening: Decadal Changes in Solar Radiation at Earth's Surface. *Science*, *308*(5723), 847–850.

Wolkoff, P., Wilkins, C. K., Clausen, P. A., & Nielsen, G. D. (2006). Organic compounds in office environments - Sensory irritation, odor, measurements and the role of reactive chemistry. *Indoor Air*, *16*(1), 7–19.

Xu, Q. (2001). Abrupt change of the mid-summer climate in central east China by the influence of atmospheric pollution. *Atmospheric Environment*, *35*(30), 5029–5040.

Yadav, A. K., Kumar, K., Bin Hj Awg Kasim, A. M., Singh, M. P., Parida, S. K., & Sharan, M. (2003). Visibility and incidence of respiratory diseases during the 1998 haze episode in Brunei Darussalam. *Pure and Applied Geophysics*, *160*(1–2), 265–277.

Yadav, R., Beig, G., & Jaaffrey, S. N. A. (2014). The linkages of anthropogenic emissions and meteorology in the rapid increase of particulate matter at a foothill city in the Arawali range of India. *Atmospheric Environment*, *85*, 147–151.

Yang, K., Ding, B., Qin, J., Tang, W., Lu, N., & Lin, C. (2012). Can aerosol loading explain the solar dimming over the Tibetan Plateau? *Geophysical Research Letters*, *39*(20), 1–5.

Yin, L., Niu, Z., Chen, X., Chen, J., Xu, L., & Zhang, F. (2012). Chemical compositions of PM2.5 aerosol during haze periods in the mountainous city of Yong'an, China. *Journal of Environmental Sciences (China)*, *24*(7), 1225–1233.

Current World Environment
An International Research Journal of Environmental Science
ISSN: 0973-4929, Online ISSN: 2320-8031

Spatial variation of Aerosol Optical Depth and Solar Irradiance over Delhi -NCR during Summer season

Purnima Bhardwaj[1]*, Alok Kumar Pandey[1,2], Krishan Kumar[1] and V. K. Jain[1]

[1]School of Environmental Sciences, Jawaharlal Nehru University, New Delhi-110067, India,

[2]Department of Environmental Sciences, Central University of Haryana, Haryana, India

Corresponding author Email: puru1939@gmail.com

Abstract:

Present study shows the spatial variation of Aerosol Optical Depth (AOD), solar irradiance and their association at the urban and rural sites in Delhi and National Capital Region (NCR) during the summer season of the year 2015. Summer-time AOD data from the NASA's Terra satellite MODIS sensor has been used to study the spatial distribution of aerosols over Delhi and its surrounding rural area. The ground data for the direct and global solar irradiances was collected over this region at urban and rural locations in Delhi and NCR using a Fieldspec Spectro-radiometer. HYSPLIT model has been used for the air mass trajectory analysis. The AOD values were observed to be higher over Delhi compared to the relatively lower AOD in rural area of NCR. The NCR site observed higher average solar irradiances than Delhi during the summer season. This may be because of the higher aerosol concentration in Delhi as compared to its outskirts. Also, this region is affected by the severe dust storm events during the summer season which further increases the aerosol load in the atmosphere. HYSPLIT results show the influence of western Thar Desert air masses on the Delhi-NCR. Windblown as well anthropogenic aerosols play a major role in scattering and absorption of the incoming solar radiation and hence, in governing the micro-climatology of the region.

Keywords:

AOD; Solar irradiance; MODIS

Copy the following to cite this article:

Bhardwaj P, Pandey A. K, Kumar K, Jain V. K. Spatial variation of Aerosol Optical Depth and Solar Irradiance over Delhi -NCR during Summer season. Curr World Environ 2017;12(2). .

Copy the following to cite this URL:

Bhardwaj P, Pandey A. K, Kumar K, Jain V. K. Spatial variation of Aerosol Optical Depth and Solar Irradiance over Delhi -NCR during Summer season. Curr World Environ 2017;12(2). Available from: http://www.cwejournal.org/?p=17313

International Journal of Applied Environmental Sciences
ISSN 0973-6077 Volume 12, Number 5 (2017), pp. 1009-1030

http://www.ripublication.com

Characterization and Morphological Analysis of Summer and Wintertime $PM_{2.5}$ Aerosols Over Urban-Rural Locations in Delhi-NCR

Purnima Bhardwaj*[1], Bhupendra P Singh[2], Alok K Pandey[1], Vinod K Jain[1], Krishan Kumar[1]

[1]School of Environmental Sciences, Jawaharlal Nehru University, New Delhi -110067, India
[2]Department of Environmental Studies, Lakshmibai College, Delhi University, New Delhi -110052, India
Email Addresses:
Corresponding author E-mail ID: puru1939@gmail.com

Abstract

Present study investigates the urban-rural variation of aerosols morphological and chemical characteristics. Summer and winter time 24 hourly sampling for $PM_{2.5}$ was carried out at an urban and rural location in Delhi and National Capital Region (NCR) using a Mini-Volume Air Sampler. High $PM_{2.5}$ concentrations were observed at the urban site (87.3μg/m^3, 155.56μg/m^3) compared to those at the rural (39.46μg/m^3, 91.62μg/m^3) in summer and winter seasons respectively. Scanning Electron Microscopy (SEM) and Energy Dispersive X-Ray Spectroscopy (EDX) were used to characterise the $PM_{2.5}$ aerosols in the urban and rural area in the two seasons. SEM images shows different particle shapes at the urban and rural site in summer and winter seasons. SEM results showed the presence of flaky, aggregates and irregular shaped particles dominated in the urban area in summer season whereas rural area was relatively cleaner. In the winter season, rural site was observed to be dominated by spherical and irregular shaped particles indicating the combustion sources whereas particles were observed in a more concentrated form at the urban site. EDX analysis indicates the varying percentages of C, Cu, Zn, Co, Ni, Fe (representative elements) at both the rural and urban sites in both the seasons. Hybrid Single-Particle Lagrangian Integrated Trajectory (HYSPLIT) three day backward air mass trajectories

indicated the influence of Western and N-W air masses over Delhi-NCR for both the summer and winter seasons respectively. Further, this study reveals the variability of $PM_{2.5}$ particles morphological and elemental composition in different seasons at urban and rural locations and highlighted the different probable sources associated with them.

Keywords: $PM_{2.5}$; SEM-EDX; urban-rural; elemental composition

INTRODUCTION

The deteriorating air quality in the megacities and the surrounding rural areas have become a matter of concern in the both the developed and developing world. In India, the $PM_{2.5}$ (particles with diameter $\leq$ 2.5μm) aerosols monitoring have gained importance over the last decade because of their vital role not only in the regional climate studies but in other aspects, such as the air quality, human health, socio-economic and cultural, as well. The National Capital, Delhi, is experiencing rapid economic growth and urbanization which has resulted in the severe air pollution scenarios in the last few years (Hazarika and Srivastava, 2016). The rapidly increasing population and therefore the increasing energy consumption have also helped in alleviating the problem. The National Capital Region (NCR), comprises of the various towns and villages of three states such as Haryana, Uttar Pradesh and Rajasthan which share their border with Delhi, is one of the commercially important and a rapidly urbanizing region. This increase in air pollution, esp. the $PM_{2.5}$ levels, play a major role in the regional/local climate change because of their small size and large residence time.

Depending upon their composition certain particles can cause "cooling" (e.g. sulphate aerosols) or "heating" (e.g. Black Carbon) by scattering/absorbing the incoming solar radiation (Massling et al. 2015). The morphological properties of the particles are useful in understanding the light scattering properties of the particles (Buseck et al. 2000). Light scattering properties depend upon the particle's shape and size and refractive index. The shape and size of the particles differ from region-to-region and seasonally, thus changing their optical properties such as Single Scattering Albedo (SSA), Extinction Efficiency (Q_{ext}) and Assymetry parameter (g) (Mishra et al. 2015). Therefore, regional and seasonal specific ground based measurements regarding the $PM_{2.5}$ aerosols physical and chemical properties is required in order to understand their optical properties and hence their role in regional climate change.

Imaging techniques, such as Scanning Electron Microscopy (SEM) or Transmission Electron Microscopy (TEM) coupled with the Energy Dispersive X-Ray Spectroscopy (EDX) are one of the very useful and powerful techniques to gain an insight into the morphological properties of the particulate matter (Paoletti et al. 1999; Casuccio et al. 2004).These properties help in identifying the possible sources of the particles. Detailed review of the particles morphology have been provided by Pośfai and Buseck (2010). These techniques have been used both nationally and internationally to study the physical and chemical properties of the $PM_{2.5}$ aerosols (Tasic et al. 2006; Rodriguez et al. 2009; Pipal et al. 2011; Tiwari et al. 2015).

Many studies regarding the $PM_{2.5}$ characteristics covering different regions/locations like urban, rural, natural background and different seasons have been carried out globally (Viana et al. 2008; Putaud et al. 2010 ; Khan et al. 2010). Various studies over Delhi have been carried out (Apte et al. 2011; Chelani et al. 2013; Trivedi et al. 2014 ; Tiwari et al. 2014 ; Tiwari et al. 2015; Pant et al. 2015) regarding the role of particulate matter and their chemical and morphological properties but the same information regarding the urban and rural scenario are very few (Pipal et al. 2011; Rastogi et al. 2016). The capital Delhi has been reported to have the highest $PM_{2.5}$ concentration among 20 cities in the world (Steering Committee Report 2015). Some studies have focussed on the indoor $PM_{2.5}$ concentration in the rural area (Massey et al. 2009; Joon et al. 2011; Mukhopadhyay et al. 2012) but the outdoor $PM_{2.5}$ studies in the rural area needs to be explored.

Present study is a comparative study of the $PM_{2.5}$ levels, their morphological and chemical properties and possible sources of these particles in the urban and rural locations in Delhi-NCR in both the summer and winter seasons.

METHODOLOGY

Study area

The Delhi-NCR comprises area of 58332 km^2 with a population of 56.88 million. The population of Delhi increased from 13 million in 2001 to 16 million in the year 2011 (Census of India, 2011). Delhi has seen a 3.63% surge in the energy demand from the year 2005 to 2015. Also, in Delhi the number of registered vehicles has been reported to be 8.8 millions (2014-15). Increase in number of vehicles such as cars, taxis, jeeps, auto rickshaws, buses etc. and two-wheelers like scooters and motor cycles has led to an increase in the pollution levels in Delhi (Economic Survey of Delhi, 2014-2015). Delhi-NCR falls in a semiarid climate zone experiencing different seasons during the course of a year namely, Summer (April-June), Monsoon (July-August), Post-Monsoon (September-November), winter (December- January) and spring (February-March). Summers are usually long with temperature going up to as high as 45°C during daytime (Guttikunda and Gurjar, 2012). The winters are generally cold with calm winds and temperatures going as low as 4-5°C. A strong inversion layer forms over the region during the winters. The average annual rainfall in this region is approximately 670mm. The wind direction is generally north-westerly throughout the year except during monsoon period when it is south-westerly. Sampling was carried out for summer (May-June) and winter (December-January) seasons for the year 2015 at two locations in Delhi-NCR briefly described below.

Sampling sites

Urban site

Shahdara, Delhi (28.68°N, 77.29°E) is one of the oldest and highly urbanized areas of Delhi, consisting both the residential as well as industrial establishments around it.

The sampling site was located near the main Loni Road which is a major arterial road connecting Delhi and Saharanpur, (Uttar Pradesh). It is one of the busiest roads experiencing heavy traffic 24 hours of the day. Loni Road comprises of many shops such as of utilities, local eateries (*dhabhas*), printing presses, mechanics shops or motor repairing shop/workshop and businesses mainly of plywood and timber. The Shahdara Railway Station and Metro Station are located around two kilometers from the sampling site.

Rural site

Sampla, Haryana (28.77°N, 76.76°E) in NCR which is situated around 60km away NW of Delhi represented the rural site which was surrounded mainly by the vast agricultural fields. A few factory establishments and one or two brick kilns are established approximately 10kms away from the sampling site. The national highway (NH-10) and Sampla railway station are located approx. 1-1.5 kms away from the sampling site. Sampla is surrounded by the four major cities/towns such as Bahadurgarh, Rohtak, Sonepat and Jhajjar which are around 20 -40 kms away from the sampling site. Nearest is the Bahadurgarh (approx. 20kms away) which is an industrial area with industries and factories ranging from shoe manufacturing, steel, textiles and chemicals.

$PM_{2.5}$ sampling

Sampling and quality control

Sampling for $PM_{2.5}$ was carried out with the Tactical Air Sampler (TAS) Mini-Vol® Air sampler (Airmetrics) with a constant flow rate of 5L/min for 24 hours a day. The sampler works with a rechargeable lead-acid battery with a 24 hour backup with low flow and low battery shut-offs. PM2.5 sampling was carried out using Whatmann quartz fibre filters (47mm) for 5 days each in both the summer and winter seasons at Shahdara and Sampla respectively. The sampler was placed at a height of 1.5 meters above the floor level of the second floors of residential buildings at each sampling site throughout the study. Filter papers were kept in dessicator with silica gel for 24 hours both pre and post-sampling. Blank filters were also treated in the same way. The sampler pump draws air at the rate of 5litres/minute, which is made to pass through an impactor leading to collection of $PM_{2.5}$ on a quartz filter paper. After sampling the samples were put in the aluminium foil covered petri dishes which were sealed with the plastic cover and cellotape and stored in the refrigerator till further analysis. Samples were weighed pre and post-sampling using microbalance (SARTORIUS GD603) with 0.0001mg accuracy. Care was taken to handle the samples with the forceps all the time. Weight of the samples was calculated gravimetrically. Field and lab blank samples were collected and their concentrations were subtracted from the measured concentrations. Total of 20 samples were collected at both the sampling sites in the summer and winter seasons. The average temperature and relative humidity during the sampling in Delhi-NCR in summer and winter months were 32.8°C, 50.7% and 13.4°C, 66.0% respectively (www.wunderground.com).

SEM-EDX Analysis

SEM-EDX technique was used to analyze $PM_{2.5}$ samples collected from the two sites at Advanced Instrumentation Research Facility (AIRF) in Jawaharlal Nehru University (JNU), New Delhi. The SEM-EDX analysis was carried out with the help of a computer controlled scanning electron microscope SEM (Carl Zeiss EVO 40, Cambridge) coupled with an energy dispersive X-ray (EDX) system (Bruker X-Flash detector 3010, Germany). Prior to the SEM analysis, the samples were mounted on aluminium stubs using double sided carbon tape for gold coating to make the samples electrically conductive. A very thin film of gold (Au) was deposited on the surface of each sample in vacuum coating unit called Gold Sputter Coater (POLARON-SC7640, UK). The samples were placed in the vacuum chamber of SEM instrument at the designated positions for analysis. The SEM working conditions were set at an accelerating voltage of 20 kV, a beam current of 40 - 50μA. The images were recorded at different magnifications 5000x, 10000x, 15000x with a resolution of 20nm. The EDX analysis system consists of Silicon Drift detector with 129eV resolutions and detection limit of 0.1% is capable of collecting spectrum from different points and elemental mapping. A quantitative and qualitative analysis of the elements was done using EDX analysis. The EDX spectra of blank quartz fiber filter was also measured and subtracted from the samples EDX spectra.

Backward trajectory Analysis

NCEP re-analysis data have been downloaded from the NOAA website (ftp://ftp.arl.noaa.gov/pub/archives/reanalysis) for Hybrid Single-Particle Lagrangian Integrated Trajectory (HYSPLIT) model configuration. HYSPLIT model control file has been configured to run model at different heights for the three days backward trajectory analysis in both the summer and winter season.

RESULTS AND DISCUSSION

Seasonal variation of $PM_{2.5}$

The average concentration of $PM_{2.5}$ at the urban (Shahdara) site was found to be relatively higher as compared to the rural site (Sampla) in both the summer and winter seasons. The average $PM_{2.5}$ concentration in the urban site was measured to be 87.33μg/m^3 and 155.56μg/m^3 and in rural was 39.46μg/m^3 and 91.62μg/m^3 in the summer and winter seasons respectively (Figure 2). The average, minimum, maximum concentrations and standard deviation at urban and rural locations in both summer and winter seasons respectively are listed in table 1.

Table 1. The average, minimum, maximum and standard deviation (S.D) of $PM_{2.5}$ concentration ($\mu g/m^3$) at urban and rural location in summer and winter season.

Location	Summer				Winter			
	Avg. ($\mu g/m^3$)	Min. ($\mu g/m^3$)	Max. ($\mu g/m^3$)	S.D	Avg. ($\mu g/m^3$)	Min. ($\mu g/m^3$)	Max. ($\mu g/m^3$)	S.D
Shahdara (Urban)	87.30	41.66	152.70	39.04	155.56	69.40	263.88	89.14
Sampla (Rural)	39.46	33.33	41.67	3.26	91.62	70.92	125.00	20.87

The standard deviation of $PM_{2.5}$ was observed to be highest at the urban site in winter than in summer and lowest at the rural site in summer season. These average daily concentrations at both the sites exceeded the 24 hourly average levels of Central Pollution Control Board (CPCB)-NAAQS $PM_{2.5}$ level (60 $\mu g/m^3$), WHO guidelines (25 $\mu g/m^3$) & US-EPA standards (35 $\mu g/m^3$) except in the summer season at the rural site which were below the prescribed 24 hourly CPCB-NAAQ Standards but exceeded those of US-EPA and WHO standards.

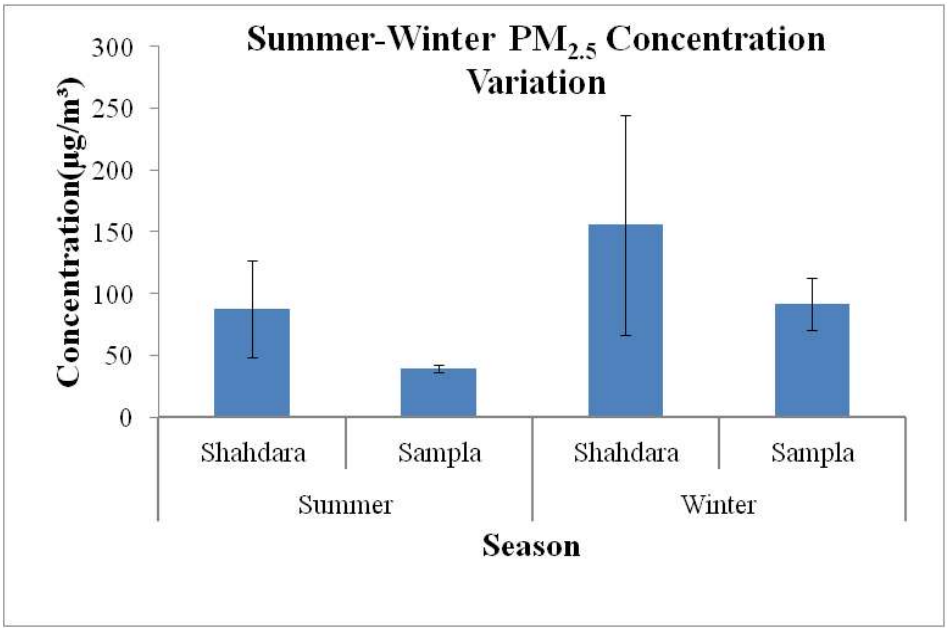

Figure 1. $PM_{2.5}$ concentration at the sites Shahdara (urban) and Sampla (rural).

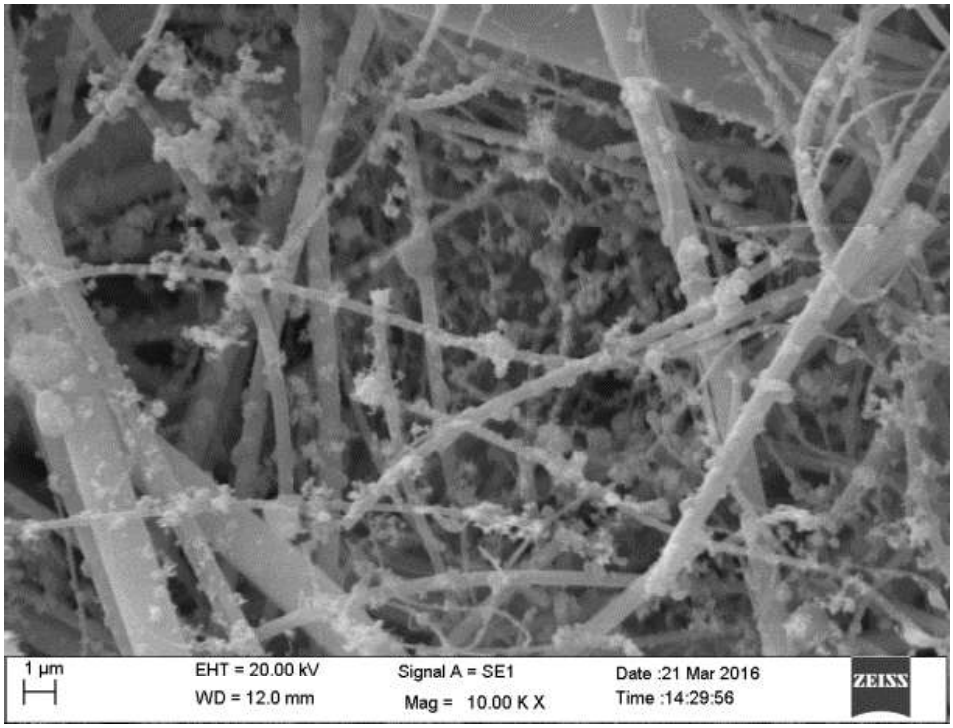

(2a)

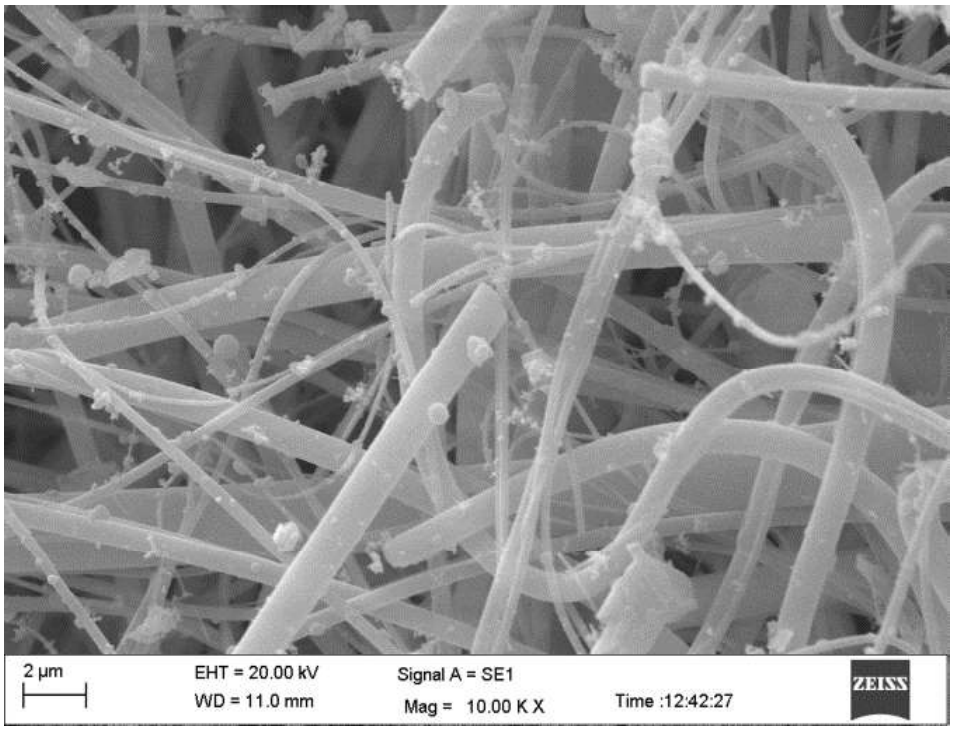

(2b)

Figure 2. SEM images of $PM_{2.5}$ particles in summer season at the urban (2a) and rural site (2b) in Delhi-NCR.

The measured $PM_{2.5}$ concentrations were found to be consistent with the previous studies. During the summer season (Table 2), the measured $PM_{2.5}$ concentration in the Shahdara area was found to be higher than the concentrations reported in various cities such as Chattisgarh (Durg City), Chennai, Pune, Lucknow and cities outside India like Yokohama (Japan) but lower than those reported in Agra and Kanpur. During the winter season, measured concentrations were found to be higher than Chennai, Pune and Yokohama (Japan) but lower than Kanpur, Chattisgarh and Jinan (China) but lie in between those reported at Lucknow. The $PM_{2.5}$ concentrations in the present study were also compared with the other studies reported previously over Delhi. $PM_{2.5}$ concentrations were observed to be higher during the winter season than those reported by Tiwari et al. (2015) but lower than other studies (Trivedi et al. 2014; Pant et al. 2015) and during the summer season, measured concentration was higher than Pant et al. (2015) but almost comparable to Trivedi et al. (2014).

Table 2. Seasonal $PM_{2.5}$ concentrations ($\mu g/m^3$) in urban areas in India and outside India.

Sites	Summer	Winter	Reference
Delhi, India	**87.3**	**155.56**	**Present study**
Kanpur, India	136-232	172-304	Behera et al., (2010)
Yokohama, Japan	20.80±6.3	21.15±9.5	Khan et al., (2010)
Agra, India	90.14±7.21	-	Pipal et al., (2011)
Chattisgarh, India	83.5	215.0	Deshmukh et al., (2011)
Shanghai, China		65.4±16.8	Hou et al., (2011)
Jinan, China	143.25	204.89	Yang et al., (2012)
Fuzhou, China	23.58	59.81	Xu et al., (2012)
Chennai, India	67.0	74.0	Srimuruganandam and Nagendra, (2012)
Lucknow, India	34.3-71.0	144.7-189.3	[a]Pandey et al., (2013)
Kerala, India	12.37-25.6	-	[b]Ragi et al., (2013)
Delhi, India	-	117±79.1	[c]Tiwari et al., (2015)
Delhi, India	86.4±26.8	221.1±94.7	Trivedi et al., (2014)
Delhi, India	58.2±35.0	276.9±99.9	[d]Pant et al., (2015)
Pune, India	76.1±25.5	97.8±30.5	Yadav et al., (2015)

[a,b] Concentrations from lower to higher level
[c] 4h sampling concentration
[d] 12h sampling concentration

From Table 3, the measured concentration at the rural site during winter season is comparable to those reported at other rural sites (Xu et al. 2002; Pachauri et al. 2013) but higher than Rachma (Jordan) and lower than that in Agra (Kulshrestha et al. 2009), Wusumu (China) and Jinan (China). Measured rural concentration during the summer season was found to be higher than Ragi et al. (2013) but lower than the rest of the other studies. The studies regarding the $PM_{2.5}$ concentrations during summer season are very few may be because winter season is most important as far as air quality of a region with respect to $PM_{2.5}$ concentration is concerned.

Table 3. Seasonal $PM_{2.5}$ concentrations ($\mu g/m^3$) in rural areas in India and outside India.

Sites	Summer	Winter	Reference
Haryana, India	**39.46**	**91.62**	**Present study**
Linan, China	-	90.0±47.0	Xu et al. (2002)
Miyun, China	-	683.1±233	Dan et al. (2004)
Rachma, Jordan	-	25.0±7.0	Schneidenesser et al. (2010)
Wusumu, China	50.7	115.6	Han et al. (2008)
Agra, India	59.6±20.6	127.0±53.9	Kulshrestha et al. (2009)
Jinan, China	69.56	146.8	Yang et al. (2012)
Agra, India	-	91.2±17.3	Pachauri et al. (2013)
Agra, India	89.12 ±37.94	-	Pipal et al. (2011)
Kerala, India	14.12-16.89	-	[a]Ragi et al. (2013)

[a] Concentrations from lower to higher level

The months of April-June characterise the summer season in the North India. During the summer season, high atmospheric boundary layer and strong surface winds leads to the proper dispersion of pollutants and therefore, less concentration near the surface. This might be true up to a point in the rural areas as anthropogenic pollution sources are far and few as compare to urban areas where they are present in large numbers, thus, effectively keeping the pollution level high even during the summer season. The other sources of $PM_{2.5}$ aerosols in the rural region may also include the biomass burning (April-May; October-December), bio-fuels (wood and cow-dung cakes) for cooking purposes, transport of pollutants by wind from the nearby industrial areas and brick kilns (Guttikunda and Calori 2013). Heavy metals along with the dust are also carried by the wind during the summer season, further aggravating the air pollution and affecting the visibility (Pandithurai et al. 2008). High level of $PM_{2.5}$ concentration over Delhi in both the summer and winter seasons could

be because of significant amount of anthropogenic emissions such as vehicular, coal based thermal power plants, which are also a source of sulphates, nitrates and carbonaceous aerosols such as black carbon, brick kilns, dust from large scale constructional activities, especially, in the urban areas, the burning of wood, coal, garden cuttings, and dead leaves (Prasad et al. 2006; Chowdhury et al. 2007; CPCB, 2010; Guttikunda and Calori, 2013; Sharma et al. 2014). $PM_{2.5}$ concentrations during winter in the Delhi-NCR are also affected by meteorological conditions (calm or no winds and lower inversion height) leading to poor dispersion of pollutants causing them to accumulate near the surface. The high level of anthropogenic aerosols during the winter greatly affects the visibility of the region which badly hits the transport sector both (air and ground), safety of the public, business and tourism (Singh and Dey, 2012). Haziness of the sky, as a resut of anthropogenic aerosols, further plays an important role in the solar irradiance attenuation studies (Ramanathan et al. 2001). As solar radiation is one of the major driving force of various earth and life processes, understanding the role of the aerosols interactions with the incoming solar radiation is very important for various scientific, academic and industrial applications. Higher the concentration of the aerosols, higher will be the attenuation of the incoming solar radiation.

SEM Analysis

Seasonal variation in the particles morphology could be seen at both the urban and rural sites through SEM application. The flaky, free, aggregated and irregular shaped particles (Figure 2a) were found to be dominated in the urban areas during the summer season. The SEM results show that the rural area samples were relatively cleaner (Figure 2b) as compared to the urban area samples. However, ultrafine and spherical shaped particles were found to be present in the rural samples during the summer season but not in significant amount. The long tubular structures represent the quartz filter fibres in all the SEM images. During winter season, the spherical, aggregated and irregular shaped particles were found to be dominated in both the urban and rural areas. The individual spherical, irregular shaped particles, which were embedded in fibre filters, were more prominently observed at the rural site (Figure 3b) as compared to the urban site where particles were observed to be in a much more concentrated form on the fibre filter strands (Figure 3a). Particles with spherical shape and smooth surfaces are generally characterised by the combustion processes at high temperatures (Tasic et al. 2006). Various atmospheric models consider the spherical shape of the particles for solar attenuation studies (Buseck et al. 2000). Irregular shaped particles could be formed as result of aggregation (Rodriguez et al. 2009). Similar results have been reported in other studies (Tasic et al. 2006; Pipal et al. 2011; Tiwari et al. 2015). Soot particles were observed as aggregates of smaller particles at both the rural and urban sites in the winter and at urban site in summer season. These aggregates are often irregular shaped of different sizes. Soot particles are also known to cause the "heating" of the atmosphere by absorbing the incoming solar irradiance (Tiwari et al. 2015). Also, different processes of particle formation results in different morphologies of the particles. Coagulation processes also result in irregular particles

in the fine mode fraction. Breed et al. (2002) reported contribution of combustion processes more to the fine mode fraction. In rural areas, combustion processes generally include burning of biomass seasonally and bio-fuels for various purposes such as cooking whereas in urban areas there are numerous combustion processes as discussed above. Though the SEM analysis is a powerful tool to determine the shape and size of the $PM_{2.5}$ particle but it still has some limitations. For example, the SEM analysis, cannot tell the presence of the hollow spherical particles. Given the complex fibre structure of the quartz fibre filter, manual SEM analysis of the collected particles is often limited by the heavily loaded samples which makes it difficult for the individual particles to be analyzed effectively (Casuccio et al. 2004).

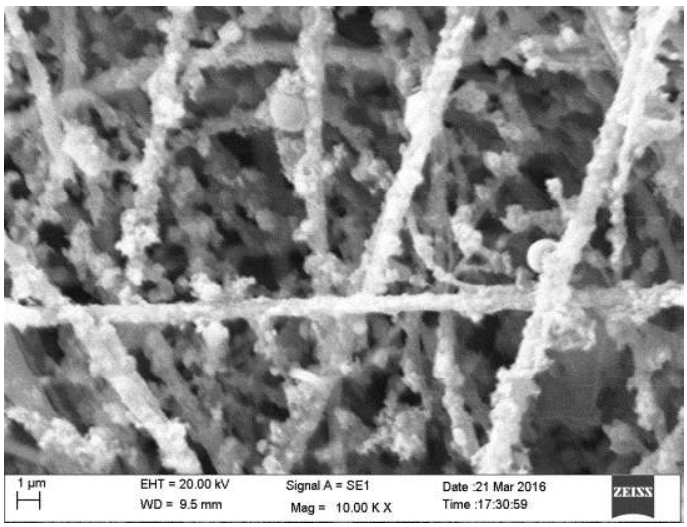

(3a)

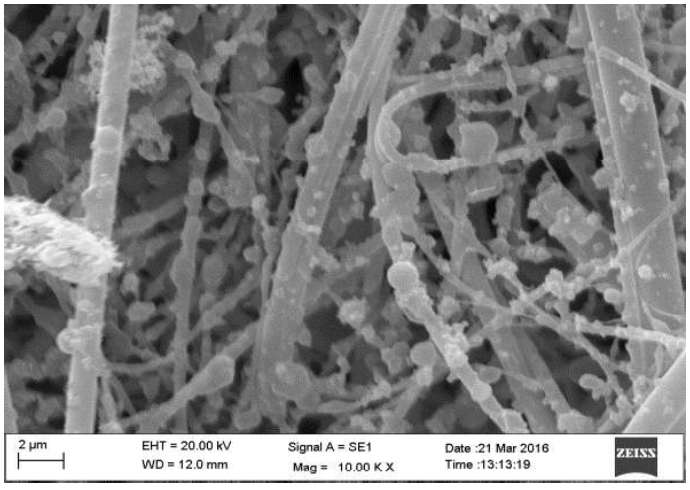

(3b)

Figure 3. SEM images of $PM_{2.5}$ particles in winter season in the urban (3a) and rural area (3b) in Delhi-NCR.

EDX Analysis:

Figures 4 and 5 respectively show summer and winter variability of the elemental composition of the $PM_{2.5}$ aerosols at the urban and rural sites in Delhi-NCR.

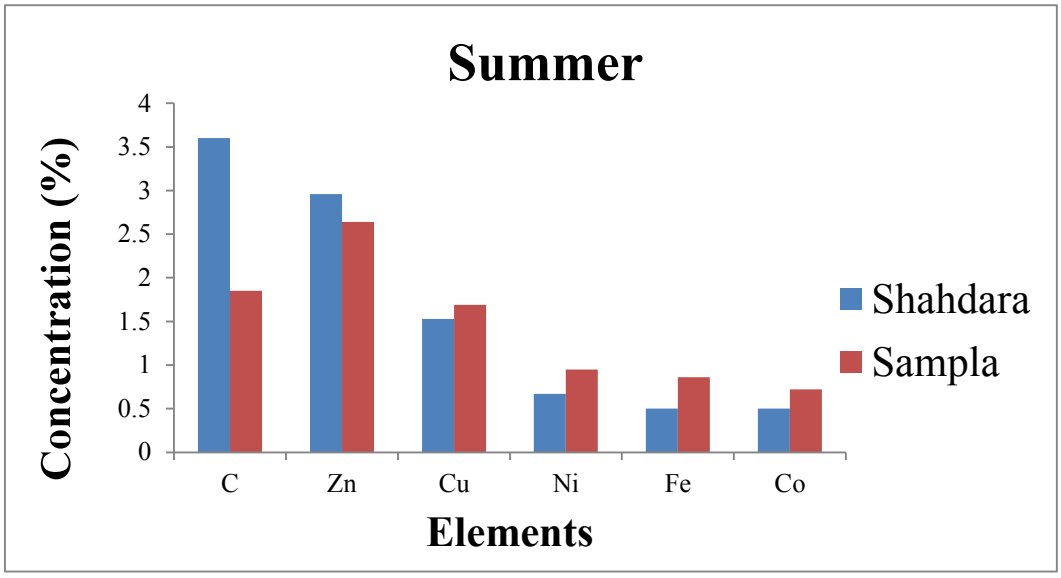

Figure 4. EDX results of elements in $PM_{2.5}$ for urban and rural sampling sites during summer.

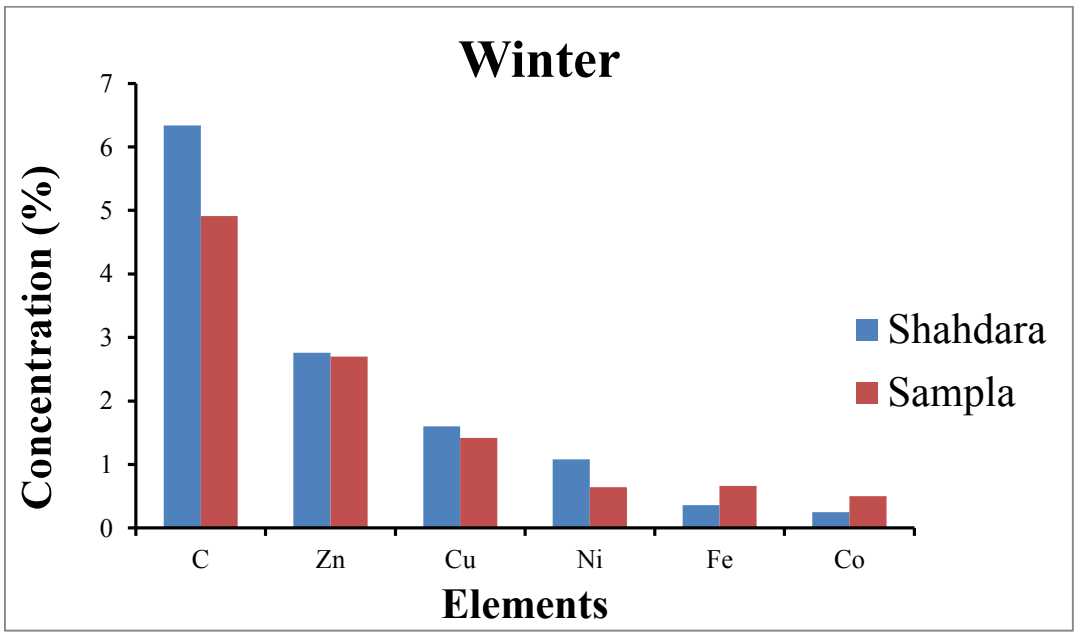

Figure 5. EDX results of elements in $PM_{2.5}$ for urban and rural sampling sites during winter.

Trace elements

In summer season, the concentration of Zn was observed to be higher at the urban site than the rural site, but was comparable in the winter season at both the sites. In urban area, Cu was found to be slightly higher in winter than summer whereas, in the rural area, Cu concentration was observed to be higher in summer season than winter. Similar variation for Ni was also observed i.e. higher values during summer (rural site) and winter (urban site) seasons. However, the concentrations of Fe and Co were found to be decreasing in winter than summer season at both the sites. Again, Fe and Co were found to be higher in rural area in both the summer and winter seasons as compare to urban area. Presence of Zn and Ni at rural site could be due to diesel-fuelled trucks plying on NH-10 throughout the day and tractors used for the agricultural purposes (Reff et al. 2009). Delhi has two major coal based thermal power plants, large amount of industrial and vehicular (including tire wear and brake lining) emissions, combustible processes using coal and oil which could be the sources of Ni, Cu, Zn and Fe (Hays et al. 2011; Sahu et al. 2011b; Patil et al. 2013; Farao et al. 2014; Pant et al. 2015). Zn has also been associated with incineration (Harrison et al. 1997). Fugitive dust, paints and varnishes for buildings doors and windows have been reported as sources of Co (Srivastava and Jain, 2007; Reff et al. 2009).

Carbon

Carbon concentration was observed to be higher during winter at both the urban and rural sites, but increase was observed to be higher in the urban area than the rural area in both the summer and winter seasons indicating the effect of numerous sources, such as biomass burning high amount of vehicular, industrial and coal based power plants emissions which are the major sources of carbonaceous aerosols in the atmosphere in urban areas (Prasad et al. 2006; Moreno et al. 2013; Singh et al. 2015) and meteorological conditions. Biannual crop residue burning, using bio-fuels like cow-dung cakes and wood for cooking and heating purposes in rural areas could be the possible sources of carbon content in the rural atmosphere (Rastogi et al. 2016, Pandey et al. 2017). The high amount of carbon in the urban area could indicate the presence of absorbing aerosols in the urban atmosphere. These aerosols absorb the incoming solar irradiance as well as outgoing terrestrial infrared radiation thereby "heating" the atmosphere. This leads to the formation of urban heat island (UHI) indicating the temperature over urban area is higher than the surrounding rural areas (Pandey et al. 2014).

The observed trend in the summer season is: C>Zn>Cu>Ni>Fe ~ Co in Shahdara whereas in Sampla it is Zn>C>Cu>Ni>Fe>Co. However, in winter season observed trend in Shahdara is C>Zn>Cu>Ni>Fe>Co and in Sampla it is C>Zn>Cu>Ni~Fe>Co. Similar trend of Zn > Cu has been observed in Navarra, Spain (Aldabe et al. 2011).

In Delhi, the diesel vehicles and industrial pollution have been ascertained to be the major contributors to the pollution (Srivastava and Jain, 2008) whereas the other sources such as mineral or soil dust, solid waste, gasoline vehicles, or paved road are

found to be variable. However, in the present study, the variability in the elemental composition at the two sampling sites is not found to be very significant. The characterization and source identification of $PM_{2.5}$ aerosols is very much important as they have large residence time in the atmosphere and can be transported to a long distance with wind thus greatly affecting the air quality and human health. The elemental composition of the aerosols can also be used to study the solar attenuation processes by various elements (e.g. Carbon).

Trajectory Analysis

Summer and winter-time three day backward air mass trajectories have been shown in the Figure 6(a) and Figure 6(b) respectively. To understand the movement of air mass at different heights, air mass trajectories were drawn at three different heights levels from ground level i.e. 50m, 500m and 1000m. This was done to understand how different air pollutants, especially aerosols, which have reasonably long residence times, are being transported across various regions. During summertime, air mass originates in the Arabian Sea and gradually moves towards Thar Desert and move further towards the Delhi and NCR (Figure 6a). Delhi-NCR is under the influence of the air masses from North-Western parts mainly Haryana-Punjab and Pakistan (Figure 6b). A downward movement of the air masses have also been seen in the trajectories plots, which depict greater stability conditions. Higher atmospheric stability favours the build up of pollutants in the atmosphere in Delhi-NCR during winter.

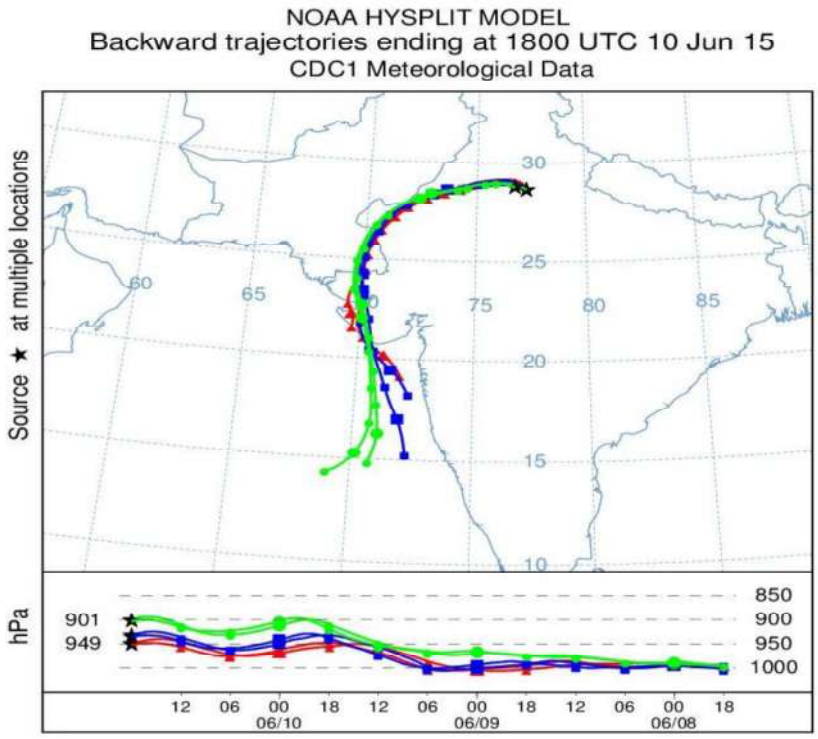

(a)

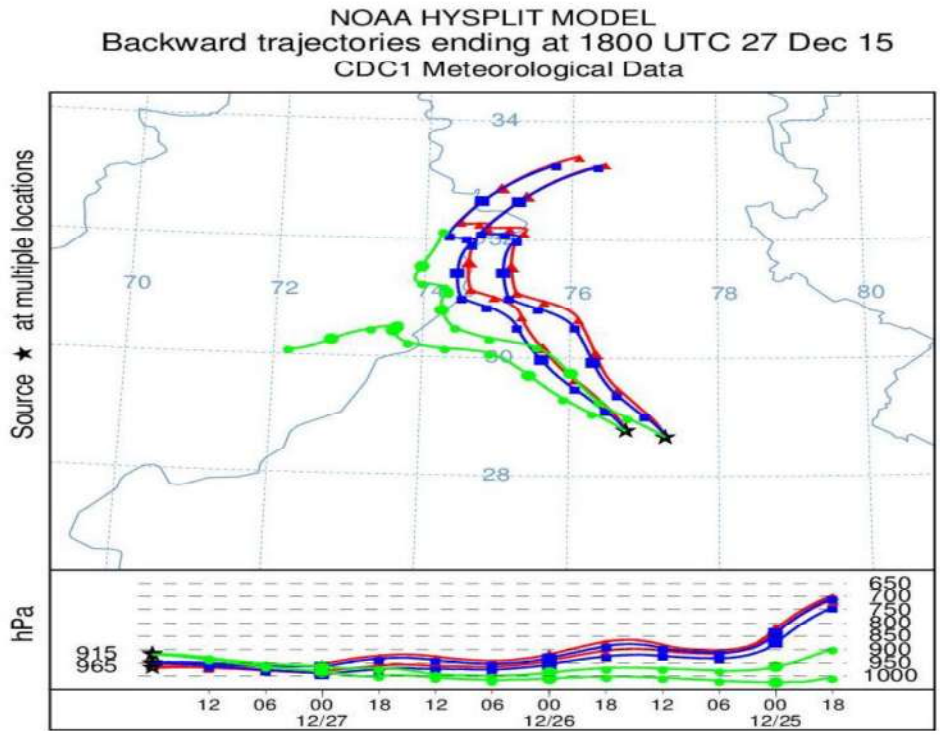

(b)

Figure 6. Three-days backward trajectory from NOAA HYSPLIT model over Delhi-NCR during the (a) summer and (b) winter season.

CONCLUSION

Measured $PM_{2.5}$ concentrations were higher at the urban site as compared to the rural site in both the summer and winter seasons. Irregular shaped and flaky particles were found to be abundant in summer season whereas in winter, particles were in a concentrated form at the urban site. Rural area SEM results show relatively cleaner with presence of a few ultrafine and spherical particles during the summer season. Spherical, irregular shaped particles dominated in the rural area in the winter season indicating the presence of combustion sources such as biomass burning. Elements such as C, Zn, Cu, Ni, Fe and Co indicating the presence of anthropogenic sources were observed in varying concentrations at both the sampling sites in both the summer and winter seasons. The HYSPLIT three day backward trajectories during the summer season showed a North and North-westerly influence apart from local sources emissions on air mass over Delhi-NCR. The air masses movements show the characteristics of the area over which they passes. The comprehensive studies regarding the aerosols properties need to be carried out further in order to understand the role of aerosols in light scattering processes and hence, the regional /local climate change.

ACKNOWLEDGEMENT

I would like to thank the University Grant Commission (UGC), Government of India for financial support for this study. Authors are also thankful to Advanced Instrumentation Research Facility (AIRF), Jawaharlal Nehru University, New Delhi for facilitating the SEM and EDX analysis.

REFERENCES

[1] Aldabe, J., Elustondo, D., Santamaría, C., Lasheras, E., Pandolfi, M., Alastuey, A., ... & Santamaría, J. M. (2011). Chemical characterisation and source apportionment of PM2. 5 and PM10 at rural, urban and traffic sites in Navarra (North of Spain). Atmospheric Research, *102*(1), 191-205.

[2] Apte, J. S., Kirchstetter, T. W., Reich, A. H., Deshpande, S. J., Kaushik, G., Chel, A., ... & Nazaroff, W. W. (2011). Concentrations of fine, ultrafine, and black carbon particles in auto-rickshaws in New Delhi, India. Atmospheric Environment, *45*(26), 4470-4480.

[3] Behera, S. N., & Sharma, M. (2010). Reconstructing primary and secondary components of $PM_{2.5}$ composition for an urban atmosphere. Aerosol Science and Technology, *44*(11), 983-992.

[4] Breed, C. A., Arocena, J. M., & Sutherland, D. (2002). Possible sources of PM 10 in Prince George (Canada) as revealed by morphology and in situ chemical composition of particulate. Atmospheric Environment, *36*(10), 1721-1731.

[5] Buseck, P. R., Jacob, D. J., Pósfai, M., Li, J., & Anderson, J. R. (2000). Minerals in the air: An environmental perspective. *International Geology Review*, *42*(7), 577-593.

[6] Casuccio, G. S., Schlaegle, S. F., Lersch, T. L., Huffman, G. P., Chen, Y., & Shah, N. (2004). Measurement of fine particulate matter using electron microscopy techniques. Fuel Processing Technology, *85*(6), 763-779.

[7] Census of India 2011, Economic Survey of Delhi (2012-13), Chapter 2 - Demographic Profile, pp. 8-26. (http://delhi.gov.in/DoIT/DoIT_Planning/ES2012-13/EN/ES_Chapter%202.pdf).

[8] Chelani, A. B. (2013). Statistical Characteristics of Ambient $PM_{2.5}$ Concentration at a Traffic Site in Delhi: Source Identification Using Persistence Analysis and Nonparametric Wind Regression. Aerosol and Air Quality Research, *13*, 1768-1778.

[9] Chowdhury, Z., Zheng, M., Schauer, J. J., Sheesley, R. J., Salmon, L. G., Cass, G. R., & Russell, A. G. (2007). Speciation of ambient fine organic carbon particles and source apportionment of $PM_{2.5}$ in Indian cities. Journal of Geophysical Research: Atmospheres, *112*(D15).

[10] CPCB-NAAQS 2009 Report (2010-2011), pp-3. (http://cpcb.nic.in/upload/Publications/Publication_514_airqualitystatus2009.pdf).

[11] Criterion Air Pollutants, Environment Protection Agency (EPA), United States. (https://www.epa.gov/criteria-air-pollutants/naaqs-table).

[12] Dan, M., Zhuang, G., Li, X., Tao, H., & Zhuang, Y. (2004). The characteristics of carbonaceous species and their sources in $PM_{2.5}$ in Beijing. Atmospheric Environment, *38*(21), 3443-3452.

[13] Deshmukh, D. K., Deb, M. K., Tsai, Y. I., & Mkoma, S. L. (2011). Water soluble ions in $PM_{2.5}$ and PM_1 aerosols in Durg city, Chhattisgarh, India. Aerosol and Air Quality Research, *11*, 696-708.

[14] Dey, S., Di Girolamo, L., van Donkelaar, A., Tripathi, S. N., Gupta, T., & Mohan, M. (2012). Variability of outdoor fine particulate (PM 2.5) concentration in the Indian subcontinent: a remote sensing approach. Remote Sensing of Environment, *127*, 153-161.

[15] Economic Survey of Delhi Report 2014-15, Chapter 8, pp:107. (http://www.delhi.gov.in)

[16] Farao, C., Canepari, S., Perrino, C., & Harrison, R. M. (2014). Sources of PM in an industrial area: comparison between receptor model results and semi-empirical calculations of source contributions. Aerosol and Air Quality Research, *14*, 1558-1572.

[17] Guttikunda, S. K., & Gurjar, B. R. (2012). Role of meteorology in seasonality of air pollution in megacity Delhi, India. Environmental Monitoring and Assessment, 184(5), pp. 3199-3211.

[18] Guttikunda, S. K., & Calori, G. (2013). A GIS based emissions inventory at 1 km× 1 km spatial resolution for air pollution analysis in Delhi, India. Atmospheric Environment, *67*, 101-111.

[19] Han, Y. M., Han, Z. W., Cao, J. J., Chow, J. C., Watson, J. G., An, Z. S., ... & Zhang, R. J. (2008). Distribution and origin of carbonaceous aerosol over a rural high-mountain lake area, Northern China and its transport significance. Atmospheric Environment, *42*(10), 2405-2414.

[20] Harrison, R. M., Smith, D. J. T., Piou, C. A., & Castro, L. M. (1997). Comparative receptor modelling study of airborne particulate pollutants in Birmingham (United Kingdom), Coimbra (Portugal) and Lahore (Pakistan). Atmospheric Environment, *31*(20), 3309-3321.

[21] Hays, M. D., Cho, S. H., Baldauf, R., Schauer, J. J., & Shafer, M. (2011). Particle size distributions of metal and non-metal elements in an urban near-highway environment. Atmospheric Environment, *45*(4), 925-934.

[22] Hazarika, N., & Srivastava, A. (2016). Estimation of risk factor of elements and PAHs in size-differentiated particles in the National Capital Region of India. Air Quality, Atmosphere & Health, 1-14.

[23] Joon, V., Kumari, H., Chandra, A., & Bhattacharya, M. (2011). Predicting exposure levels of respirable particulate matter (PM2.5) and carbon monoxide for the cook from combustion of cooking fuels. In International Conference on Chemistry and Chemical Process (Vol. 10, pp. 229-232).

[24] Khan, M. F., Shirasuna, Y., Hirano, K., & Masunaga, S. (2010). Characterization of $PM_{2.5}$, $PM_{2.5–10}$ and $PM_{> 10}$ in ambient air, Yokohama, Japan. Atmospheric Research, *96*(1), 159-172.

[25] Kulshrestha, A., Satsangi, P. G., Masih, J., & Taneja, A. (2009). Metal concentration of $PM_{2.5}$ and PM_{10} particles and seasonal variations in urban and rural environment of Agra, India. Science of the Total Environment, *407*(24), 6196-6204.

[26] Massey, D., Masih, J., Kulshrestha, A., Habil, M., & Taneja, A. (2009). Indoor/outdoor relationship of fine particles less than 2.5 μm (PM 2.5) in residential homes locations in central Indian region. Building and Environment, *44*(10), 2037-2045.

[27] Massling, A., Nielsen, I. E., Kristensen, D., Christensen, J. H., Sørensen, L. L., Jensen, B., ... & Skov, H. (2015). Atmospheric black carbon and sulfate concentrations in Northeast Greenland. Atmospheric Chemistry and Physics, *15*(16), 9681-9692.

[28] Middleton, N. J. (1986), A geography of dust storms in south west Asia, Int. J. Climatol., 6, 183–196, doi:10.1002/joc.3370060207.

[29] Mishra, S. K., Agnihotri, R., Yadav, P. K., Singh, S., Prasad, M. V. S. N., Praveen, P. S., ... & Sharma, C. (2015). Morphology of atmospheric particles over Semi-Arid region (Jaipur, Rajasthan) of India: Implications for optical properties. Aerosol and Air Quality Research, *15*(3), 974-984.

[30] Moreno, T., Karanasiou, A., Amato, F., Lucarelli, F., Nava, S., Calzolai, G., ... & Borge, R. (2013). Daily and hourly sourcing of metallic and mineral dust in urban air contaminated by traffic and coal-burning emissions. Atmospheric Environment, *68*, 33-44.

[31] Mukhopadhyay, R., Sambandam, S., Pillarisetti, A., Jack, D., Mukhopadhyay, K., Balakrishnan, K., ... & Smith, K. R. (2012). Cooking practices, air quality, and the acceptability of advanced cookstoves in Haryana, India: an exploratory study to inform large-scale interventions. Global Health Action, *5*.

[32] National Capital Region Planning Board, Ministry of Urban development, Govt. of India, Annual Report 2015-16, pp-3. (http://ncrpb.nic.in/pdf_files/Annual%20Report%202015-16.pdf).

[33] Pachauri, T., Satsangi, A., Singla, V., Lakhani, A., & Kumari, K. M. (2013). Characteristics and sources of carbonaceous aerosols in $PM_{2.5}$ during wintertime in Agra, India. Aerosol and Air Quality Research, *13*(3), 977-991.

[34] Pandey, P., Patel, D. K., Khan, A. H., Barman, S. C., Murthy, R. C., & Kisku, G. C. (2013). Temporal distribution of fine particulates ($PM_{2.5}$, PM_{10}), potentially toxic metals, PAHs and Metal-bound carcinogenic risk in the population of Lucknow City, India. Journal of Environmental Science and Health, Part A, *48*(7), 730-745.

[35] Pandey, A. K., Mishra, A. K., Kumar, R., Berwal, S., Devadas, R., Huete, A., & Kumar, K. (2017). CO variability and its association with household cooking fuels consumption over the Indo-Gangetic Plains. Environmental Pollution. 222, 83 – 93

[36] Pandey, A. K., Singh, S., Berwal, S., Kumar, D., Pandey, P., Prakash, A., ... & Kumar, K. (2014). Spatio–temporal variations of urban heat island over Delhi. Urban Climate, *10*, 119-133.

[37] Pandithurai, G., S. Dipu, K. K. Dani, S. Tiwari, D. S. Bisht, P. C. S. Devara, and R. T. Pinker (2008), Aerosol radiative forcing during dust events over New Delhi, India. Journal of Geophysical Research 113, D13209.

[38] Pant, P., Shukla, A., Kohl, S. D., Chow, J. C., Watson, J. G., & Harrison, R. M. (2015). Characterization of ambient $PM_{2.5}$ at a pollution hotspot in New Delhi, India and inference of sources. Atmospheric Environment, *109*, 178-189.

[39] Paoletti, L., Diociaiuti, M., De Berardis, B., Santucci, S., Lozzi, L., & Picozzi, P. (1999). Characterisation of aerosol individual particles in a controlled underground area. Atmospheric Environment, *33*(22), 3603-3611.

[40] Patil, R. S., Kumar, R., Menon, R., Shah, M. K., & Sethi, V. (2013). Development of particulate matter speciation profiles for major sources in six cities in India. Atmospheric Research, *132*, 1-11.

[41] Pipal, A. S., Kulshrestha, A., & Taneja, A. (2011). Characterization and morphological analysis of airborne $PM_{2.5}$ and PM_{10} in Agra located in north central India. Atmospheric Environment, *45*(21), 3621-3630.

[42] Pósfai, M., & Buseck, P. R. (2010). Nature and climate effects of individual tropospheric aerosol particles. Annual Review of Earth and Planetary Sciences, *38*, 17-43.

[43] Prasad, A. K., Singh, R. P., & Kafatos, M. (2006). Influence of coal based thermal power plants on aerosol optical properties in the Indo- Gangetic basin. Geophysical Research Letters, *33*(5).

[44] Putaud, J. P., Van Dingenen, R., Alastuey, A., Bauer, H., Birmili, W., Cyrys, J., & Harrison, R. M. (2010). A European aerosol phenomenology–3: Physical

and chemical characteristics of particulate matter from 60 rural, urban, and kerbside sites across Europe. Atmospheric Environment, *44*(10), 1308-1320.

[45] Ragi, M.S., Muralidharan V., Nita Sukumar and Neethu Sha A.P (2013). Short-term assessment of fpm concentration in the urban and rural ambient air environments of an Indian tropical area at thiruvananthapuram, Kerala. International Journal of Geology, Earth & Environmental Sciences, Vol.3 (3) 52-60.

[46] Ramanathan, V., Crutzen, P. J., Lelieveld, J., Mitra, A. P., Althausen, D., Anderson, J., and Clarke, A. D. (2001). Indian Ocean Experiment: An integrated analysis of the climate forcing and effects of the great Indo-Asian haze. Journal of Geophysical Research: Atmospheres, 106(D22), pp. 28371-28398.

[47] Rastogi, N., Singh, A., Sarin, M. M., & Singh, D. (2016). Temporal variability of primary and secondary aerosols over northern India: impact of biomass burning emissions. Atmospheric Environment, *125*, 396-403.

[48] Reff, A., Bhave, P. V., Simon, H., Pace, T. G., Pouliot, G. A., Mobley, J. D., & Houyoux, M. (2009). Emissions inventory of $PM_{2.5}$ trace elements across the United States. Environmental Science & Technology, *43*(15), 5790-5796.

[49] Report of the Steering Committee on Air Pollution and Health Related Issues, August 2015, pp: 7-8. http://www.mohfw.nic.in/showfile.php?lid=3650.

[50] Rodríguez, I., Galí, S., & Marcos, C. (2009). Atmospheric inorganic aerosol of a non-industrial city in the centre of an industrial region of the North of Spain, and its possible influence on the climate on a regional scale. Environmental Geology, *56*(8), 1551-1561.

[51] Sahu, M., Hu, S., Ryan, P. H., Le Masters, G., Grinshpun, S. A., Chow, J. C., & Biswas, P. (2011). Chemical compositions and source identification of $PM_{2.5}$ aerosols for estimation of a diesel source surrogate. Science of the Total Environment, *409*(13), 2642-2651.

[52] Schneidemesser, E.V., Zhou, J., Stone, E.A., Schauer, J.J., Qasrawi, R. *et al*. (2010). Seasonal and Spatial Trends in the Sources of Fine Particle Organic Carbon in Israel, Jordan, and Palestine. Atmospheric Environment, 44: 3669–3678.

[53] Sharma, M., Kaskaoutis, D. G., Singh, R. P., & Singh, S. (2014). Seasonal variability of atmospheric aerosol parameters over Greater Noida using ground sunphotometer observations. Aerosol and Air Quality Research, 14(3), pp. 608-622.

[54] Singh, A., & Dey, S. (2012). Influence of aerosol composition on visibility in megacity Delhi. Atmospheric Environment, *62*, 367-373.

[55] Singh, A., Rastogi, N., Sharma, D., & Singh, D. (2015). Inter and intra-annual variability in aerosol characteristics over northwestern Indo-Gangetic Plain. Aerosol and Air Quality Research, *15*, 376-386.

[56] Singh, R., Kulshrestha, M. J., Kumar, B., & Chandra, S. (2016). Impact of anthropogenic emissions and open biomass burning on carbonaceous aerosols in urban and rural environments of Indo-Gangetic Plain. Air Quality, Atmosphere & Health, *9*(7), 809-822.

[57] Srivastava, A., & Jain, V. K. (2007). Seasonal trends in coarse and fine particle sources in Delhi by the chemical mass balance receptor model. Journal of Hazardous Materials, *144*(1), 283-291.

[58] Srivastava, A., & Jain, V. K. (2007). Size distribution and source identification of total suspended particulate matter and associated heavy metals in the urban atmosphere of Delhi. Chemosphere, *68*(3), 579-589.

[59] Srivastava, A., Gupta, S., & Jain, V. K. (2009). Winter-time size distribution and source apportionment of total suspended particulate matter and associated metals in Delhi. Atmospheric Research, *92*(1), 88-99.

[60] Srivastava, A., Jain, V. K., & Srivastava, A. (2009). SEM-EDX analysis of various sizes aerosols in Delhi India. Environmental Monitoring and Assessment, *150*(1-4), 405.

[61] Srimuruganandam, B., & Nagendra, S. S. (2012). Application of positive matrix factorization in characterization of PM_{10} and $PM_{2.5}$ emission sources at urban roadside. Chemosphere, *88*(1), 120-130.

[62] Tasić, M., Đurić-Stanojević, B., Rajšić, S., Mijić, Z., & Novaković, V. (2006). Physico-Chemical Characterization of PM. Acta Chimica Slovenica, *53*, 401-405.

[63] Tiwari, S., Bisht, D. S., Srivastava, A. K., Pipal, A. S., Taneja, A., Srivastava, M. K., & Attri, S. D. (2014). Variability in atmospheric particulates and meteorological effects on their mass concentrations over Delhi, India. Atmospheric Research, *145*, 45-56.

[64] Trivedi, D. K., Ali, K., & Beig, G. (2014). Impact of meteorological parameters on the development of fine and coarse particles over Delhi. Science of the Total Environment, *478*, 175-183.

[65] Tiwari, S., Pipal, A. S., Hopke, P. K., Bisht, D. S., Srivastava, A. K., Tiwari, S., ... & Pervez, S. (2015). Study of the carbonaceous aerosol and morphological analysis of fine particles along with their mixing state in Delhi, India: a case study. Environmental Science and Pollution Research, *22*(14), 10744-10757.

[66] Viana, M., Kuhlbusch, T. A. J., Querol, X., Alastuey, A., Harrison, R. M., Hopke, P. K., ... & Hueglin, C. (2008). Source apportionment of particulate

matter in Europe: a review of methods and results. Journal of Aerosol Science, *39*(10), 827-849.

[67] WHO Air quality guidelines for particulate matter, ozone, nitrogen dioxide and sulfur dioxide, Global Update, 2005, pp-9. (http://apps.who.int/iris/bitstream/10665/69477/1/WHO_SDE_PHE_OEH_06.02_eng.pdf).

[68] Xu, J., Bergin, M. H., Yu, X., Liu, G., Zhao, J., Carrico, C. M., & Baumann, K. (2002). Measurement of aerosol chemical, physical and radiative properties in the Yangtze delta region of China. Atmospheric Environment, *36*(2), 161-173.

[69] Xu, L., Chen, X., Chen, J., Zhang, F., He, C., Zhao, J., & Yin, L. (2012). Seasonal variations and chemical compositions of $PM_{2.5}$ aerosol in the urban area of Fuzhou, China. Atmospheric Research, *104*, 264-272.

[70] Yadav, S., Praveen, O. D., & Satsangi, P. G. (2015). The effect of climate and meteorological changes on particulate matter in Pune, India. Environmental Monitoring and Assessment, *187*(7), 402.

[71] Yang, L., Zhou, X., Wang, Z., Zhou, Y., Cheng, S., Xu, P., Gao, X., Nie, W., Wang, X. and Wang, W. (2012). Airborne Fine Particulate Pollution in Jinan, China: Concentrations, Chemical Compositions and Influence on Visibility Impairment. Atmospheric Environment. 55: 506–514.

CURRICULUM-VITAE

Purnima Bhardwaj
Ph.D. Student
School of Environmental Sciences
Jawaharlal Nehru University
New Delhi-110067, India
Email : puru1939@gmail.com
Contact No. + 91-9811434673

CURRENT POSITION

Ph.D. Student
School of Environmental Sciences, Jawaharlal Nehru University **July 2011 - Present**

RESEARCH INTERESTS

- Atmospheric Sciences
- Remote Sensing & GIS

EDUCATION

Jawaharlal Nehru University New Delhi, India

Ph.D., Environmental Sciences Ongoing

Thesis Title: Urban-Rural Aerosol Characteristics and Solar Insolation over Delhi-NCR

Jawaharlal Nehru University New Delhi, India

M.Phil., Environmental Sciences (Course work only) 2012

Delhi University Delhi, India

M.Sc., Physics 2010

Professional Qualification

- ❖ Short Course in **Remote Sensing and Image Interpretation - Indian Institute of Remote Sensing, Dehradun, India**

ACADEMIC ACHIEVEMENTS

- ❖ Recipient of **Basic Scientific Research (Fellowship) –** University Grants Commission (UGC), India
- ❖ Secured Ist Rank in JNU Entrance Examination for M. Phil./Ph.D Program (2011)

PUBLICATIONS

Peer-reviewed Refereed Journals:

- Bhardwaj, P., Singh, B. P., Pandey, A. K., Jain, V. K., & Kumar, K. (2017). Characterization and Morphological Analysis of Summer and Wintertime $PM_{2.5}$ Aerosols Over Urban-Rural Locations in Delhi-NCR. *International Journal of Applied Environmental Sciences*, *12*(5), 1009-1030. (ISSN No. 0974-0260)

- **Bhardwaj, P.**, Pandey, A. K., Kumar, K., & Jain, V. K. (2017). *Spatial variation of Aerosol Optical depth and Solar Irradiance over Delhi-NCR during Summer season.* **Current World Environment**, 12(2). (ISSN: 2320-8031). (In-Press)

PROFICIENCY

Computer:

- User level proficiency in Operating Systems – Mac, Windows
- Mathematical software's like : SPSS
- Remote sensing-GIS Software's like: ArcGIS, ENVI, and Erdas Imagine

Instrumentation:

- Handheld Field Spectro – Radiometer
- DRI Thermal Optical Carbon Analyzer

CONFERENCE/WORKSHOP PRESENTATIONS

- **Purnima Bhardwaj,** Krishan Kumar and V. K. Jain; Poster entitled: "Urban-Rural solar irradiance and AOD variations over Delhi – NCR during summer season " at the **National Conference on Environmental Pollutants - Impact Assessment and Remediation (NCEPIAR) at School of Environmental Sciences, Jawaharlal Nehru University, New Delhi, India** (29^{th} March 2017)
- **Purnima Bhardwaj,** Alok K. Pandey, Krishan Kumar and V. K. Jain; Paper Title: "Seasonal-Spatial Variations of AOD and Solar Irradiance over Delhi - NCR" at the **International Conference on Urban Geoinformatics,** at **The Energy and Research Institute (TERI), New Delhi, India** (22^{nd} – 23^{rd} February 2017)
- **Purnima Bhardwaj,** Krishan Kumar and V. K. Jain; Poster entitled – "Seasonal physical and chemical characteristics of $PM_{2.5}$ over urban and rural location in Delhi-NCR" at "**American Geophysical Union Fall Meeting 2016**" in **San Francisco, California, USA** (12^{th} – 16^{th} December 2016)

Training / Workshop / School / Symposium

- Attended winter school on "**Aerosol Measurement and Monitoring Techniques**" held in **IIT-Madras, Chennai, India**. (Feb 16-19 2016).
- Participated in the training program titled " **Fundamentals of GIS, GPS & Remote Sensing**" held at **Department of Geography &**

Geoinformatics, Bangalore University, Bangalore, India under the financial assistance of National Natural Resource Management System (NNRMS), Department of Space, Government of India. Duration of the training: 21 days (27th July to 16th August 2015).

- Participated in the **Board of Research in Nuclear Sciences (BRNS) Tenth School on Analytical Chemistry (SAC-10)** organized by Association of Environmental Analytical Chemistry of India (AEACI), c/o **Analytical Chemistry Division, Bhabha Atomic Research Centre (BARC), Trombay, Mumbai, India**. (May18- 25 2015).
- TROPMET-2012 Pre-Symposium tutorial (18th – 19th Nov'12) on "**Satellite observations for regional climate modelling**" and **National Symposium on "Frontiers of Meteorology with special reference to the Himalayas**" (20-22 Nov'12) organised by the **Indian Meteorological Society, Dehradun chapter at Indian Institute of Remote Sensing (IIRS), Dehradun, India.**
- Participated in TERI-BCCR Climate Research School 2012 "**Beyond Regional Climate Modelling- Best Practices and New Insights**" from 1-5 October 2012 organized by The Energy and Resources Institute (TERI) and Bjerknes Centre for Climate Research(BCCR) with support from Royal Norwegian Embassy at **TERI University, New Delhi, India**.
- **National Seminar on Environmental Pollution and Bioremediation** (Dec 28-29, 2011) in JNU organised by the **School of Environmental Sciences, JNU, New Delhi, India**.
- Participated in **ASSOCHAM National Waste to Wealth Conference** (Nov 14, 2011) held in **New Delhi**.
- Participated in **First National Students Conference on River Basin Planning (BRiP-2011)** held at the **Indian Institute of Technology, Kanpur, India** (Nov 04-05, 2011).

Membership

Name of body	Type of membership	From Date	Positions held
SPIE	STUDENT	29/05/2017	Member

References

Prof. V. K. Jain
Vice-Chancellor,
Doon University,
Dehradun-248012, India
Phone No. - +91 - 9868585788
E-mail: vkj0400@mail.jnu.ac.in
http://www.jnu.ac.in/Faculty/vkjain/

Prof. Krishan Kumar
School of Environmental Sciences,
Jawaharlal Nehru University,
New Delhi-110067, India
Phone No. - +91-9899718492
E-mail: kklab301@gmail.com,
krishan_kumar@mail.jnu.ac.in